



UNIVERSITA' DEGLI STUDI DI PADOVA

**DIPARTIMENTO DI SCIENZE ECONOMICHE ED AZIENDALI
"M.FANNO"**

**CORSO DI LAUREA MAGISTRALE IN
ECONOMICS AND FINANCE**

TESI DI LAUREA

**Analysis of carbon prices with both a Variance-Gamma (VG) model and a
Mean-Reverting process and a Real Options Valuation for an alternative
energy switch**

RELATORE:

CH.MO PROF. MICHELE MORETTO

LAUREANDA: MARIA FLORA

MATRICOLA N. 1058971

ANNO ACCADEMICO 2014 – 2015

Il candidato dichiara che il presente lavoro è originale e non è già stato sottoposto, in tutto o in parte, per il conseguimento di un titolo accademico in altre Università italiane o straniere.

Il candidato dichiara altresì che tutti i materiali utilizzati durante la preparazione dell'elaborato sono stati indicati nel testo e nella sezione "Riferimenti bibliografici" e che le eventuali citazioni testuali sono individuabili attraverso l'esplicito richiamo alla pubblicazione originale.

Firma dello studente

Ai miei genitori ed ai miei nonni

Abstract

After the recent international environmental agreements (UNFCCC and Kyoto Protocol, among others), the European Union has decided to adopt the EU ETS (European Emission Trading Scheme), in order to cap the total amount of emissions of greenhouse gases. The aim of this work is to give a quantitative view on the evolution of the EU ETS carbon market, analyzing the emission reduction problem from the point of view of an electricity producer running an oil-fired power plant. First, an analysis of the emission allowances price distribution is performed, using both a Variance-Gamma model and a Brennan-Schwartz process to fit the data, and assessing their mutual advantages and shortcomings. Subsequently, using real option approach, the effectiveness of the EU ETS is evaluated, analyzing the time of grid parity, in which it is profitable to invest in a renewable energy project (a photovoltaic plant), as opposed to continuing production using fossil fuels. The results show how the combined dynamics of the prices of oil, photovoltaic technology and emission allowances influence the optimal timing of the investment.

Abstract

In seguito ai recenti trattati internazionali a salvaguardia dell'ambiente (UNFCCC, protocollo di Kyoto ed altri), l'Unione Europea ha deciso di istituire l'EU ETS (European Emission Trading Scheme), in modo da regolamentare le emissioni di gas serra. Lo scopo di questa tesi è di fornire una prospettiva quantitativa sull'evoluzione del mercato del carbonio EU ETS, analizzando il problema della riduzione di emissioni dal punto di vista di un produttore di elettricità che gestisce una centrale alimentata a petrolio. Inizialmente, viene svolta un'analisi della distribuzione dei prezzi dei permessi di emissione, utilizzando sia un modello Variance-Gamma che un processo di Brennan-Schwartz, e valutando i vantaggi e svantaggi reciproci. Successivamente, utilizzando la teoria delle opzioni reali, viene valutato se il sistema EU ETS sia in grado di incentivare l'investimento in un impianto ad energia rinnovabile (una centrale fotovoltaica), in sostituzione di un tipo di produzione elettrica basata sull'uso di combustibili fossili. I risultati mostrano come le dinamiche combinate dei prezzi di petrolio, costi della tecnologia fotovoltaica e valore dei permessi di emissione influenzino il tempo ottimale dell'investimento.

Contents

Introduction	5
1 The Emission Trading System	9
1.1 Environmental awareness retrospective	9
1.2 Taxes and tradable permits	11
1.3 The EU ETS	16
2 The Carbon Price Path	21
3 The VG Model	33
3.1 Description of the model	35
3.2 Model calibration	40
4 The Brennan-Schwartz Model	45
4.1 Description of the model	45
4.2 Model calibration	46
4.3 VG vs. BS comparison	50
5 A Real Option Valuation for a Power Plant Switch	55
5.1 The investment project	55
5.1.1 The oil-fired plant	56
5.1.2 The PV plant	58
5.1.3 The Levelized Cost of Electricity	59
5.2 The variables involved	65

5.2.1	The carbon price	65
5.2.2	The LCOE	65
5.2.3	The oil price	66
5.2.4	The benefits and costs deriving from switching	67
5.3	The option value	69
5.3.1	Analytical solution of the real option problem	70
5.3.2	Results	79
Conclusions		85
Appendix		89
A	Codes (created for the Matlab [®] environment)	89
B	Emission by year and country	104
C	Option value and benefit function derivatives	109
Bibliography		111

List of Figures

All the following figures are our own elaborations of the data, excluding fig 1.1, 1.2, 5.1, 5.2 and 5.3, whose sources are indicated in the caption.

1.1	Total EU environmental tax revenue as percentage of total taxes and of GDP, 2012	12
1.2	Map of existing, emerging and potential emissions trading schemes	13
1.3	EUA prices 2005-2014 (€/tCO ₂ e)	18
1.4	EUA log-returns 2005-2014	20
2.1	Histogram of EUA log-returns with fitted normal model	24
2.2	Histogram of EUA log-returns with fitted normal model, first partition (1 st phase)	25
2.3	Histogram of EUA log-returns with fitted normal model, second partition (2 nd and 3 rd phase)	25
2.4	Autocorrelations of absolute log-returns	28
2.5	Autocorrelation function of $ r_t ^\theta$ for $\theta=0.1, 0.2, \dots, 2.0$	29
2.6	Autocorrelations of the square root of absolute log-returns	29
3.1	Empirical data compared to the fitted VG pdf obtained with the estimated parameters	42
3.2	Empirical data vs. fitted VG density, zoom-in on central data	42
4.1	EUA spot prices, theoretical PDF plotted against histogram of empirical data	49
4.2	EUA spot prices, theoretical CDF plotted against empirical one	49
4.3	EUA empirical prices vs. forecasted ones, simulated with a VG, BS, GBM process, respectively	52
5.1	Global irradiation and solar electricity potential, optimally-inclined photovoltaic modules	61
5.2	2014 capital expenditures for a ground-mounted PV system	61
5.3	Price of solar modules and experience curve	63
5.4	Oil spot prices 1986-2015 in USD/barrel, real and fitted curve	67
5.5	Trigger point P^* for $t = 4$	81
5.6	Trigger prices P^* for each fixed time (first scenario)	81
5.7	Trigger prices P^* for each fixed time (second scenario)	83
5.8	Trigger prices P^* for each fixed time (third scenario)	83

Introduction

Fossil fuels have long been the cornerstone of electricity production and of the exponential socio-economic growth of the human society. Nevertheless, in the past decades, it has become increasingly clear that a development model based on such energy sources is hardly sustainable in the long term and presents two main shortcomings: the first one is the depletion of fossil fuel reserves themselves, and the second one is that, when burnt, such fuels release into atmosphere a huge amount of GHG (greenhouse gases), with negative effects on the environment, health and society.

The recent international environmental agreements (UNFCCC, Kyoto Protocol) have stressed the need for intervention and urged countries to adopt emission reduction measures and to invest in alternative energy projects as a mean to decrease human-related emissions.

One of the tools which have been implemented, aimed at internalizing the negative externalities generated through the production processes, is the adoption of emission-trading programs, establishing markets in which emission allowances are traded. The carbon market is a fast changing environment: over 40 countries and 20 sub-national jurisdictions are putting a price on carbon, with about 12% of global annual GHG emissions covered (World Bank, 2014).

In this work, we focus on the EU ETS, the European Emission Trading Scheme, which is the world's biggest emissions trading market, established in 2005 and accounting for more than 75% of international carbon trading. The aim of this thesis is to give a quantitative view on the evolution of the EU ETS carbon market, analyzing the emission reduction problem from the point of view of an electricity producer running an

oil-fired power plant, who is confronted with the choice of either submitting to the ETS jurisdiction, as opposed to changing the production model, by switching production to alternative sources of energy, such as the solar one.

In order to do this, first, we perform a statistical analysis of EUA (European Union Allowances) prices. The particular distribution of returns, characterized by leptokurtosis and lack of shoulders, motivates the search for a model able to adequately describe the data, while keeping tractability from an analytical standpoint. We analyze two specific stochastic models, the Variance Gamma (VG) and the Brennan-Schwartz (BS), defining their advantages and shortcomings with respect to each other, in terms of capacity to adequately fit the carbon data and in terms of computational tractability. On the basis of such results, we proceed to evaluate the problem the electric utility has. Considering the uncertainty involving future EUA prices and the irreversible costs connected to a new PV plant investment, the opportunity of switching production method can be viewed as a real option.

Real option theory, whose theoretical foundations rely on the seminal work of Dixit and Pindyck (1994), enables us to value such an investment opportunity in a very similar way to the one in which financial options are usually priced. The goal of this valuation is to find the EUA trigger price which makes it convenient to switch to alternative sources of energy, as opposed to continuing production by means of fossil fuels. Such threshold is linked to a certain point in time, thus ultimately leading to the break-even cost of an alternative energy source.

The work is organized as follows: Chapter 1 provides a summarizing overview of the history of environmental awareness and of the different economic tools which have been used over the years to address the GHG emissions issue. Furthermore, it describes the mechanisms regulating the EU ETS and the historical performance of the EU carbon market. Chapter 2 describes the main problems and features arising from financial time series analysis, while delineating the statistical properties of carbon prices. Given the presence of fat tails in the distribution, we choose a stochastic process able to address this feature. There are different processes which could serve this purpose, such as the GBM with log-normal jumps, the GARCH model or the VG process. The latter is the one we selected and its detailed description and calibration are provided in Chapter 3. The VG model is obtained by time changing a Brownian motion with an independent

subordinator and it belongs to the class of generalized hyperbolic distributions (GH), which are useful to capture high kurtosis features in the data. In Chapter 4, we fit the data using a different class of stochastic processes, the mean-reverting one. The BS belongs to this category, since the asset is assumed to drift towards a mean level in the long-run, with a certain speed of mean-reversion. After calibrating the BS model, we compare the results with the ones obtained in the previous chapter, performing a simulation via Monte Carlo in order to define the predictive capacity of both models, and assessing which of the two stochastic processes helps better grasping the essential features of the data under analysis. Basing our dynamics choice on the previous findings, in Chapter 5 we get to the core of the real options valuation approach, showing the results of its application to our motivating example and defining the relationship linking EUA prices to the convenience of an alternative energy investment project.

The quantitative analysis of carbon price data and the numerical resolution of the real option pricing problem have been performed using the technical computing software Matlab[®].

Chapter 1

The Emission Trading System

1.1. Environmental Awareness Retrospective

The roots of the relationship between business and the natural environment can be traced back to the late '60s and early '70s, when both in Europe and in the USA the modern environmental movement was rising.

In Europe, the idea of making the polluter pay for the damage done to the environment came up during the 1972 Stockholm Conference on the Human Environment and, in October 1972, the EU environmental policy was formally founded through the European Council declaration¹. During that same year, environmental awareness had become a hot topic, and growing public and scientific concerns were generated also by the publication of *Limits to Growth*, an eye-opening book stressing the importance of the environment and the long term unsustainability of economic growth, written by the Club of Rome, which at the time was a small group of people from the fields of academia and industry. Subsequently, in November 1973, the EU adopted its first ambitious Environment Action Programme, where the Polluter Pays Principle (PPP), which states that whoever is responsible for damage to the environment should bear the costs associated with it, was taken on as a guideline, along with the idea that being proactive is better than reactive. During the '80s, the main body of EU environmental legislation enlarged, embodying some key pieces such as the Environmental Impact Assessment Directive (1985) and the environmental policy approach started being more

¹ European Environment Agency website (<http://www.eea.europa.eu/environmental-time-line/1970s>).

and more emission-oriented. In 1987, environmental protection was given its own chapter in the European Community Treaty, and the year was designated as the European Year of the Environment. At the end of the '80s, there was a mounting wave of environmentalism and, in several EU countries, a lot of green political parties were on the rise, achieving good results. In 1994, the European Environmental Agency was born.

In the US, the modern environmental movement was forged in the social and political turbulence of the '60s and '70s², with the tipping point coming with the publication of Rachel Carson's *Silent Spring* (1962), a book that "helped bring about a growing awareness that chemicals were damaging the environment and ultimately ourselves"³. The creation of the US Environmental Protection Agency (1970), partly triggered by the massive public demonstration that was called "Earth Day" on April 1970, provided a governmental agency to oversee policy-making and regulation in respect of environmental problems⁴. Later, the Superfund legislation debate (1980) proved to be a milestone in the long march toward corporate environmental accountability⁵ and, in 1987, the Brundtland Declaration, sponsored by the United Nations, traced the roots to the contemporary environmental movement⁶, and led to the increasing internalization of environmental sustainability carried on by corporations.

On an international level, a number of agreements have tried to address the climate change issue. Among the most relevant environmental treaties, we mention the United Nations Framework Convention on Climate Change (UNFCCC) and the Kyoto Protocol. The former was negotiated at the United Nations Conference on Environment and Development, known as the Earth Summit, held in Rio de Janeiro in June 1992. Such treaty was non-binding, in the sense that it contained no enforcement mechanisms, while providing a framework for negotiating other international treaties to address the

² Post, Chapter 29, *The Oxford Handbook of Business and the Natural Environment*, Oxford University Press, 2012.

³ Hoffman, Bansal. Chapter 1, *The Oxford Handbook of Business and the Natural Environment*, Oxford University Press, 2012

⁴ Lounsbury, Fairclough & Lee. Chapter 12, *The Oxford Handbook of Business and the Natural Environment*, Oxford University Press, 2012.

⁵ Carrol, Lipartito, Post, Werhane. *Corporate Responsibility – The American Experience*, p. 288, Cambridge University Press, 2012.

⁶ Carrol, Lipartito, Post, Werhane. *Corporate Responsibility – The American Experience*, p. 397-398, Cambridge University Press, 2012.

GHG issue. In 1997, according to the UNFCCC framework, the Kyoto protocol established legally binding obligation for developed countries to reduce emissions.

1.2. Taxes and Tradable Permits

Over the years, environmental regulation has tried to integrate the social costs entailed by environmental pollution into the price of the products, and this was done essentially in two ways: through Command-and-Control instruments or using economic instruments.

The first group of instruments dominated the past decades and the rationale behind those tools was to diminish the overall emission level by imposing a quantitative restriction on each player, for example by setting emission standards for individual sources. This plain quantitative restriction was definitely not efficient, since it didn't take into account the different marginal abatement costs of each company.

The latter group, namely the market-based instrument one, instead comprehends taxes and tradable permits and has emerged as a more cost-effective alternative⁷. Pollution fees and marketable permits in the US were introduced in the 1990 Clean Air Act Amendments (even though environmental taxation has never been popular nor really used in the US), while in Europe only environmental taxes have been used since 1990, when Finland and Sweden acted as pioneers in launching CO₂ abatement taxes, with other European countries following the policy trend a few years later⁸.

⁷ Tietenberg, (1990). *Economic Instruments for Environmental Regulation*. Oxford Review of Economic Policy, 6, 1, 17-33.

⁸ Andersen & Ekins, (2009). *Carbon-Energy Taxation. Lessons from Europe*. New York: Oxford University Press.

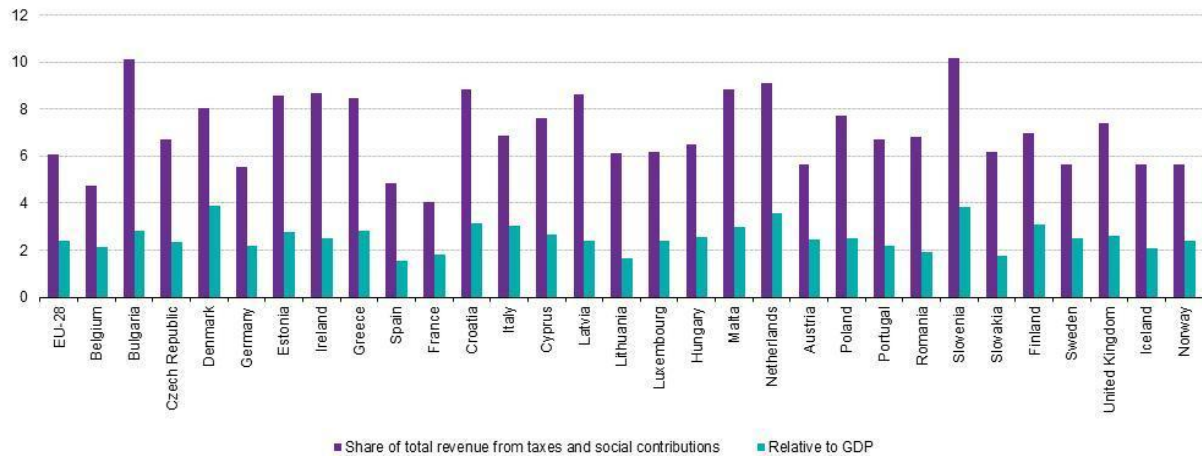


FIG. 11 Total EU environmental tax revenue as percentage of total taxes and of GDP, 2012. Source: Eurostat (online data code: env_ac_tax).

After the agreement of the Kyoto Protocol, tradable permits in Europe were introduced on a large scale, as a mean to tackle environmental pollution, with the set up of an emission trading scheme, established by the European Directive 2003/87/EC, namely the EU ETS, the largest carbon emissions trading scheme in the world, covering about 45% of EU carbon emissions.

The common feature of both taxes and tradable permits is that the process of internalization of negative externalities occurs in such a way that the marginal abatement costs are equalized between different companies. In fact, the firms which incur higher emission reduction costs will find it more convenient to pay the tax/buy more permits rather than reducing emissions, and vice versa, in this way increasing the overall efficiency of the system.

What differentiates these two tools, instead, is the object of the political decision: when the government imposes a tax on the emitters, it indirectly fixes the price of a ton of CO₂, while it lets the quantity float; in a trading scheme, the price of a ton of CO₂ is determined by the market, while the overall quantity is fixed (there's a cap determined by the legislator).

Before deepening the topic, we should better explain what exactly tradable permits are. As of 2014 there are currently 11 emission trading schemes in place⁹, along with many others under implementation/consideration (see Fig.1.2).

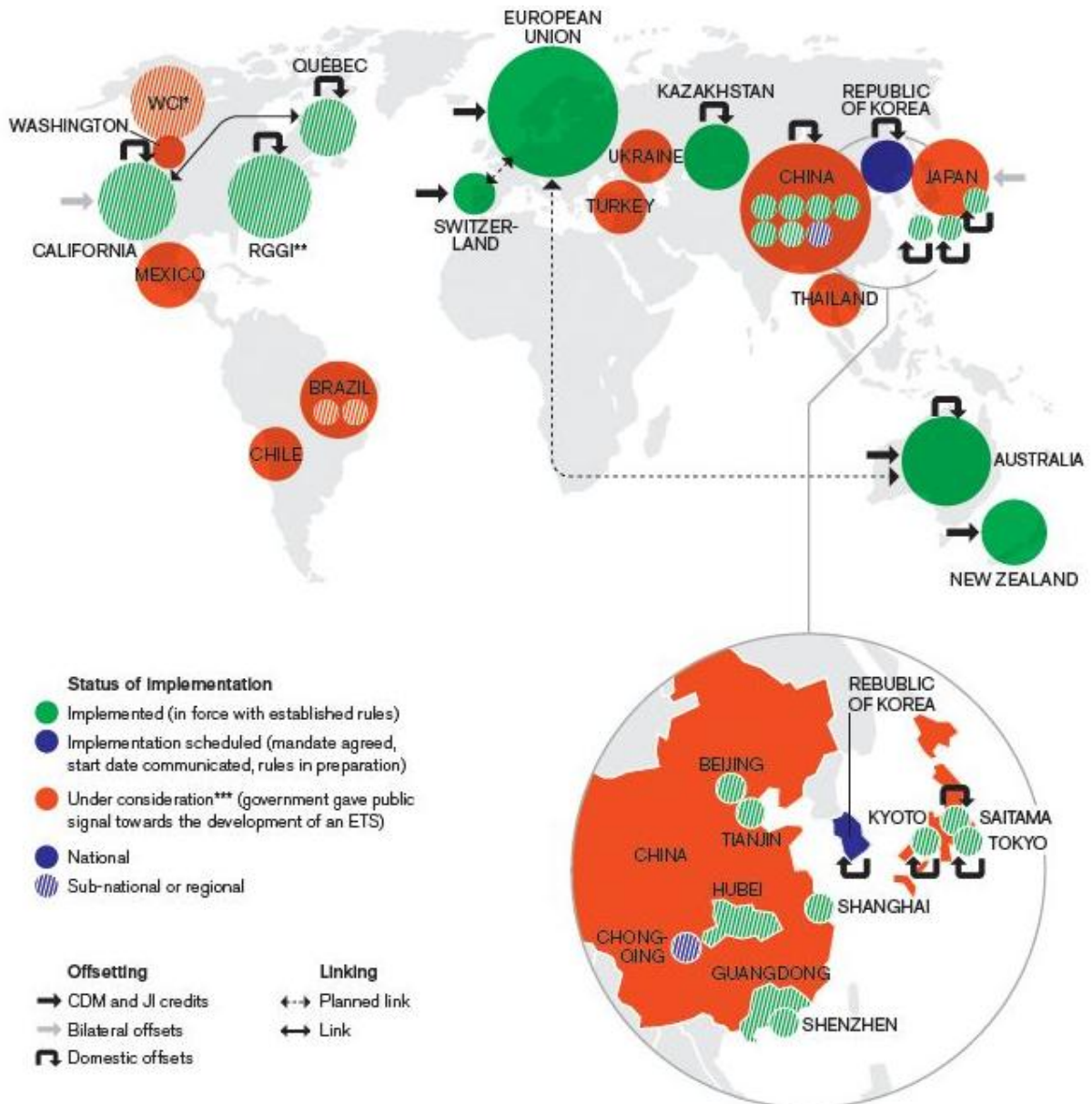


FIG. 1.2 Map of existing, emerging and potential emissions trading schemes. Source: World Bank (2014). States and Trends of Carbon Pricing 2014. Washington, DC: World Bank.

⁹ *States and Trends of Carbon Pricing*, (2014). World Bank Group, Washington DC. (http://www-wds.worldbank.org/external/default/WDSContentServer/WDSP/IB/2014/05/27/000456286_20140527095323/Rendered/PDF/882840AR0Carbo040Box385232B00OUO090.pdf)

These instruments were initially proposed by Dales (1968) and Coase (1960) in their influencing papers and first examples of tradable permits systems can be traced back to the 1980s in the US, when the Environmental Protection Agency offered states such tools in order to control localized air pollutants. One of the first cases of successful implementation of an emission trading system on a large scale was in the US indeed, when Title IV of Clean Air Act amendments established a sulfur dioxide allowance trading program in 1990, in order to control the acid rain issue. Such a program turned out to outperform the expectations, with the achievement and the overcoming of the targets and with the total abatement costs having been significantly less than what they would have been without the program¹⁰.

Emission trading can be credit-based or allowance-based. The allowance-based system is a “cap-and-trade” one, meaning that the legislator sets a cap, a total maximum amount of CO₂ or other GHG (greenhouse gases), and then injects in the market a proportional number of allowances, the price of whom is determined by supply and demand. Credits, instead, do not enter the market consequently to an allocation process, but are granted to over-complying emitters, who are then free to trade them in the secondary market.

In other words, credit-based systems are schemes in which firms voluntarily decide to participate and they do so by reducing their emissions below a defined baseline, through the implementation of a project. In this way a proportional credit is generated and the developer of the reduction project can sell its credit, gaining a profit. The difficulty policymakers encounter, when designing a credit-based system, is defining which projects are worthy credits. In fact, it’s not always easy to measure the effective emission reduction obtained through the implementation of the project, because it’s not easy to tell what the emissions would have been, had the project not taken place.

In allowance-based systems, instead, participation is mandatory. There’s a cap on overall emissions defined by the policymaker and, according to that cap, a certain number of allowances is distributed among regulated sources through an allocation process. Each allowance corresponds to a certain amount of CO₂ or other GHG. For example, in the EU ETS, which is a cap-and-trade system, every allowance gives the right to emit 1 ton of CO₂, or the equivalent amount of N₂O or PFCs. Each firm has to

¹⁰ Stavins, (1998). *What Can We Learn from the Grand Policy Experiment? Lessons from SO₂ Allowance Trading*. *Journal of Economic Perspectives*, **12**, 3, 69-88.

surrender allowances for every ton of GHG that they emitted in the previous year. The opportunity to trade the allowances ensures that only firms which incur higher abatement costs will surrender the permits instead of undertaking an emission reduction project, thus leading to the implementation of such projects where it is the most cost-effective.

As Anger (2008), Jaffe & Stavins (2008) and many other authors pointed out, linkage between different emission trading schemes would be desirable, since it would induce marginal economic benefits. In a linked trading environment, emitters would be able to meet their compliance obligations not only by acquiring emission permits in their domestic market, but also using allowances or credits from another system. In a joint trading system, the access to emission reduction options of developing countries would increase cost savings, and other potential benefits would be given by boosted market liquidity and, consequently, by a more stable carbon price. This proposal is currently under development, and the EU ETS is seen as an important building block for the construction of an international carbon market. In fact, the European Commission and Australia have agreed that their respective trading schemes, the EU ETS and the Australian Carbon Market, will be fully linked by mid-2018, and similar negotiations are under way on a possible linkage between the EU ETS and the Swiss ETS¹¹.

EUAs (European Union Allowances) can be traded in an organized exchange or in an OTC (over the counter) market. Generally speaking, in an ETS, carbon is traded as an energy commodity, even if there are some distinctive features that differentiate the carbon market from a commodity one. Just to name a few, there is only one underlying asset, the corresponding derivative market is not equally active nor liquid, and, most importantly, demand can vary, but the same cannot be said for supply, which is by definition fixed by the policymakers.

¹¹ European Commission (2013). *The EU Emissions Trading System (EU ETS)*. European Union Publications Office.

1.3. The EU ETS

The EU ETS is the largest carbon market in the world, accounting for over three-quarters of international carbon trading and covering more than 11,000 power stations and manufacturing plants in the EU territory, as well as airline companies operating flights in the EU. The GHG covered are CO₂ emitted from energy-intensive industry sectors and civil aviation, N₂O (nitrous oxide) from the production of acids and PFCs (perfluorocarbons) from aluminum production. The cap is set in order to achieve, by 2020, a 20% emission reduction with respect to 1990 levels. In this way, by that date, the maximum amount regulated firms will be allowed to emit will be 1,777 million MtCO₂e.

There is a number of ways in which allowances can be allocated among regulated emitters, and each of these ways has been object of studies (Harrison and Radov (2002), Cramton and Kerr (2002)). During the first years of functioning of the EU ETS, the preferred mode was the so-called “grandfathering”. This is essentially a free allocation, in which allowances are distributed free of charge, in proportion of each source’s past emission. In this way, a firm will only buy allowances if, in a given year, it emits more than what it did during the previous year.

Updating is another way of allocating permits, similar to grandfathering: allowances are distributed for free, the only difference with respect to the previous method is that the amount each firm will receive in the following period is updated on the basis of its production output: if its output in a given year is higher than the one of other firms in the industry, its allotted number of allowances will increase.

The third mode in which permits can be allocated is auctioning. In this way businesses have to buy their necessary amount of allowances at a competitive auction. Starting from 2013, there has been an increasing share of allowances given away in this way in the EU ETS, even if free allocation is still implemented in some sectors. The EU goal is to phase it out completely by 2027, keeping auctioning as the only method of distribution.

Contrarily to updating, which is perceived as a less efficient allocation method¹², grandfathering and auctioning have coexisted in EU ETS, and the reason the latter method has not been favored since the beginning, having actually been the former the preferred one in early years indeed, is that free allocation does not harm firms in terms of the so-called “stranded costs”, and it’s obviously preferred by regulated actors, since allowances are for free. However, as Cramton and Kerr (2002) point out, auctioning is more desirable since it provides greater incentive for innovation and reduced tax distortions. Furthermore, the ongoing shift toward auctioning is also beneficial in terms of transparency and coherence to the polluter pays principle we mentioned above.

The development of EU ETS has been marked by three different phases:

- 1st trading period: 2005-2007. This was the launching phase of the emission trading system. It didn’t exactly start off with a bang, since the set cap was too high and, consequently, the price of the permits fell to zero in 2007 (in fact, banking was not allowed during this phase).
- 2nd trading period: 2008-2012. In this phase, aviation was included among the regulated emitters, the non-compliance penalty was increased to € 100 per ton of CO₂e (during the first phase it was € 40), the proportion of permits given away for free decreased to 90% and the cap was reduced by 6.5% for the period. Nevertheless, the global recession deeply hit the economy and, consequently, emissions, causing overcapacity and negatively affecting the carbon price.
- 3rd trading period: 2013-2020. The system underwent some important reforms and the cap was set to be reduced by 1.74% per year. A progressive shift toward auctioning takes place. Carbon price remains low, with a surplus of over 2.1 billion allowances at the end of 2013¹³, mainly due to the lingering economic crisis and high imports of international credits.
- 4th trading period: 2021-2028. Starting from the beginning of this phase, the EC proposal is to increase the annual reduction of the cap from 1.74% to 2.2%

¹² Harrison, Radov (2002). *Evaluation of Alternative Initial Allocation Mechanisms in a European Union Greenhouse Gas Emissions Allowance Trading Scheme*. Report by National Economic Research Associates prepared for DG Environment, European Commission.

¹³ Source: European Commission, *Structural Reform of the European Carbon Market*, accessed January 8, 2015, <http://ec.europa.eu/clima/policies/ets/reform/>.

(World Bank, 2013). Another measure to be implemented in 2021 is the creation of a market stability reserve, in order to address the allowance surplus problem.

Figure 1.3 illustrates the evolution of the EUA spot price during 2005-2014; this data, provided by Bloomberg[®], will constitute the historical sample object of study in the following chapters.

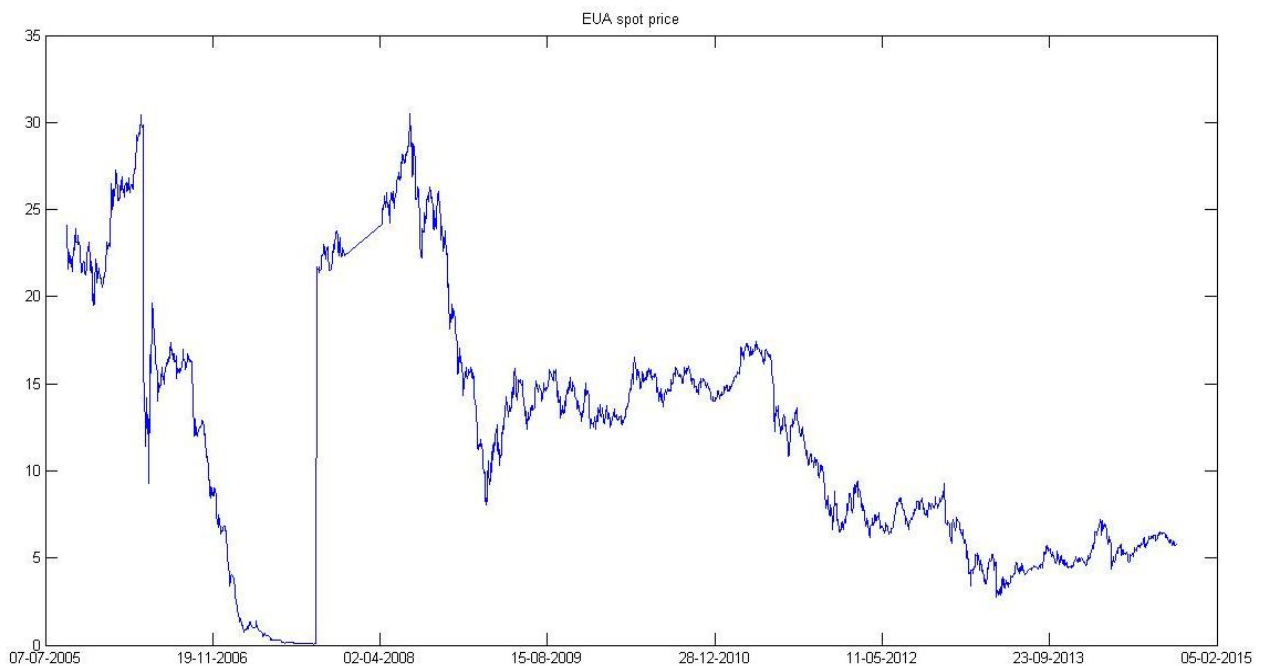


FIG. 1.3 EUA prices 2005-2014 (€/tCO₂e)

As we can see in Figures 1.3 - 1.4, the huge spike marks the transition from the first to the second phase. In fact, as we said above, during the first trading period, the price declined sharply, due to the fact that the allowances could not be banked for use in phase two and the cap was set too high. This miscalculation of the effective number of permits needed was caused by the lack of reliable emissions data, forcing the policymakers to make the decision on the basis of best guesses. After the pilot phase, verified annual emissions data were produced, which helped setting the cap in a more accurate way.

During the second phase, thanks to the Linking Directive (2004/101/EC), the use of Joint Implementation and Clean Development Mechanism credits, respectively named ERUs and CERs, was allowed in order to meet compliance obligations, thus enlarging the set of options available to businesses. Banking of allowances was permitted, reducing the exposure by extending the time span in which permits could be used. However, the economic downturn deeply affected the price development in this phase, leading to declining and unstable prices.

During the beginning of the third trading period, from January 2013 until February 2014, the EUA price was characterized by a fluctuating trend. This was caused by the debate surrounding the so-called “back-loading” proposal. In fact, phase three started carrying over a 2 billion allowance surplus, which grew further to 2.1 billion allowances by the end of 2013 (see Appendix B for comprehensive data on allocated allowances and effective emissions). This structural surplus had led to weak carbon prices and, in order to fix the situation at least in the short-term, the European Commission proposed a price-stabilization mechanism called “back-loading”. The back-loading consisted in postponing the auctioning of 900 million allowances from the beginning until the end of the third trading phase, in 2020, in order to allow demand to rise again. However, the proposal went through several votes and delays, causing market uncertainty and numerous ups and downs in the price development. For example, in April 2013, the Parliament rejection of the back-loading draft amendment caused the price to drop by 40%¹⁴. Finally, the proposal was approved and put into legislation in February 2014, causing a positive response of the market and soaring prices.

As a more long-term oriented solution, besides back-loading, the EU has also proposed another measure, namely a market stability reserve. This structural change would enable a realignment between demand and supply and would be implemented through an automatic and predictable mechanism, which wouldn't leave any need for political decisions, both addressing the surplus problem and increasing resilience to future shocks. Such a reserve is planned to be implemented by 2021 and the way it works is that it would be triggered when the surplus of allowances reached a certain level,

¹⁴ Source: Reuters, *EU Parliament Rejects Carbon Market Rescue Fix*, April 16, 2013, <http://www.reuters.com/article/2013/04/16/us-eu-ets-vote-idUSBRE93F0NT20130416>.

withholding the excess allowances from the auction volumes and adding them to the reserve.

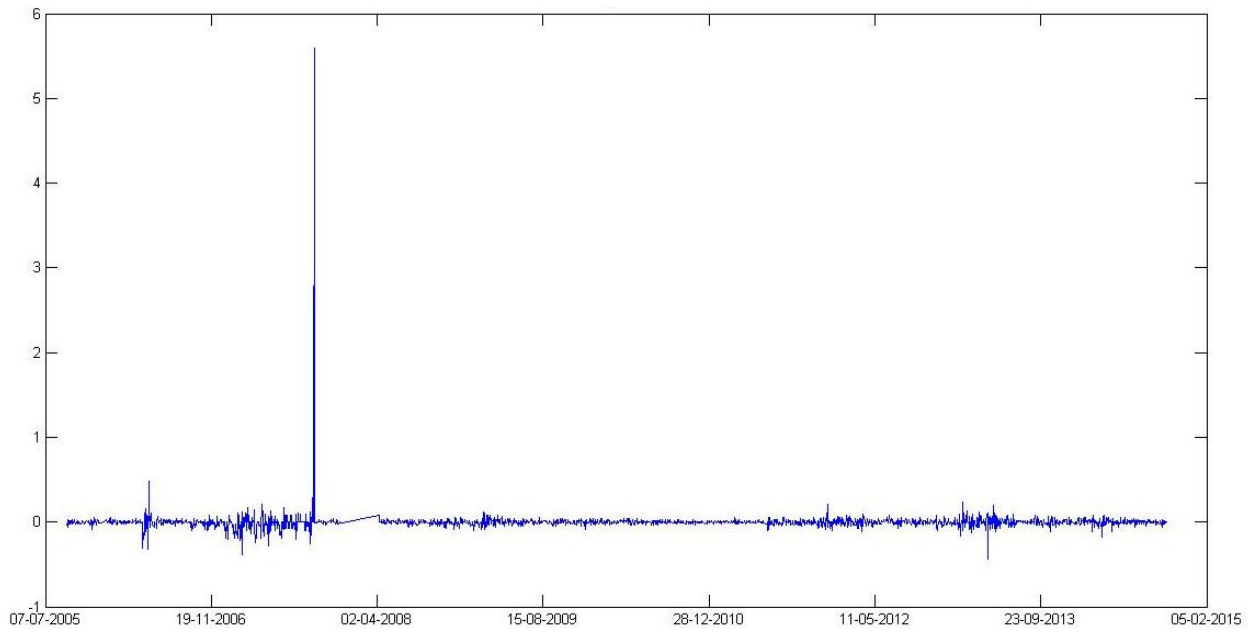


FIG. 1.4 EUA log-returns 2005-2014

Chapter 2

The Carbon Price Path

Since the Black-Scholes model in 1973, the natural assumption for asset price behavior has usually been the Geometric Brownian Motion (GBM), which has provided the financial world with numerous insights into the functioning of markets and has been one of the fundamental building blocks for the modeling of asset prices. Assuming a GBM for an asset price is equivalent to considering that the logarithm of the underlying variable follows a generalized Wiener process.

Proposition 2.1 *The GBM equation is given by*

$$dS_t = \alpha S_t dt + \sigma S_t dW_t$$

$$S_0 = s_0$$

whose solution is

$$S(t) = s_0 e^{(\alpha - \frac{1}{2}\sigma^2)t + \sigma W(t)}$$

where S_t is the asset price, W_t is a Wiener process, $\alpha \in \mathbb{R}$ and $\sigma > 0$.

As we can see, the GBM can be viewed as a linear ordinary differential equation, with a stochastic coefficient driven by white noise.

If we further define $X_t := \log \frac{S_t}{S_{t-1}}$ as the logarithmic return process, we can write the equation above as

$$X_t = \log S_t - \log S_{t-1} = \left(\alpha - \frac{1}{2}\sigma^2 \right) + \sigma W_t$$

which implies that the log-returns are independent and identically distributed normal random variables.

To check whether our data on carbon emission certificates match such a model, we begin with a basic statistical analysis.

First, we test whether a unit root is present in our time series. To do this, we implement the Augmented Dickey-Fuller test, which is a more sophisticated version of the original test proposed by Dickey and Fuller in 1979, using the Matlab[®] built-in function `adftest`. This function assesses the null hypothesis of a unit root in a time series and returns the p-value of the test statistic.

In particular, the model proposed is

$$\Delta y_t = \alpha + \beta t + \gamma y_{t-1} + \delta_1 \Delta y_{t-1} + \delta_2 \Delta y_{t-2} + \dots + \delta_k \Delta y_{t-k} + u_t$$

where u_t is the innovations process and y_t , in our case, is the logarithmic price at time t . The null hypothesis is $\gamma = 0$, tested against the default alternative one, which is $\gamma < 0$, that is, the process would be stationary (the other alternative hypothesis could be $\gamma > 0$, which would imply an explosive process, but this is not usually of interest, given that it would mean that the price may grow indefinitely).

The result we obtain is

```
h =
    0

pvalue_dickey =
    0.1308
```

meaning we cannot reject the unit-root null hypothesis, with a default 95% confidence level.

After having tested that the price process is not stationary, we must check if the log-returns are normally distributed, a natural consequence given by the prices following a GBM. To do this, we implement the Jarque-Bera test, through the Matlab[®] function `jbtest`, which performs a Jarque-Bera test of the null hypothesis that the sample comes

from a normal distribution with unknown mean and variance. Specifically, the test statistic, which for large sample sizes has a chi-squared distribution with two degrees of freedom, is:

$$JB = \frac{n}{6} \left(s^2 + \frac{(k - 3)^2}{4} \right)$$

where n is the sample size, s represents the sample skewness, defined as $s = E \left(\frac{(X-\mu)^3}{\sigma^3} \right)$ and k the sample kurtosis, defined as $k = E \left(\frac{(X-\mu)^4}{\sigma^4} \right)$. The result we obtain is:

```
d =
```

```
1
```

```
pvalue_jarque =
```

```
1.0000e-003
```

meaning the hypothesis of normality is rejected. In fact, if we check the values of kurtosis and skewness of our time series, we can see that the former is definitely high compared to the value of the Gaussian distribution, which is 3, and the latter is far from zero, meaning the distribution is not symmetric.

```
Kurtosis =
```

```
1.7414e+003
```

```
Skewness =
```

```
39.0531
```

This higher peakedness about the mean and lack of shoulders, consequences of such a high kurtosis, can also be seen graphically (Fig.2.1). In Figure 2.1 we can also notice there's a value out of range, definitely farther from the rest of the observations, which is the main cause to such a high skewness. This is mainly due to the big jump in prices that occurred in September 2007, in concomitance with the beginning of the second trading period, after the drastic drop of the price of first-period allowances during phase 1, which was mentioned in the previous chapter.

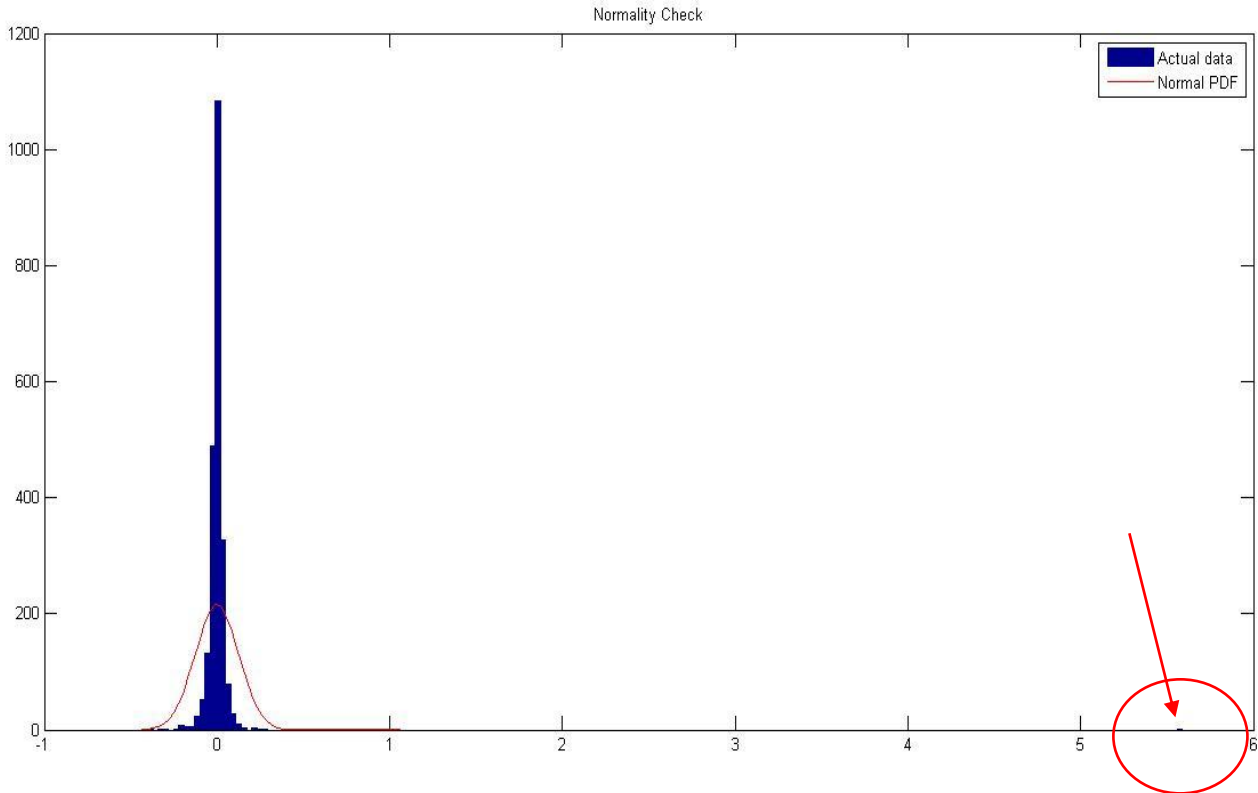


FIG. 2.1 Histogram of EUA log-returns with fitted normal model.

In fact, if we split the time series into two separate partitions, before and after the aforementioned jump, we obtain results which are still far from the ones we would obtain if the distribution was normal, but at least much more similar to what we're used to see in the scope of financial analysis (see also Fig. 2.2 and 2.3):

Kurtosis_1st =	Kurtosis_2nd3rd =
13.4738	23.6432
Skewness_1st =	Skewness_2nd3rd =
-0.3138	-1.0542

The distribution is still really leptokurtic, but it's definitely more symmetric. This is a frequent phenomenon in financial time series; in fact, the presence of both volatility clustering (observed dependence of time-varying pattern of the volatility) and conditional non-normality can induce leptokurtosis¹⁵.

¹⁵ Bai, Russel, Tiao, (2001). *Kurtosis of GARCH and Stochastic Volatility Models with Non-normal Innovation*. University of Chicago.

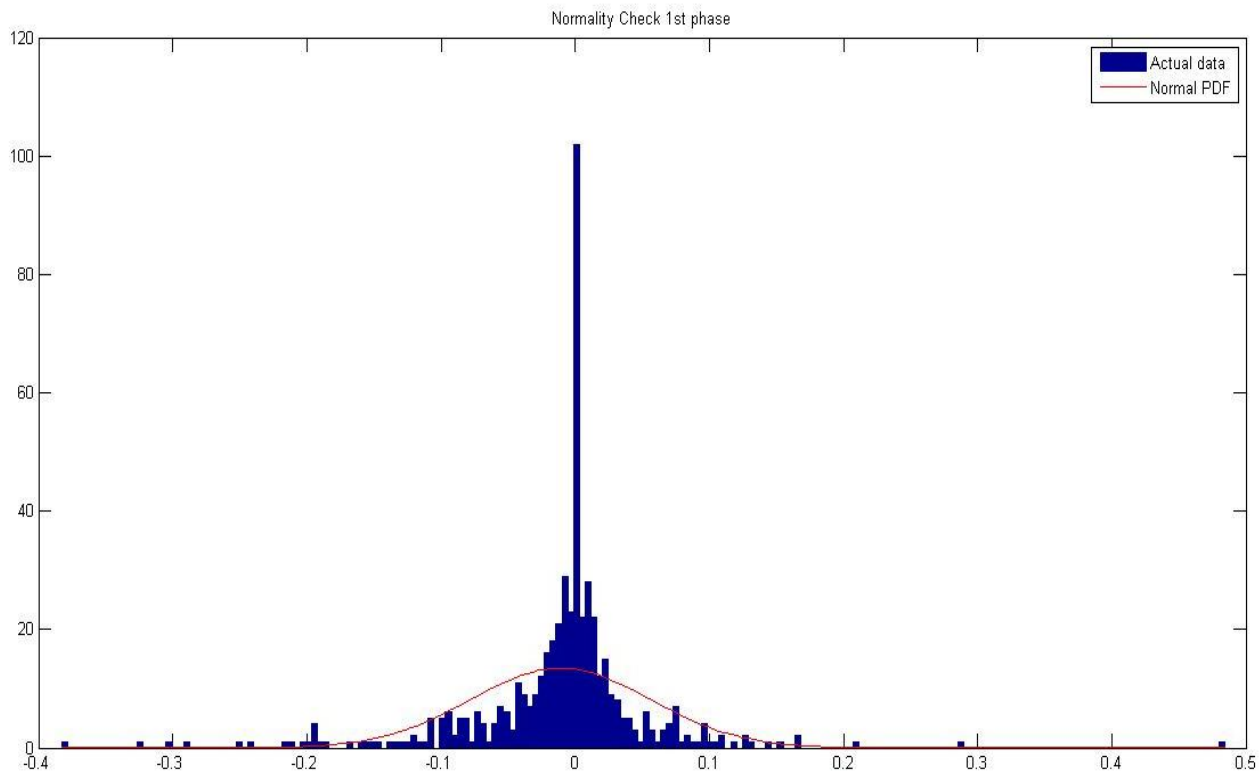


FIG. 2.2 Histogram of EUA log-returns with fitted normal model, first partition (1st phase)

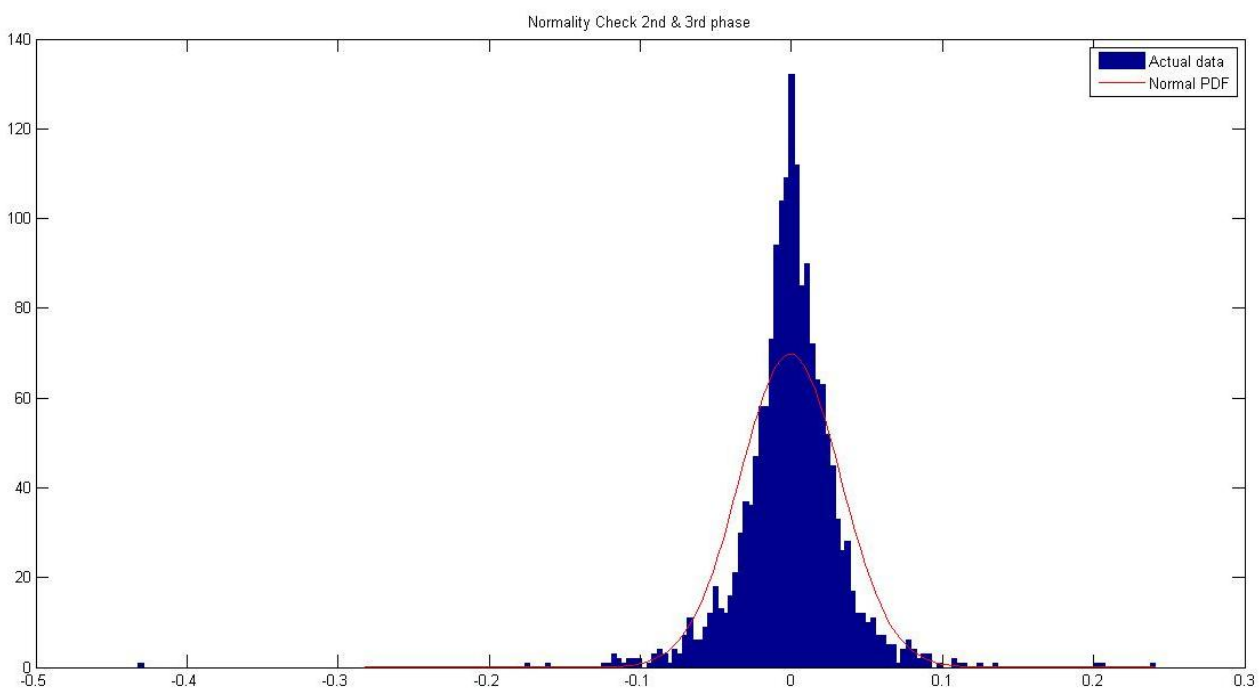


FIG. 2.3 Histogram of EUA log-returns with fitted normal model, second partition (2nd and 3rd phase)

In fact, such high values of kurtosis are no surprise at all in the scope of financial data analysis: typical values for $T=5$ minutes are $k \simeq 74$ for USD/DEM exchange rate futures, $k \simeq 60$ for USD/CHF exchange rate futures, $k \simeq 16$ for the S&P500 index futures¹⁶, while, if considering daily data, the kurtosis value of the S&P500 index (SPX) has been found equal to 42.23, during the period 1980-2005¹⁷.

If we try to reduce the frequency of returns, namely using monthly returns rather than daily ones, the empirical distribution exhibits both lower kurtosis and skewness, but still the Jarque-Bera test rejects the hypothesis of normality:

Kurtosis =

75.0176

Skewness =

7.6727

which may represent an improvement compared to the previous values of 1741.40 and 39.05, respectively. This result is consistent with the so called “aggregational Gaussianity”, by which, at the increasing of the time scale over which returns are computed, their distribution looks more and more normal. However, even on a monthly level, these values are still too far from the ones we would obtain if the distribution was Gaussian, suggesting that a GBM may not be the best assumption for our price data.

A lot of studies on financial modeling show that the typical asset price behavior is far from being similar to a GBM. Instead, as Heyde and Liu point out¹⁸, log return data usually show:

- a pronounced leptokurtic distribution;
- occasionally skewed distributions;

¹⁶ Cont, Potters, Bouchaud, (1997). *Scaling in stock market data: stable laws and beyond - Scale Invariance and Beyond*. (Proc. CNRS Workshop on Scale Invariance, Les Houches, 1997) ed. Dubrulle, Graner and Sornette (Berlin: Springer).

¹⁷ Kou, (2008). *Jump-Diffusion Models for Asset Pricing in Financial Engineering*. Handbooks in OR & MS, Vol 15, 73-116.

¹⁸ Heyde & Liu (2001). *Empirical Realities for a Minimal Description Risky Asset Model. The Need for Fractal Features*. Journal of the Korean Mathematical Society (5), **38**, 1047-1059.

- a high volatility and heteroskedastic time series, quite unlike Gaussian white noise;
- evidence of long range dependence structure in absolute and squared returns, even if log-returns are not serially correlated.

These and other properties have been found to be common across a wide range of financial instruments and have been referred to as “stylized facts”. To name a few more, the aforementioned aggregational Gaussianity, the volatility clustering, the Taylor effect (see below) and the intermittency (presence of irregular bursts in time series of a wide variety of volatility estimators)¹⁹ all fall into the “stylized facts” category. As we will later see, these stylized facts, which are usually formulated in terms of qualitative properties, are quite constraining and make it really difficult to find even an *ad hoc* stochastic process which possesses the same set of features.

The fact that, for various financial series, the sample autocorrelations of the absolute log-returns $|r_t|$ decline slowly as a function of lags was first discovered by Taylor in 1986²⁰. He also noticed that this slowly decaying autocorrelation behavior is more significant for absolute returns rather than for squared returns. This phenomenon was further investigated by Granger et al., who studied the behavior of the ACF of $|r_t|^\theta$, finding that the sample ACF tends to assume higher values for $\theta=1$. This “stylized fact” was later referred to as “Taylor effect” in a paper by Granger and Ding (1995)²¹, and states the following:

$$\text{corr}(|r_n|, |r_{n+k}|) > \text{corr}(|r_n|^\theta, |r_{n+k}|^\theta), \quad \text{for any } \theta \neq 1$$

In our case, while performing an analysis of autocorrelations on emission allowances data, we found that the log-returns are not significantly serially correlated (as we should expect indeed), but neither the absolute log-returns are (Fig. 2.4).

¹⁹ Cont, (2001). *Empirical Properties of Asset Returns: Stylized Facts and Statistical Issues*. Quantitative Finance, **1**, 223-236.

²⁰ Taylor, (1986). *Modelling Financial Time Series*. John Wiley & Sons, New York.

²¹ Granger, Ding, (1995). *Some Properties of Absolute Returns: an Alternative Measure of Risk*. Annales d'Économie et de Statistique, **40**, 67-91.

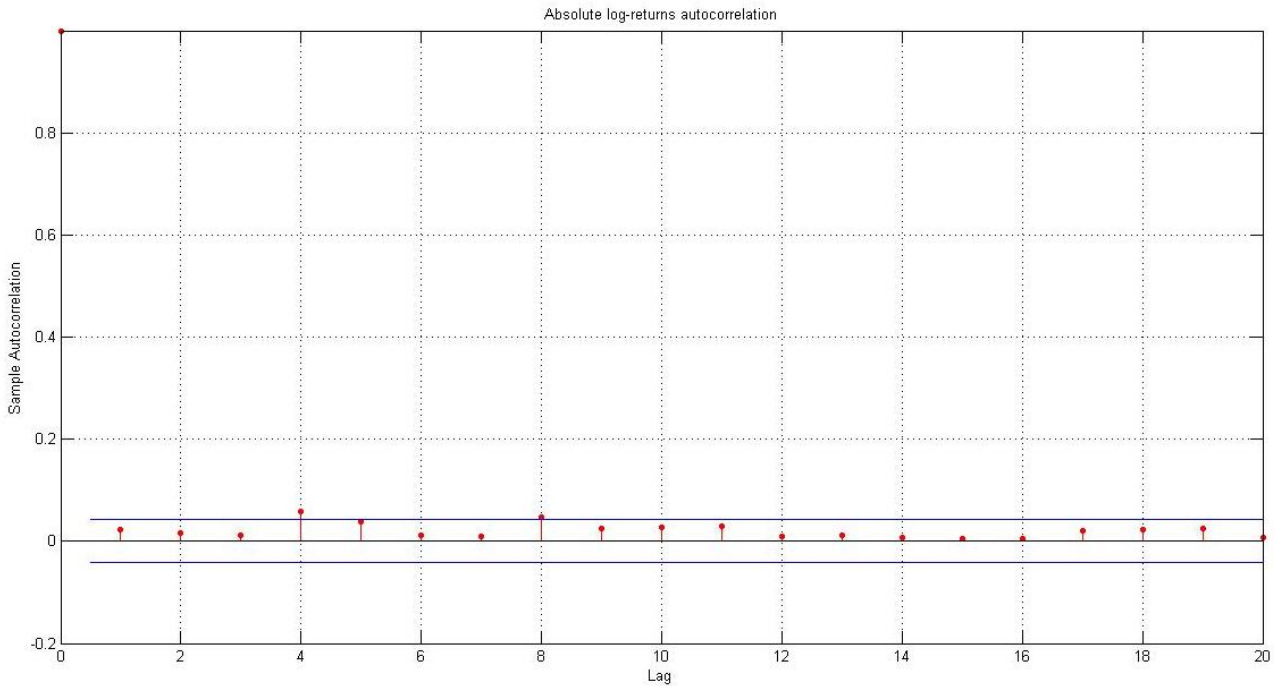


FIG. 2.4 Autocorrelations of absolute log-returns

However, if we further investigate the presence of a so called Taylor effect on our data, we find that, even if a significantly high autocorrelation is not reached for $\theta=1$, for lower values of θ the ACF values become quite high (Fig. 2.5). Specifically, we noticed that the maximum autocorrelation values are reached when $\theta \in [0.4, 0.5]$. In Fig. 2.6 we reported the ACF for $\theta=0.5$ and we can see that the values are definitely out of the 95% significance levels. This means that our sample follows a slightly different pattern from that of other financial data: a significant autocorrelation is present in the square root of the absolute log-returns, rather than in the absolute log-return. However, this is not too worrying since even Granger, in a later study²², found that also values of $\theta < 1$ may lead to the absolute returns having this “long memory” property for some kind of financial assets (the exchange rates in his case) and Muller and Dacorogna (1998) confirmed this finding, assessing that $|r_t|^\theta$ is maximized with $\theta=0.5$ for certain types of financial products²³. The interesting fact however, which may differ from other authors’ findings, is that the autocorrelations, instead of slowly decaying, in our case seem to follow a cyclical pattern.

²² Granger, Ding, Spear, (1997). *Stylized Facts on the Temporal and Distributional Properties of Daily Data from Speculative Markets*. Department of Economics, UC San Diego.

²³ Müller, Dacorogna, Pictet, (1998). *Heavy tails in high-frequency financial data. A Practical Guide to Heavy Tails: Statistical Techniques and Applications*. Boston: Birkhäuser, 55-77.

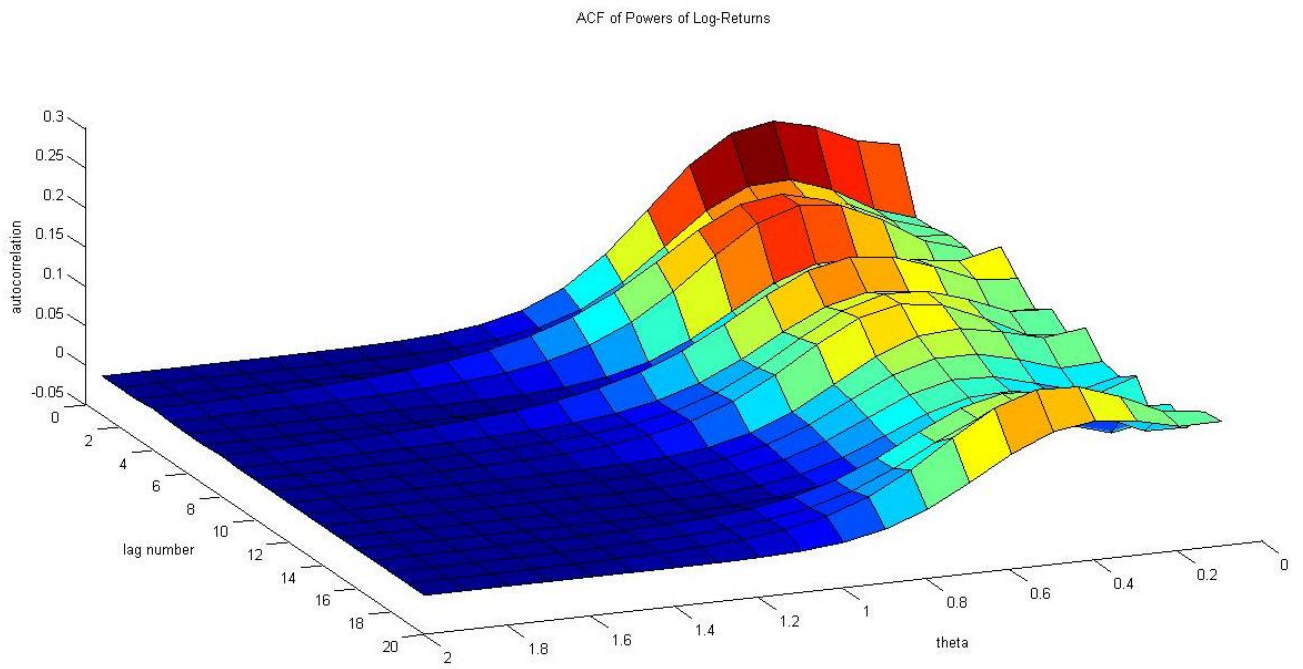


FIG. 2.5 Autocorrelation function of $|r_t|^\theta$ for $\theta=0.1, 0.2, \dots, 2.0$

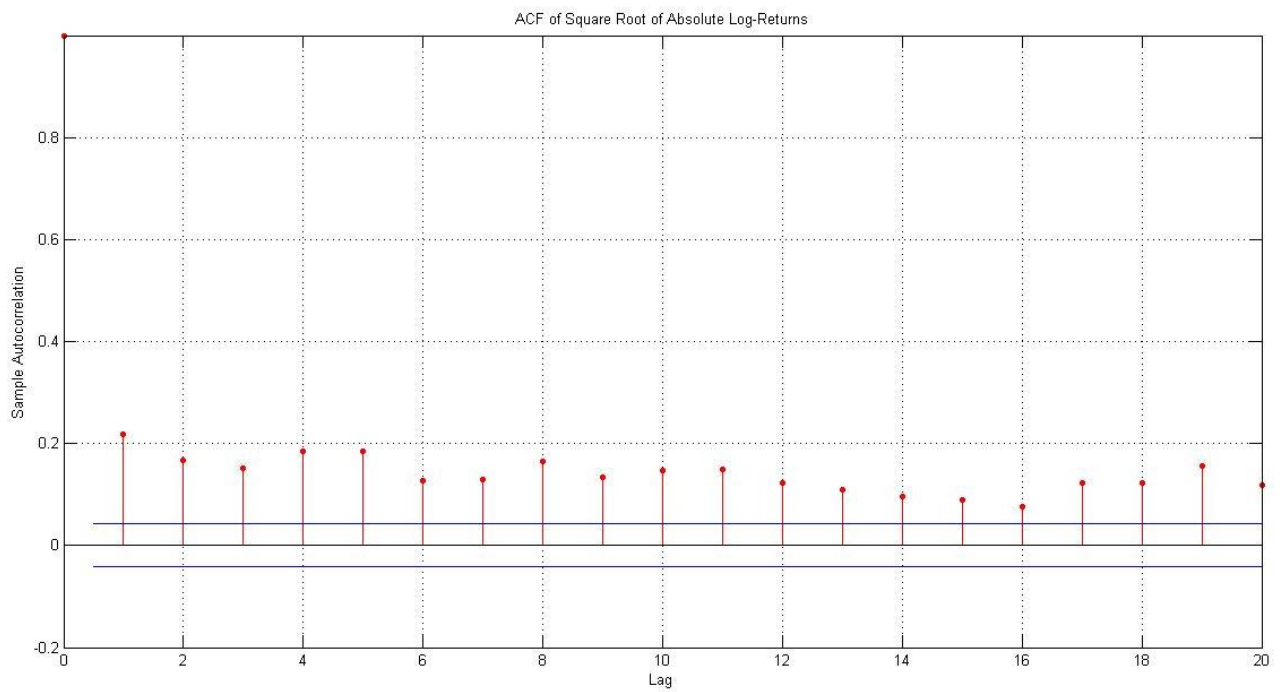


FIG. 2.6 Autocorrelations of the square root of absolute log-returns

To explain the numerous empirical properties described above, various models have been proposed to substitute the framework assumed by Black and Scholes. To name a few, these include: generalized hyperbolic models, stochastic volatility and GARCH models, fractal Brownian motions, constant elasticity of variance (CEV) models, jump-diffusion models, time-changed Lévy processes. Each one of them has its strengths and its shortcomings, and one must decide whether to gain in analytical tractability or consistency to reality. In the next chapter, we'll choose to focus on an alternative version of the Variance Gamma (VG) model as proposed by Madan, Carr and Chang (1998), created modifying a Lévy process in order to take into account the long range dependence of the asset return structure.

Let's start by relaxing the assumptions of the Black and Scholes model: of course we first need to remove the Gaussian character of the log-returns and replace it with an unspecified distribution F_h , depending only on the time span h . Then, we assume that the price path S_t exhibits only jump discontinuities (the process is *càdlàg*, right continuous and with a left limit) and finally we still suppose (as in the GBM) that log-returns on disjoint time periods are stationary and mutually independent. These are the conditions necessary to define a general Lévy process. For every infinitely divisible distribution we can define a Lévy process and such a process will be useful in finance if it's able to represent skewness and kurtosis adequately²⁴. One of the first responses to generate non-normality using a Lévy process different from the GBM was the one by Merton (1976), who incorporated a Poisson process into the standard underlying process, creating the so called jump-diffusion process. Being the jump component modeled with a compound Poisson process, only rare event are captured by the model. There are other jump models which exhibit higher jump frequencies, such as the log stable model (LS) of Carr and Wu (2003) and the aforementioned VG model, and both of them allow an infinite number of jumps within any finite interval.

The problem with Lévy processes, however, as with any other model for asset returns with independent increments, is that they cannot incorporate the volatility clustering effect. In fact, the particular property we acknowledged before, that the absolute log-

²⁴ Schoutens, W. (2003). *Lévy Processes in Finance. Pricing Financial Derivatives*. John Wiley & Sons, England.

returns are serially correlated, is not consistent with assuming independent increments, since the volatility of returns is correlated. This is why jump processes are usually combined with stochastic volatility processes. However, adding a stochastic volatility component makes it more difficult to obtain an analytical solution and results in a more complicated calibration process.

Chapter 3

The VG Model

The VG model, as it was first conceived, had finite moments and was a pure jump process with infinite activity and with no diffusion component. Most importantly, it was a Lévy process. Early forms of the VG model appear as far back as 1929, when Pearson, Jeffery & Elderton defined a density function which was a particular case of the VG density function, while in 1957 Teichroew obtained the VG pdf. However, the most important contribution to describing the VG process came from Madan & Seneta in 1990. In their work, they presented a symmetric variance gamma process, with stationary and independent increments, which was in all respects a Lévy process. They also pointed out that the process could also be represented as the difference between two i.i.d. gamma variates, namely between the gains process and the losses process, both with the same mean and variance rates.

The two parameter stochastic process studied in Madan & Seneta (1990) only controlled for volatility and kurtosis, while Madan, Carr & Chang (1998) generalized it, adding a third parameter to address skewness as well.

Even if the independent increment VG models by Madan & Seneta (1990) and by Madan, Carr & Chang (1998) don't solve the problem of long range dependence, there's still a way to modify the models in order to incorporate dependence in increments: the solution is to time-change the Lévy process by a positive increasing process, independent of the original process, with dependent increments. In this way, the observed term structure of implied volatility can be accommodated and the model can explain the autocorrelation structure of the increments. This happens stochastically altering the clock on which the Lévy process is run, and one can see the original clock

as calendar time and the new random clock as activity time²⁵. This difference arises from the volume traded and the flow of new price-sensitive information: at heavy trading hours, one hour on a clock, for example, may generate two hours worth of business activity. In this sense, if we randomize time $t \rightarrow T_t$ and we apply the random time change to $X_t \rightarrow X_{T_t}$, with $T_t = \int_0^t v_s ds$, following our example, we have that $v_t = 2$. If we wisely choose the subordinator model, that is, the “time deformation” applied to the Lévy process, we can determine both the distribution of the log price increments and their correlation structure in a favorable way.

This is what Carr, Geman, Madan & Yor (2003) did, time-changing the Brownian motion by a mean-reverting process, but even other authors tried to follow such a path in previous works. For example in 1982, McLeish studied the VG distribution and model, describing it as a normal multiplied by the square root of a gamma random variable, but also suggested a way for incorporating a long range dependence structure.

In particular, he presented two alternatives for the X_t process. First, he considered a simple stationary first order autoregressive model:

$$X_{t+1} = \sqrt{B_t} X_t + e_t$$

However, the correlation structure implied by this process displays short range dependence both for X_t and for X_t^2 , and makes it impossible to obtain a situation in which the log-returns show no autocorrelation, while the squared log-returns do. The second alternative he considered is closer to the one we’ll adopt in this thesis:

$$X_t = \sqrt{\tau_t} Z_t$$

where Z_t is the standard normal and τ_t is gamma distributed, they are both stationary and independent of each other. Here τ_t is what we previously defined “activity time” and it’s a possibly internally dependent process, which we’ll return to later on. This time, if Z_t consists of normal Gaussian i.i.d. variables, the process has no apparent correlation of the first order, while the autocorrelation of squared or absolute log-returns can be statistically significant.

²⁵ Carr, Wu, (2004). *Time-changed Lévy Processes and Option Pricing*. Journal of Financial Economics, **71**, 113-141.

In the next section, in order to find the parameters useful to describe our emission allowance prices, we will rely on Finlay (2009) findings, following the procedure described there to fit the VG model to the financial data.

3.1. Description of the model

In his work, Finlay extended the Madan, Carr & Chang (1998) model in order to obtain a long range dependence structure through a subordinator model that is fairly similar to the one presented by McLeish (1982).

A subordinator is an almost surely increasing process used to “time-change” other Lévy processes, which are independent of the subordinator²⁶. In Finlay (2009), the price of the risky asset S_t follows a subordinated geometric Brownian motion:

$$S_t = S_0 e^{\mu t + \theta T_t + \sigma B(T_t)}$$

where $\mu, \theta, \sigma \in \mathbb{R}$, $\sigma > 0$, $B(t)$ is a standard Brownian motion independent of T_t , which is a positive non-decreasing random process with stationary but not necessarily independent increments and which is denoted by $\tau_t = T_t - T_{t-1}$ over a time unit²⁷. This means that the price log increments, as we defined them in chapter 2, are given by:

$$\begin{aligned} X_t &= \log S_t - \log S_{t-1} \\ &= \mu + \theta \tau_t + \sigma (B(T_t) - B(T_{t-1})) \\ &\stackrel{\mathcal{D}}{\rightarrow} \mu + \theta \tau_t + \sigma \sqrt{\tau_t} B(0,1) \end{aligned} \tag{3.1}$$

The idea of having a subordinator is that of controlling the most important properties of

²⁶ Cont, Tankov, (2004). *Financial Modelling with Jump Processes*. Chapman and Hall/CRC Press, London.

²⁷ Finlay, (2009). *The Variance Gamma (VG) Model with Long Range Dependence*. Doctoral Thesis, School of Mathematics and Statistics, University of Sidney.

X_t through the τ_t process. In fact, defining the τ_t dynamics in the proper way can lead to the particular degree of autocorrelation which provides the best fit to our data.

As we can see, the activity time process τ_t shapes the covariances of the X_t process:

$$Cov(X_t, X_{t+k}) = Cov(\theta\tau_t + \sigma\sqrt{\tau_t}B_1(0,1), \theta\tau_{t+k} + \sigma\sqrt{\tau_{t+k}}B_2(0,1))$$

If B_1 and B_2 are Brownian motions and independent of each other, then

$$\begin{aligned} &= E[\theta^2\tau_t\tau_{t+k} + \sigma\theta\tau_t\sqrt{\tau_{t+k}}B_2(0,1) + \sigma\theta\tau_{t+k}\sqrt{\tau_t}B_1(0,1) + \sigma^2\sqrt{\tau_t}\sqrt{\tau_{t+k}}B_1(0,1)B_2(0,1)] \\ &\quad - E[\theta\tau_t + \sigma\sqrt{\tau_t}B_1(0,1)]E[\theta\tau_{t+k} + \sigma\sqrt{\tau_{t+k}}B_2(0,1)] \\ &= E[\theta^2\tau_t\tau_{t+k}] - E[\theta\tau_t]E[\theta\tau_{t+k}] \\ &= \theta^2\{E[\tau_t\tau_{t+k}] - E[\tau_t]E[\tau_{t+k}]\} \\ &= \theta^2Cov(\tau_t, \tau_{t+k}) \end{aligned}$$

which means that the autocorrelation depends on the τ_t dynamics and in the symmetric case, that is $\theta=0$, we have

$$Cov(X_t, X_{t+k}) = 0.$$

In regards to $|X_t|$, always assuming the symmetric case and for $\mu = 0$, we have:

$$Cov(|X_t|, |X_{t+k}|) = Cov(|\sigma\sqrt{\tau_t}B_1(0,1)|, |\sigma\sqrt{\tau_{t+k}}B_2(0,1)|)$$

Since

$$Cov(xy, zw) = Cov(x, z)Cov(y, w) + Cov(x, w)Cov(y, z) + E(x)E(z)Cov(y, w) + E(x)E(w)Cov(y, z) + E(y)E(z)Cov(x, w) + E(y)E(w)Cov(x, z),$$

$$\begin{aligned} \Rightarrow Cov(|X_t|, |X_{t+k}|) &= \sigma^2 E(|B_1(0,1)|)E(|B_2(0,1)|)Cov(\sqrt{\tau_t}, \sqrt{\tau_{t+k}}) \\ &= \frac{2}{\pi}\sigma^2 Cov(\sqrt{\tau_t}, \sqrt{\tau_{t+k}}) \end{aligned}$$

where the last passage derives from the following:

$$\begin{aligned}
E(|x|) &= \int_{-\infty}^{+\infty} |x| \frac{e^{-\frac{x^2}{2}}}{\sqrt{2\pi}} dx = \\
&= 2 \int_0^{+\infty} x \frac{e^{-\frac{x^2}{2}}}{\sqrt{2\pi}} dx \\
&= -\frac{2}{\sqrt{2\pi}} \left[e^{-\frac{x^2}{2}} \right]_0^{\infty} = \frac{2}{\sqrt{2\pi}}
\end{aligned}$$

for $x \sim N(0,1)$.

Assuming that $Cov(\sqrt{\tau_t}, \sqrt{\tau_{t+k}}) \neq 0$, we have thus obtained a null log-return autocorrelation and a significant autocorrelation for the absolute log-returns. The autocovariance of squared log-returns displays a non-zero value as well:

$$\begin{aligned}
Cov(X_t^2, X_{t+k}^2) &= Cov \left[\left(\mu + \theta \tau_t + \sigma \sqrt{\tau_t} B_1(0,1) \right)^2, \left(\mu + \theta \tau_{t+k} + \sigma \sqrt{\tau_{t+k}} B_2(0,1) \right)^2 \right] \\
&= Cov \left[\left(\mu^2 + \theta^2 \tau_t^2 + \sigma^2 \tau_t B_1^2(0,1) + 2\mu\theta \tau_t + 2\mu\sigma \sqrt{\tau_t} B_1(0,1) + 2\theta \tau_t^{\frac{3}{2}} B_1(0,1) \right), \right. \\
&\quad \left. \left(\mu^2 + \theta^2 \tau_{t+k}^2 + \sigma^2 \tau_{t+k} B_2^2(0,1) + 2\mu\theta \tau_{t+k} + 2\mu\sigma \sqrt{\tau_{t+k}} B_2(0,1) + 2\theta \tau_{t+k}^{\frac{3}{2}} B_2(0,1) \right) \right] \\
&= E \left(\theta^4 \tau_t^2 \tau_{t+k}^2 + \theta^2 \tau_t^2 \sigma^2 \tau_{t+k} B_2^2(0,1) + 2\theta^3 \mu \tau_t^2 \tau_{t+k} + 2\theta^2 \tau_t^2 \mu \sigma \sqrt{\tau_{t+k}} B_2(0,1) + \right. \\
&\quad 2\theta^3 \tau_t^2 \tau_{t+k}^{\frac{3}{2}} B_2(0,1) + \theta^2 \sigma^2 \tau_t \tau_{t+k}^2 B_1^2(0,1) + \sigma^4 \tau_t \tau_{t+k} B_1^2(0,1) B_2^2(0,1) + \\
&\quad 2\sigma^2 \mu \theta \tau_{t+k} \tau_t B_1^2(0,1) + 2\sigma^3 \mu \tau_t \sqrt{\tau_{t+k}} B_1^2(0,1) B_2(0,1) + \\
&\quad 2\theta \sigma^2 \tau_t \tau_{t+k}^{\frac{3}{2}} B_1^2(0,1) B_2(0,1) + 2\theta^3 \mu \tau_t \tau_{t+k}^2 + 2\sigma^2 \mu \theta \tau_t \tau_{t+k} B_2^2(0,1) + 4\mu^2 \theta^2 \tau_t \tau_{t+k} + \\
&\quad \left. 4\mu^2 \sigma \theta \tau_t \sqrt{\tau_{t+k}} B_2(0,1) + 4\mu \theta^2 \tau_t \tau_{t+k}^{\frac{3}{2}} B_2(0,1) \right) + 0 - [\theta^4 E(\tau_t^2) E(\tau_{t+k}^2) + \\
&\quad \theta^2 \sigma^2 E(\tau_t^2) E(\tau_{t+k}) + 2\mu \theta^3 E(\tau_t^2) E(\tau_{t+k}) + \theta^2 \sigma^2 E(\tau_t) E(\tau_{t+k}^2) + \sigma^4 E(\tau_t) E(\tau_{t+k}) + \\
&\quad 2\theta \mu \sigma^2 E(\tau_t) E(\tau_{t+k}) + 2\mu \theta^3 E(\tau_t) E(\tau_{t+k}^2) + 2\mu \theta \sigma^2 E(\tau_t) E(\tau_{t+k}) + \\
&\quad 4\mu^2 \theta^2 E(\tau_t) E(\tau_{t+k})]
\end{aligned}$$

$$\begin{aligned}
&= \theta^4 \text{Cov}(\tau_t^2, \tau_{t+k}^2) + (\sigma^4 + 4\sigma^2\mu\theta + 4\mu^2\theta^2) \text{Cov}(\tau_t, \tau_{t+k}) \\
&\quad + (\theta^2\sigma^2 + 2\theta^3\mu) [\text{Cov}(\tau_t^2, \tau_{t+k}) + \text{Cov}(\tau_t, \tau_{t+k}^2)]
\end{aligned}$$

In the symmetric case, this reduces to:

$$\text{Cov}(X_t^2, X_{t+k}^2) = \sigma^4 \text{Cov}(\tau_t, \tau_{t+k})$$

thus confirming that, if τ_t has a dependence structure, so does X_t^2 .

In this thesis, we choose τ_t to follow a gamma (Γ) distribution, which results in the X_t increments having the VG distribution.

Proposition 3.1 *The probability density function of the gamma distribution is given by:*

$$f_{\Gamma}(x; \alpha, \lambda) = \frac{\lambda^{\alpha}}{\Gamma(\alpha)} x^{\alpha-1} e^{-\lambda x}, \quad x > 0$$

where α is the shape parameter, λ is the rate parameter and $\Gamma(\alpha)$ is the gamma function evaluated at α .

The gamma function at the denominator is an extension of the factorial function to real numbers:

$$\begin{aligned}
\Gamma(\alpha) &= (\alpha - 1)! && \text{if } \alpha \in \mathbb{Z}^+ \\
\Gamma(\alpha) &= \int_0^{\infty} x^{\alpha-1} e^{-x} dx && \text{if } \alpha \in \mathbb{R}_{\neq 0} - \mathbb{Z}^-
\end{aligned}$$

In this case we choose the shape parameter to be equal to the rate parameter, namely $\alpha = \lambda$, so that $E(\tau_t) = 1$ and $\text{Var}(\tau_t) = \frac{1}{\alpha}$. In fact, the mean and variance for a gamma distributed variable are equal, respectively, to the following formulas:

$$\begin{aligned}
E(x) &= \int_0^{\infty} x \frac{\lambda^{\alpha}}{\Gamma(\alpha)} x^{\alpha-1} e^{-\lambda x} dx \\
&= \frac{\lambda^{\alpha}}{\Gamma(\alpha)} \int_0^{\infty} x^{\alpha} e^{-\lambda x} dx
\end{aligned}$$

Now, letting $y = \lambda x$ so that $dy = \lambda dx$, we have:

$$\begin{aligned}
&= \frac{\lambda^\alpha}{\Gamma(\alpha)} \int_0^\infty \frac{y^\alpha}{\lambda^\alpha} e^{-y} \frac{dy}{\lambda} \\
&= \frac{1}{\lambda \Gamma(\alpha)} \int_0^\infty y^\alpha e^{-y} dy \\
&= \frac{\Gamma(\alpha + 1)}{\lambda \Gamma(\alpha)} = \frac{\alpha}{\lambda}
\end{aligned}$$

And

$$\begin{aligned}
\text{Var}(x) &= E(x^2) - E(x)^2 = \int_0^\infty x^2 \frac{\lambda^\alpha}{\Gamma(\alpha)} x^{\alpha-1} e^{-\lambda x} dx - \frac{\alpha^2}{\lambda^2} \\
&= \frac{\lambda^\alpha}{\Gamma(\alpha)} \int_0^\infty x^{\alpha+1} e^{-\lambda x} dx - \frac{\alpha^2}{\lambda^2} \\
&= \frac{\lambda^\alpha}{\Gamma(\alpha)} \int_0^\infty \frac{y^{\alpha+1}}{\lambda^{\alpha+1}} e^{-y} \frac{dy}{\lambda} - \frac{\alpha^2}{\lambda^2} \\
&= \frac{\Gamma(\alpha + 2)}{\lambda^2 \Gamma(\alpha)} - \frac{\alpha^2}{\lambda^2} = \frac{\alpha(\alpha - 1) - \alpha^2}{\lambda^2} = \frac{\alpha}{\lambda^2}
\end{aligned}$$

If τ_t follows the gamma distribution and X_t is defined according to equation (3.1), then X_t has the following Variance Gamma pdf (see Madan, Carr, Chang (1998) and Finlay(2009)):

$$f_{VG}(x) = \sqrt{\frac{2}{\pi}} \frac{\lambda^\alpha e^{\frac{(x-\mu)\theta}{\sigma^2}}}{\sigma \Gamma(\alpha)} \left(\frac{|x-\mu|}{\sqrt{\theta^2 + 2\lambda\sigma^2}} \right)^{\alpha-\frac{1}{2}} K_{\alpha-\frac{1}{2}} \left(\frac{|x-\mu|\sqrt{\theta^2 + 2\lambda\sigma^2}}{\sigma^2} \right)$$

for $x \in \mathbb{R}$ and

$$K_\eta(\omega) = \frac{1}{2} \int_0^\infty z^{\eta-1} e^{-\frac{\omega}{2}(z+\frac{1}{z})} dz \quad \eta \in \mathbb{R}, \omega > 0$$

which is a modified Bessel function of the second kind.

3.2. Model calibration

We now proceed with the estimation of the parameters, choosing the maximum likelihood estimation (MLE) technique to fit the VG model to our EUA financial data, that is, we maximize $\sum_{t=1}^n \log f_{VG}(X_t)$ as a function of the parameters.

The results of the parameter estimation are shown in Table 3.1.

Parameter	Estimated value
$\hat{\sigma}$	0.0479
$\hat{\mu}$	$-4.61 \cdot 10^{-11}$
$\hat{\theta}$	$8.96 \cdot 10^{-4}$
$\hat{\alpha}$	0.188

TABLE 3.1. Estimated parameters for data fitted via MLE using a VG model.

One could note that there is something quite questionable about this result: every parameter shows a reasonable value but one: the α value is quite low. In fact, we should recall that $E(\tau_t) = 1$ and $Var(\tau_t) = \frac{1}{\alpha}$, and such a low value for α would imply a variance of about 5.3 for our activity time process, which is extremely high. In spite of that, if we consider that the variance of our activity time process τ_t is sort of a variance of the variance of the process X_t , since $X_t \stackrel{\mathcal{D}}{\rightarrow} \mu + \theta\tau_t + \sigma\sqrt{\tau_t}B(0,1)$, then even if $Var(\tau_t)$ equals about 5.3, this should not be too worrying. As regards the drift, τ_t is present as well and affects the overall mean of the process X_t , but since it is multiplied by a very low number, $\hat{\theta}$, the effect of a very high variance of τ_t is not so overwhelming.

If we now compare graphically our data to the VG distribution, using the estimated parameters, we can see the VG pdf provides a much better fit than the Gaussian distribution we analyzed before (Figures 3.1 - 3.2).

Nevertheless, performing a χ^2 goodness of fit test, the χ^2 statistic returns an extremely high value of 1.1247e+30, which would of course make us reject the null hypothesis at any given significance level. This is because of the one outlier we evidenced before, due to the jump that occurred at the end of the first trading phase. In fact, the Pearson's chi squared test statistic works comparing the observed frequencies (O_i) to the theoretical ones (T_i), according to the following formula:

$$\chi^2 = \sum_{i=1}^n \frac{(O_i - T_i)^2}{T_i}$$

The resulting value is then compared to the critical value from a χ^2 distribution, since the statistic asymptotically approaches a χ^2 with as many degrees of freedom as the number of bins (n) minus the number of parameters of the fitted distribution. Since the outlier has observed frequency 1, but lies very far from the rest of the data, its corresponding theoretical value tends to zero, consequently causing the explosion of the test statistic. We can choose to exclude this value from the computation of the Pearson's test, in order to see if the VG distribution fitted to our data is an acceptable model. The result we obtain is the following:

```
chi2_test_statistic =
```

```
802.2118
```

```
critical_value =
```

```
965.7095
```

Since the critical value at a 95% confidence level is above the test statistic value, we cannot reject the null hypothesis and a VG distribution with such parameter values as the ones we estimated before is a good approximation for our data, thus confirming our graphical perception.

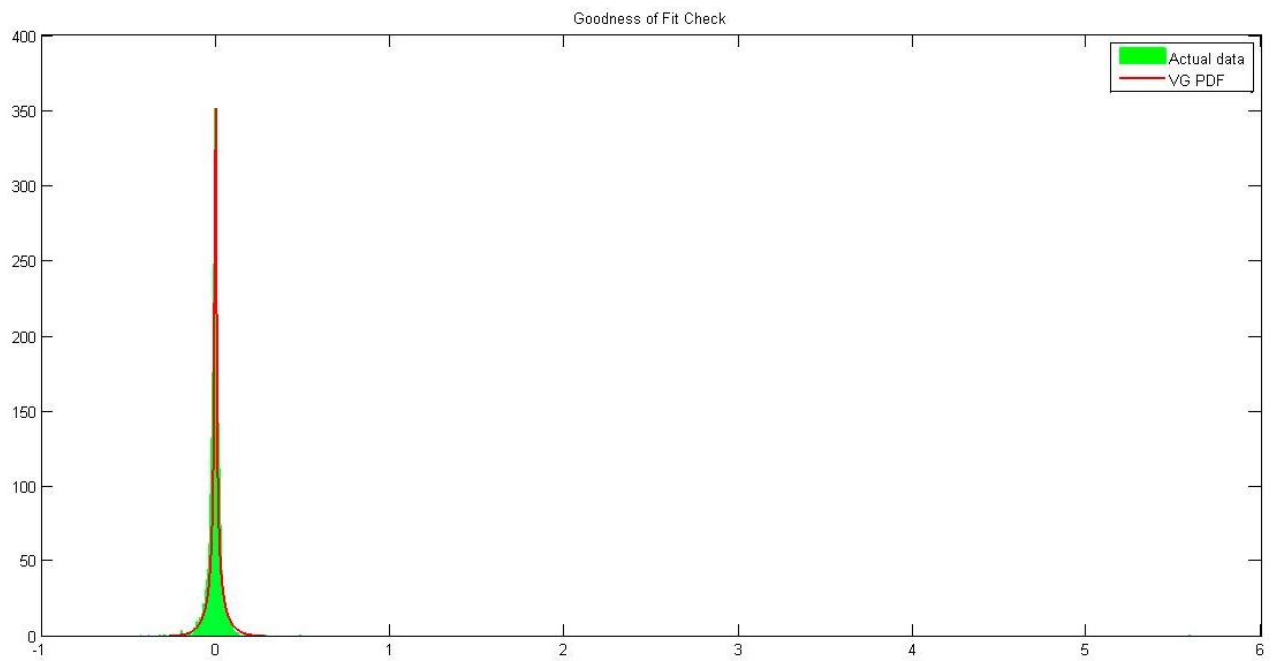


FIG. 3.1 Empirical data compared to the fitted VG pdf obtained with the estimated parameters

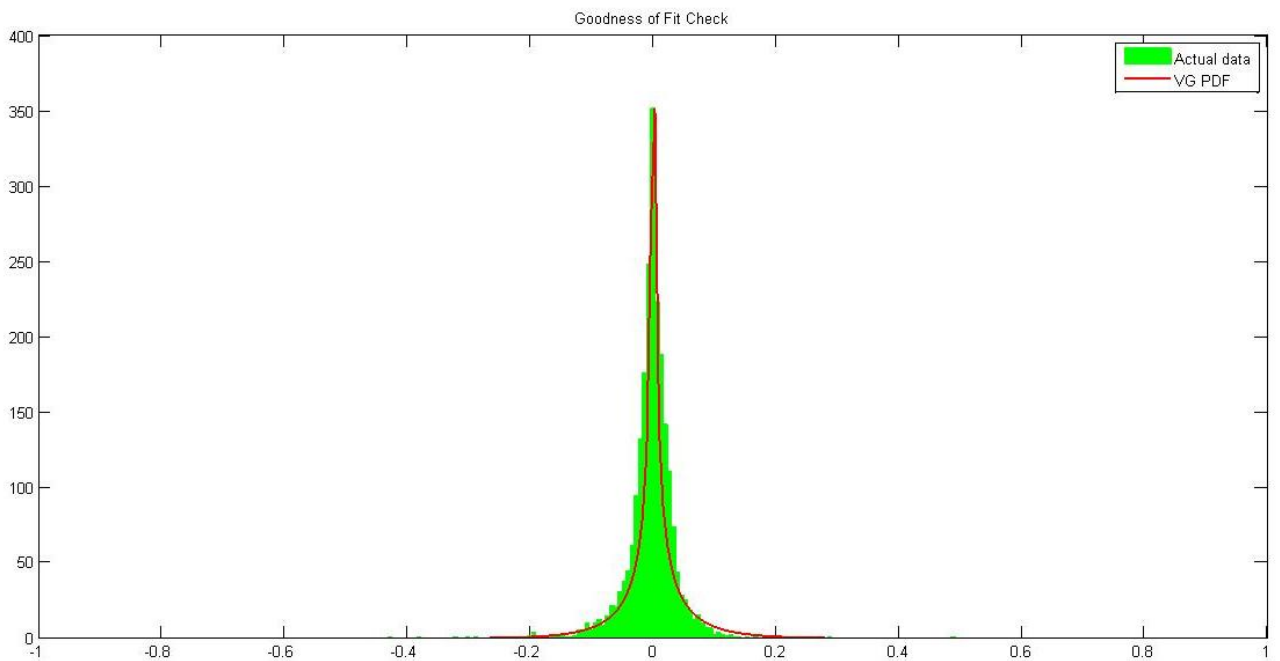


FIG. 3.2 Empirical data vs. fitted VG density, zoom-in on central data

Since the sample size is quite large ($N=2260$), we can use a normal approximation on the errors distribution in order to compute the confidence intervals on the parameters.

95% Confidence Interval	
$\hat{\sigma}$	[0.0478; 0.0480]
$\hat{\mu}$	$[-1.2624 \cdot 10^{-7}; 1.2614 \cdot 10^{-7}]$
$\hat{\theta}$	[0.000837; 0.000955]
$\hat{\alpha}$	[0.1877; 0.1882]

TABLE 3.2. Confidence intervals for the fitted VG parameters.

Chapter 4

The Brennan-Schwartz model

As we saw in the previous chapter, the VG model is very suitable for fitting the distribution of EUA prices. However, it is quite complex when it comes to analytical tractability. In this chapter, we will then analyze the same sample of EUA prices using another process, the Brennan-Schwartz (BS) one, simpler and more tractable, and then compare the convenience of using one model rather than the other.

4.1. Description of the model

The Brennan-Schwartz process belongs to the mean-reverting family. Such processes are named after the fact that they tend to drift towards its long-term mean value, and they do this with a certain speed of reversion. Mean reverting processes can take various forms, the one of the model in consideration is:

$$dP_t = k(\theta - P_t)dt + \sigma P_t dz$$

where P_t is the price in EUR of one ton of CO₂ (price of one EUA), k is the speed of reversion toward the mean, θ is the long run mean price level, σ is the volatility of the process and dz is the increment of a Wiener process.

This process is the so called Brennan-Schwartz process, from the names of the two authors who first used it to describe the interest rate path (Brennan, Schwartz (1980)²⁸), and it is the mean reversion process also chosen by Tsekrekos (2009) and Sarkar (2003).

Other choices belonging to the mean-reverting family could have been the famous Ornstein-Uhlenbeck (OU) process (or Vasicek model), $dP_t = k(\theta - P_t)dt + \sigma dz$, or its geometric version, $dP_t = k(\theta - P_t)P_t dt + \sigma P_t dz$, for example. However, the latter seems a less plausible process than the chosen one, since its drift is not a homogeneous function of degree one of the pair (P_t, θ) , as we would expect from a price process. In fact, if P_t is the price of one EUA, we expect that a number n of allowances reverts to a mean level $n\theta$. As for the former, the drift is indeed a homogeneous function of degree one of the pair (P_t, θ) , but the diffusion term is not. Instead, we want the variance to grow with P_t . Our selected process satisfies such properties.

4.2. Model calibration

As before, we must evaluate the parameters characterizing the price dynamics, using the maximum likelihood estimation method. In this case, the drawback of the selected process is that, unlike the OU process or the VG process, its transition density does not have a closed-form analytic expression. As a result, the exact ML method cannot be applied. To address this problem, we can first use an Euler scheme to approximate the general diffusion process by a discrete time model, and then apply the approximate ML method in order to find the parameter estimates.

According to the Euler scheme, the corresponding discrete model of our selected process is:

$$P_i = P_{i-1} + k(\theta - P_{i-1})\Delta t + \sigma P_{i-1}\sqrt{\Delta t} \eta_i$$

where $\eta_i \sim N(0,1)$. This implies that the transition probability density of P_i has the following expression:

²⁸ Brennan, Schwartz (1980). *Analyzing Convertible Bonds*. The Journal of Financial and Quantitative Analysis, 15, 4, Proceedings of 15th Annual Conference of the Western Finance Association, June 19-21, 1980, San Diego, California, 907-929.

$$p(P_i|P_{i-1}) \approx \frac{1}{\sqrt{2\pi\sigma_i^2}} \exp\left(\frac{-(P_i - \mu_i)^2}{2\sigma_i^2}\right) \quad (40)$$

where $\mu_i = P_{i-1} + k(\theta - P_{i-1})\Delta t$ and $\sigma_i = \sigma P_{i-1}\sqrt{\Delta t}$.

Now, according to the approximated ML method, and defining the vector of parameters by $\mathbf{\Lambda}$, the optimal vector of parameter estimators $\mathbf{\Lambda}^*$ is found by maximizing over $\mathbf{\Lambda}$ the joint density $\ell(\mathbf{\Lambda})$, equal to

$$\ell(\mathbf{\Lambda}) = p(P_0|\mathbf{\Lambda}) \prod_{i=1}^N p(P_i|P_{i-1}; \mathbf{\Lambda})$$

or, equivalently, by minimizing the function $\log \ell(\mathbf{\Lambda}) = -\ln \ell(\mathbf{\Lambda})$, given by

$$\log \ell(\mathbf{\Lambda}) = -\ln p(P_0|\mathbf{\Lambda}) - \sum_{i=1}^N \ln p(P_i|P_{i-1}; \mathbf{\Lambda})$$

Substituting,

$$\begin{aligned} \log \ell(k, \theta, \sigma; P_0, \dots, P_N) &= \sum_{i=0}^N \ln \sqrt{2\pi\sigma_i^2} + \sum_{i=0}^N \frac{(P_i - \mu_i)^2}{2\sigma_i^2} = \\ &= \frac{1}{2} \sum_{i=0}^N \ln(2\pi\sigma^2 P_{i-1}^2 \Delta t) + \sum_{i=0}^N \frac{(P_i - P_{i-1} - k(\theta - P_{i-1})\Delta t)^2}{2\sigma^2 P_{i-1}^2 \Delta t} = \\ &= \frac{N}{2} \ln \sigma^2 + \frac{1}{2} \sum_{i=0}^N \ln(2\pi P_{i-1}^2 \Delta t) + \frac{1}{2\sigma^2} \sum_{i=0}^N \frac{(P_i - P_{i-1} - k(\theta - P_{i-1})\Delta t)^2}{P_{i-1}^2 \Delta t} \end{aligned}$$

Now, to minimize this function, we must solve the following system of equations:

$$\begin{cases} \frac{\delta \log \ell}{\delta k} = 0 \\ \frac{\delta \log \ell}{\delta \theta} = 0 \\ \frac{\delta \log \ell}{\delta \sigma} = 0 \end{cases}$$

Which leads to the following parameter estimators:

$$\hat{\sigma} = \sqrt{\frac{1}{N} \sum_{i=0}^N \frac{(P_i - P_{i-1} - \hat{k}(\hat{\theta} - P_{i-1})\Delta t)^2}{P_{i-1}^2 \Delta t}}$$

$$\hat{k} = \frac{\sum_{i=0}^N \frac{(P_i - P_{i-1})(\hat{\theta} - P_{i-1})}{P_{i-1}^2}}{\sum_{i=0}^N \frac{(\hat{\theta} - P_{i-1})^2 \Delta t}{P_{i-1}^2}}$$

$$\hat{\theta} = \frac{\sum_{i=0}^N \frac{(P_i - P_{i-1})\hat{k}}{P_{i-1}^2} + \sum_{i=0}^N \frac{P_{i-1}\hat{k}^2 \Delta t}{P_{i-1}^2}}{\sum_{i=0}^N \frac{\hat{k}^2 \Delta t}{P_{i-1}^2}}$$

However, this method has a drawback: the Euler discretization offers a good approximation only when the frequency of data recording is at least daily or higher. In fact, the transition density obtained through the Euler approximation and the real transition density are equal for $\Delta t \rightarrow 0$ only, and thus it would be desirable to implement a bias reduction technique, such as the Indirect Inference (II) method²⁹.

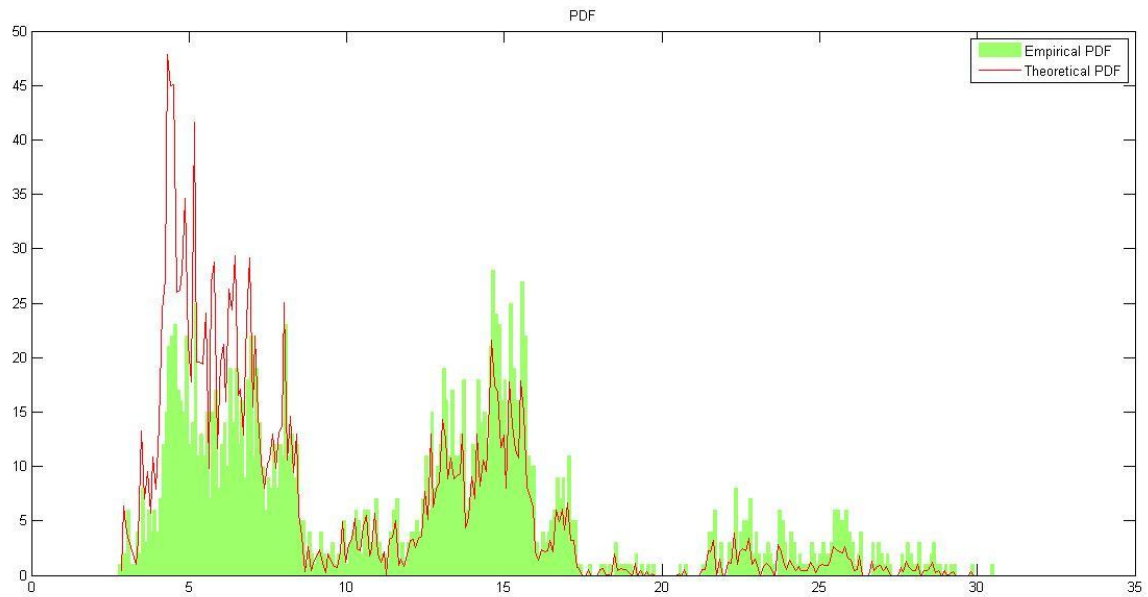
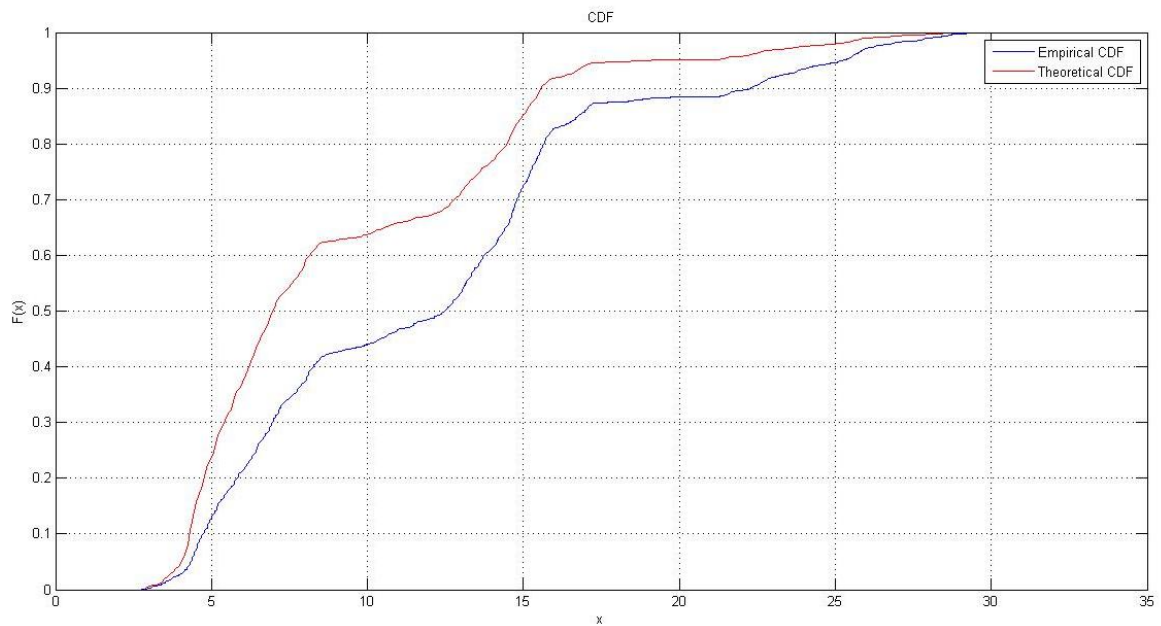
Nevertheless, in our case, the error due to the application of the Euler scheme (the so called *discretization bias*) should be quite low, given the daily frequency and the large sample size, thus we didn't perform a bias reduction procedure, considering the estimates we found through the approximate ML method to be enough for the purposes of this chapter.

The estimators obtained through the distribution fitting procedure are reported in Table 4.1.³⁰

²⁹ The II method is a simulation-based procedure, first introduced by Gouriéroux, Monfort and Renault (1993), which makes it possible to overcome the inconsistency problem of the approximate ML method, while keeping the good asymptotic properties typical of ML estimators (see Phillips, Yu (2006) as a reference).

³⁰ While performing the distribution fitting, we didn't take into consideration the whole sample of data, we just considered the second and third trading periods, thus avoiding the jump in prices which occurred between the first and second trading periods.

\hat{k}	$\hat{\theta}$	$\hat{\sigma}$
0.3640	8.38	0.5195

TABLE 4.1 Carbon BS parameter estimators**FIG. 4.1** EUA spot prices, theoretical PDF plotted against histogram of empirical data.**FIG. 4.2** EUA spot prices, theoretical CDF plotted against empirical one.

4.3. VG vs. BS comparison

In order to compare the models, let us first calibrate them on the same sample data. Since the BS model is not able to adequately explain the jump in prices occurring between the first and second ETS trading periods (the estimator of σ would return the incredibly high value of 87.62), we calibrate both models on the price data following the jump. The BS estimators are the ones reported in Table 4.1, while the VG estimated parameters are the following:

$\hat{\sigma}$	$\hat{\mu}$	$\hat{\theta}$	$\hat{\alpha}$
0.0318	4.60e-16	-7.55e-04	0.830

TABLE 4.2 Carbon VG parameter estimators

In order to compare different models, there are a number of model selection criteria, which consider goodness-of-fit and parsimony in order to declare which model is the best. Goodness-of-fit is generally determined using the likelihood approach, or an approximation of this, leading to a chi-squared test; parsimony is defined by the number of parameters in the model. In fact, additional parameters may lead to adapt the model shape to better fit the data, but sometimes too many parameters could lead to overfitting, causing poor predictive performance, since the model failed in generalizing the data trend.

A widely used model selection technique is the Bayesian Information Criteria (BIC), defined as:

$$BIC = -2(\log L) + numParam \cdot \log(n) \quad [10]$$

where $\log L$ is the maximized log-likelihood function, $numParam$ is the number of parameters in the model and n is the sample size. The “best” model has the lowest BIC.

In fact, having the lowest BIC means having the maximum likelihood and the least penalty for the number of parameters in the model.

The problem, though, is that, as obviously most criteria demand, the numerical values of the dependent variable must be identical for all models being compared. Instead, in our case, the VG model applies to log-returns, while the BS model explains prices. This means that, when evaluating the likelihood function, we will get values on different scales, which lead to BICs that cannot be compared. In fact, starting from the log-returns VG pdf, we are not able to derive the analytic expression of the prices pdf, and vice-versa as for the BS. Instead, what we can do is trying to compare the two models to another one, for which we know the distribution of both prices and log-returns. Such a model is, for example, the GBM. In the GBM, prices distribute log-normally, while log-returns have a Gaussian distribution. The results of the comparison are reported in Table 4.3.

	K	logL	BIC
VG	4	3687.40	-7345
GBM	2	3438.40	-6862
BS	3	-585.35	1193
GBM*	2	-606.39	1228

TABLE 4.3 Number of parameters (K), log-likelihood (logL) and Bayesian Information Criteria (BIC) for the EUAs. Note: in GBM, the logL function is evaluated on the log-returns distribution, while in GBM* the logL function is evaluated on the price distribution.

As we can see, when the likelihood function for GBM is evaluated on log-returns, the BIC value is comparable to the one we obtain when log-returns are modeled using a VG, and the same is valid when looking at BIC values found using BS and a normal distribution for prices. Looking at BIC values, both VG and BS perform better than the GBM, since their values are lower. However, even if we can tell they are both better than the GBM, we cannot rank them using BIC.

A possible idea in order to get a feeling of the models' performances is to try to forecast prices using both models through a Monte Carlo simulation. This can be done by creating a matrix whose rows represent different simulated price paths, and then taking the mean of each column in order to get a single path as a result of all the possible trajectories. Then, we analyze the root mean square error (RMSE), a measure of the difference between observed values and predicted ones, which should be as small as possible.

The results of the forecast are reported in Fig. 4.3.

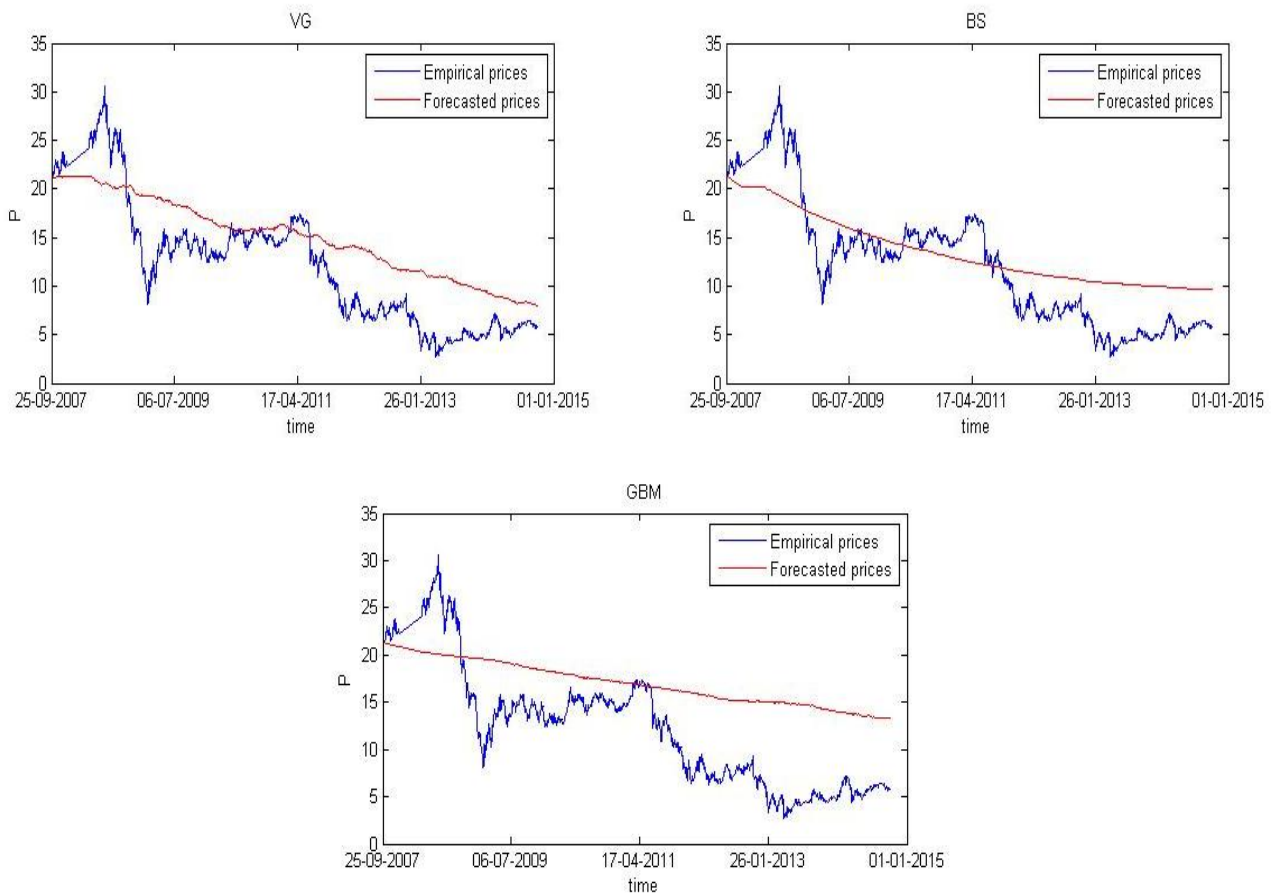


FIG. 4.3 EUA empirical prices vs. forecasted ones, simulated with a VG, BS, GBM process, respectively.

	RMSE
VG	2.84
BS	1.36
GBM	4.75

TABLE 4.4 Root mean square error (RMSE) for VG, BS, GBM processes

As we can see from Fig. 4.3, both VG and BS seem to predict the future trend of prices much better than the GBM. However, the RMSE for BS is slightly lower than the one for VG, suggesting a mild preference towards the BS model, when it comes to the ability of effectively forecasting data.

In conclusion, both models have their strengths and drawbacks. The VG model is able to accurately explain the distribution of log-returns, even when the process is fitted on the whole data sample, despite the shift in prices occurring between the first and second trading phase. However it is a quite complex model, and its analytical tractability is limited when it comes to solving option pricing problems. On the other hand, the BS model is not able to explain particular events such as large jumps occurring in prices, but it is simpler and more tractable. It also seems to be able to predict prices slightly more accurately.

Chapter 5

A real option valuation for a power plant switch

5.1. The investment project

In what follows, we will now focus on a real option problem, as a concrete application of the choice a firm faces when entering an ETS.

Our basic setting considers an oil-fired power plant with 10,000 kW capacity, located in Italy, which, under the current legislation, is obliged to surrender a certain amount of allowances, proportional to the tons of CO₂ it emits. Such a firm can thus choose whether to submit to the ETS framework or to completely switch the production process in order not to be subject to the aforementioned regulation anymore. Were it to choose this second option, a possible alternative to a fossil fuel facility could be to invest in a photovoltaic (PV) plant producing the same amount of electricity as the initial oil-fired plant. In this way, the electricity output would be the same, but the firm wouldn't have to face the cost of buying the required EUAs every year. This investment option the firm has is called a “real option” and its value can be computed in a very similar fashion to the way in which financial options' values are determined.

In order to support the relevance of the choice of the industry sector we've made, namely the sector of electricity production by means of fuel combustion, we refer the reader to the table reported in Appendix B.2, which shows the percentage of verified emissions produced by this sector with respect to the total emissions generated by all industry sectors. As we can see from the table, in each country the emission quota

imputable to this sector is fairly large with respect to the other ones (including, among others, production of coke, ferrous metals, aluminum, pulp, paper, pig iron and steel, nitric acid, ammonia and other chemicals, manufacture of glass, ceramics and mineral wool) , with Italy being no exception.

5.1.1. The oil-fired plant

These are the hypothesis we considered for our basic setting:

- Hp 1. The capacity of the oil-fired power station is 10 MW³¹;
- Hp 2. The plant is located in Italy;
- Hp 3. There's no initial investment (the oil-fired plant is already in function);
- Hp 4. The electricity price is denoted by $E(t)$, which is the price in EUR for each kWh of electricity;
- Hp 5. The residual lifetime of the plant is 25 years;
- Hp 6. The capacity factor³² is assumed equal to 80%³³;
- Hp 7. The efficiency of the plant is equal to 40%³⁴.

³¹ This capacity can appear rather low for an oil plant. The choice of such a value is for practicality reasons, so that it can be comparable to a big PV plant. On the other hand, the capacity choice does not really make the difference in our model, since the cost of kWh for PV plants above 1 MW is only slightly dependent on the plant dimensions.

³² The capacity factor is the ratio of a power station's actual generation to its maximum potential generation. Thus, it depends on the percentage of time a fleet of generators is run.

³³ This value represents the theoretical capacity factor of an oil-fired power station in good condition. The actual capacity factor of generators using petroleum is usually much lower, in a range of 10-20% over the 2014-2015 period (see http://www.eia.gov/electricity/monthly/epm_table_grapher.cfm?t=epmt_6_07_a as a reference for US utilities). This is due to the fact that, over the world, oil-fired generators are usually kept as peaking generators, while other types of generators, like nuclear ones, are used as baseload units, because of their very low variable costs. In our hypothetical scenario, oil-fired plants are for baseload production and thus the capacity factor is the theoretical one. In Italy there are some examples of fuel oil plants which have been running in full swing over the recent years: the Livorno Marzocco powerplant, Tuscany, operating since 1965, in 2007 had a capacity factor of 79% (see http://enipedia.tudelft.nl/wiki/Livorno_Powerplant).

³⁴ The efficiency of a power station is a percentage measure given by the ratio between the electricity produced and the heat energy needed in order to produce it. According to IEA (2008), the average efficiency of oil-fired electricity production in Italy, over the 2001-2005 period, was 41%. Such a value depends on the technology used and on the type of plant, where more advanced plants, such as the

Given such hypothesis, we can compute the total electricity produced each year by the plant, which is:

$$\text{Electricity produced} = 10,000 \text{ kW} \cdot 0.8 \cdot 365 \cdot 24 \text{ h} = 7.01 \cdot 10^7 \text{ kWh/year}$$

Using this data and the efficiency factor we stated above, we can then find the total energy needed every year in order to produce the aforementioned amount of electricity:

$$\text{Energy need} = \frac{\text{electricity produced}}{\text{efficiency}} = \frac{7.01 \cdot 10^7 \text{ kWh/year}}{0.4} = 1.75 \cdot 10^8 \text{ kWh/year}$$

To gain insight on how much fuel is actually consumed each year, we should consider that each different material has a peculiar calorific value, that is the specific amount of energy produced by the complete combustion of one unit mass of such material. Crude oil, which is what we're combusting in our oil plant in order to obtain electricity, has a calorific value of about 42.5 MJ/kg, namely 11,800 kWh/ton. Using this data, we can compute the number of tons of crude oil which is employed each year:

$$B = \text{tons of oil per year} = \frac{\text{energy consumption}}{\text{calorific value of oil}} = \frac{1.75 \cdot 10^8}{11,800} = 1.48 \cdot 10^4 \text{ tons/year}$$

Now that we know the total consumption of oil per year, we must find the corresponding quantity of CO₂ which is emitted in response to such a consumption.

The default CO₂ emission factor for crude oil, as stated by IPCC (Intergovernmental Panel on Climate Change)³⁵, is 73,300 kg/TJ. Since 1 kWh equals 3.6 MJ, we have:

$$\begin{aligned} \text{CO}_2 \text{ emission factor} &= 73.3 \text{ tons/TJ} = 73.3 \cdot 10^{-6} \text{ tons/MJ} = \\ &= 73.3 \cdot 10^{-6} \cdot 3.6 \text{ tons/kWh} = 2.64 \cdot 10^{-4} \text{ tons/kWh} \end{aligned}$$

Multiplying this factor by the energy consumption we found above, we obtain the total CO₂ emissions per year produced by our plant:

$$X = \text{CO}_2 \text{ emissions per year} = 46,200 \text{ tons}$$

combined cycle ones, experience higher efficiency rates compared to more traditional technologies, such as the steam generator. For ease of calculation, we took 40% as a proxy.

³⁵IPCC 2006, *2006 IPCC Guidelines for National Greenhouse Gas Inventories*, prepared by the National Greenhouse Gas Inventories Programme, Eggleston H.S., Buendia L., Miwa K., Ngara T., and Tanabe K. (eds). Published: IGES, Japan.

To complete the overview of our oil-fired plant, we must point out that, in order to properly function, it will require a certain amount of operating costs, Op , which we assumed equal to 0.5 million € per year³⁶. Finally, if we decide to shut down the facility, we will incur some decommissioning expenses³⁷ equal to $c_1 = 1$ million €.

5.1.2. The PV plant

Our environmentally friendly alternative to fossil fuel combustion, in order to produce electricity, is to invest in a PV plant. In order to obtain the same yearly output³⁸ we had before, we want the annual amount of electricity produced to be equal to $7.01 \cdot 10^7$ kWh. The average PV plant lifetime, based on current technical level, is $T_{pv} = 25$ years³⁹, thus the total electricity produced is equal to:

$$Q = \text{electricity produced during lifetime} = 7.01 \cdot 10^7 \text{ kWh} \cdot 25 = 1.75 \cdot 10^9 \text{ kWh}$$

In order to properly define the cost necessary to build the plant, we must now introduce what is called Levelised Cost Of Electricity (LCOE).

³⁶ According to the EIA website (http://www.eia.gov/electricity/annual/html/epa_08_04.html), the operation and maintenance expenses for oil plants over the 2003-2013 period varied in a range of 0.53-0.89 \$cent/kWh. Using the average value expressed in euro-cents/kWh and considering the total electricity output of our plant, we obtained a value of about 450,000 € per year. We took EUR 0.5 million as a proxy.

³⁷ As for decommissioning costs, since there is not much disclosure about the actual expenses, we rely on a decommissioning plan of a biomass cogeneration plant in Foggia, Italy (available at http://www.ambiente.provincia.foggia.it/attachments/article/201/10-625-SAG-S-002_01_%20Relazione%20Dismissione.pdf). Even if it is a type of plant different from the one we are analyzing, the cost items in case of divestment are very similar. The scope of the expense depends very much on the size of the plant, related to the capacity. The biomass plant has a 25 MW capacity, while our plant has less than half the capacity. Since the estimated decommissioning cost of the Foggia plant is 2,300,000 €, we estimated a 1 million € expense for our plant.

³⁸ In order to get the same output we produced before in terms of electricity, we must install a capacity far superior to the one we had previously (10 MW). In fact, the theoretical capacity factor for PV plants is significantly lower than the one of oil-fired plants, on the order of 10-20% as for Italy, depending on the location, solar insolation and weather.

³⁹ IEA (2014). *Technology Roadmap: Solar Photovoltaic Energy*. OECD/IEA, Paris.

5.1.3. The Levelised Cost Of Electricity

The LCOE is an indicator summarizing the various costs of building and operating a generating plant over an assumed financial life.

Its value is usually time-dependent, since the cost of electric and other components, fuel, financing and maintenance varies with time. This is especially true in our PV plant case, since PV technology benefits from the so called learning curves. Such curves, in economics, were first theorized by Wright (1936) and explain the behavior of one economic variable with respect to another according to a power law, namely varying the dependent variable (proficiency) as a power of the independent one (experience). If we use the unitary cost as a proxy for cumulated experience and consider cumulated production as dependent variable, inverting the relation we have:

$$C_n = C_0 N^a$$

where C_n is the n^{th} unit cost, C_0 is the cost necessary to produce the first unit, N is the cumulated production and a is the learning curve coefficient (typically $a < 0$).

If we consider our LCOE as the unit cost C_n , the pattern according to which it decreases with time can be seen as a decreasing exponential, as shown in Biondi and Moretto (2013)⁴⁰. We thus obtain:

$$\frac{dLCOE_t}{LCOE_t} = \alpha_c dt$$

or, equivalently:

$$LCOE_t = LCOE_0 e^{\alpha_c t}$$

where $\alpha_c = a \cdot growth$, that is the product between the learning curve coefficient and the average growth rate of the PV industry ($\alpha_c < 0$, since $a < 0$).

In order to define some possible values for these parameters and for the initial value $LCOE_0$ in the equation, we need to better understand the components of the LCOE and the current state of affairs of the PV industry.

⁴⁰ Biondi, Moretto, 2014. *Solar Grid Parity Dynamics in Italy: a Real Option Approach*. Energy (2014), <http://dx.doi.org/10.1016/j.energy.2014.11.072>

As outlined before, the LCOE is a synthetic indicator which depends on a number of factors, including the price of PV modules, the price of other electrical components, the capacity factor of the plant, assembly and installation costs, ongoing maintenance, insurance costs and decommissioning costs, while (in our case) it does not include volatile and variable components, such as subsidies or government incentives. It is a tool used to compare the unit costs of different power generation technologies, considering the lifetime generated electricity and costs, to estimate a price per unit of electricity produced⁴¹.

As we said, this unitary cost decreases with time, mainly thanks to technological improvement (causing decreasing pricing of system components (= decreased costs) and increased efficiency of solar modules (= increased production)). In order to come across a possible value for $LCOE_0$, taking as a reference year $t_0 = 2014$, we must have an idea of the magnitude of each cost we'll incur and of the full load hours (FLH) characterizing the location in which our ground-mounted plant will be built on.

Since the plant will be built in North/Central Italy, we assume an average FLH value of 1250 kWh/kW, which corresponds to a 14.3% capacity factor (see Fig. 5.1). As for the costs estimates, we rely on a 2015 Fraunhofer ISE study⁴², which estimated each component impacting on the total investment cost for the year 2014. The study considers a 1 MW PV utility plant in Germany, and we decided to take its results as a proxy, even if they probably slightly overestimate our costs, since our larger plant would benefit more from the economies of scale.

⁴¹ It is found according to this formula:

$$\sum_{t=1}^N \frac{Electricity_t \cdot LCOE}{(1+r)^t} = \sum_{t=1}^N \frac{Capex_t + Opex_t + Insurance_t}{(1+r)^t}$$

where $Capex_t$ represents the annualized capital expenditures, $Opex_t$ the yearly operating and maintenance costs, $Insurance_t$ the annual insurance cost, N the economic lifetime of the plant, r is the discount factor, assumed constant at 5%, and $Electricity_t$ is the amount of electricity produced each year by the plant.

⁴² Fraunhofer ISE, 2015. *Current and Future Cost of Photovoltaics. Long-term Scenarios for Market Development, System Prices and LCOE of Utility-Scale PV Systems*. Study on behalf of Agora Energiewende.

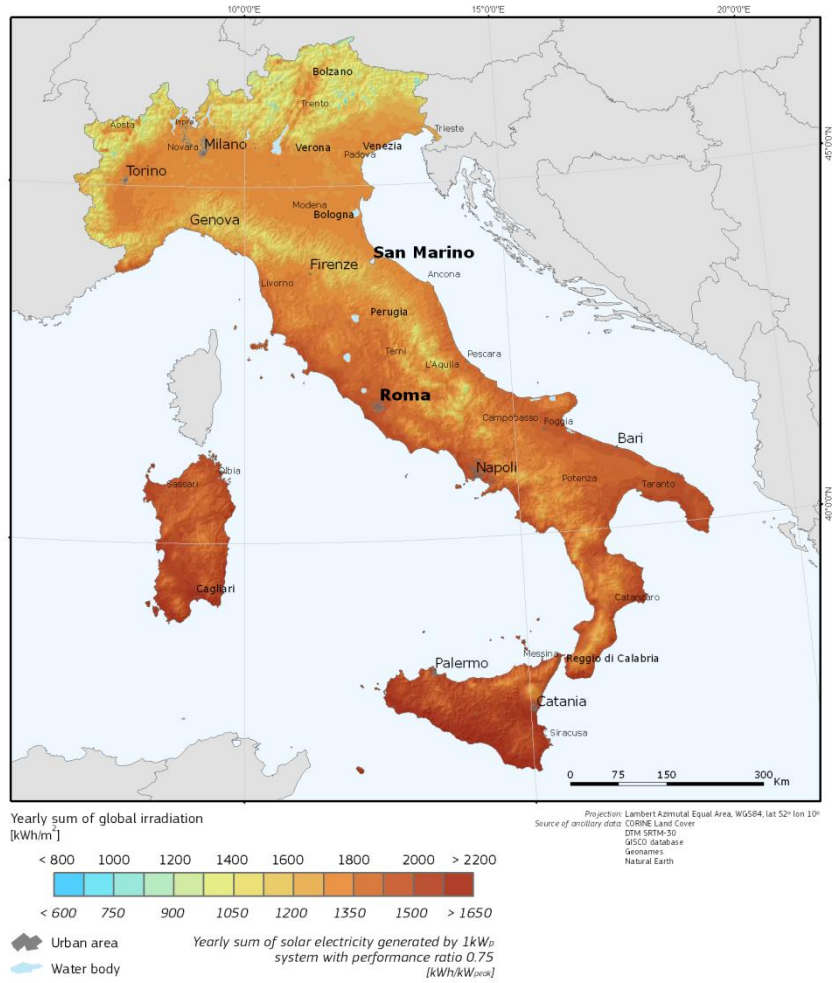


FIG. 5.1 Global irradiation and solar electricity potential, optimally-inclined photovoltaic modules. Source: PVGIS © European Union, 2001-2012.

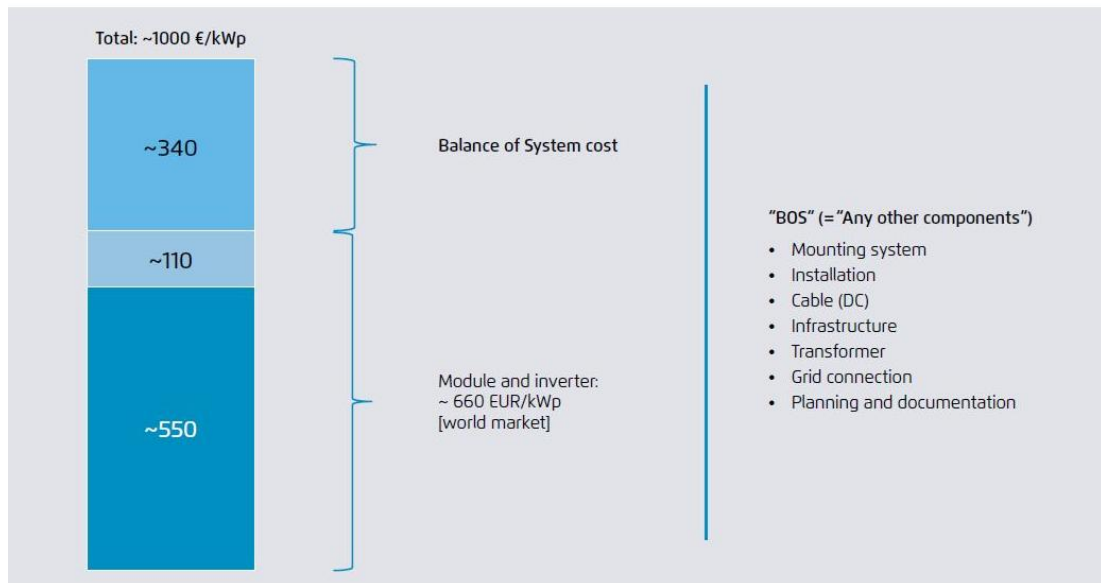


FIG. 5.2 2014 capital expenditures for a ground-mounted PV system. Source: Fraunhofer ISE, 2015. *Current and Future Cost of Photovoltaics. Long-term Scenarios for Market Development, System Prices and LCOE of Utility-Scale PV Systems.* Study on behalf of Agora Energiewende.

As we can see in Fig. 5.2, the modules have the larger share of the capital expenditures, which also include the inverter, transformer and mounting system costs, installation, cabling, grid connection, planning and infrastructure costs.

The study then considers a 20 EUR/kW operating expenditure (to which we added a 10 EUR/kW insurance expenditure), a WACC ranging from 5% to 10% (given the large scale of our plant we've decided to use a 5% discount rate), a reduction in production of 0.2% per year, due to the degradation of solar modules, and a system lifetime of 25 years. However, the inverter will need to be replaced in 15 years, since its economic lifetime is supposed to be shorter, and this leads to an additional cost, which has been included as well.

As we can see in Table 5.1, the $LCOE_{2014}$ resulting from all these assumptions is equal to 0.087 EUR/kWh (if we used a 10% WACC we could see the results are quite in line with the 2014 estimates for PV plants reported in the Bloomberg New Energy Finance 2015 factbook⁴³, where a 10% discount factor was considered). The calculation have been made using the Excel[®] spreadsheet provided by the author of the aforementioned study⁴⁴.

Discount rate	Plant lifetime	Capacity factor	Capex €/kW	Opex €/kW year	Insurance €/kW year	$LCOE_{2014}$ €/kWh
5%	25	14.3%	1,055	20	10	0.087
10%	25	14.3%	1,055	20	10	0.120

TABLE 5.1 Assumptions and results for $LCOE_{2014}$

As regards the parameter α_C , in order to compute it, we need to find some possible values for the average growth rate of the PV industry and for a , the learning coefficient. To better define such learning coefficient, we label PR (progress ratio) as the cost improvement at each doubling of cumulated capacity, that is, $PR = 2^a$ (in fact, recall

⁴³ Bloomberg New Energy Finance, 2015. *Sustainable Energy in America: 2015 Factbook*. London, UK: Bloomberg New Energy Finance; Washington, DC: The Business Council for Sustainable Energy.

⁴⁴ Agora Energiewende (2015): Calculator of Levelized Cost of Electricity for Photovoltaics; www.agora-energiewende.org/pv-cost.

that $\frac{C_n}{C_0} = N^a$). Equivalently, $a = \frac{\ln PR}{\ln 2}$. The learning coefficient a can be found analyzing the historical data on the PV module prices plotted against cumulated production on a logarithmic scale and computing the angular coefficient of the regression line.

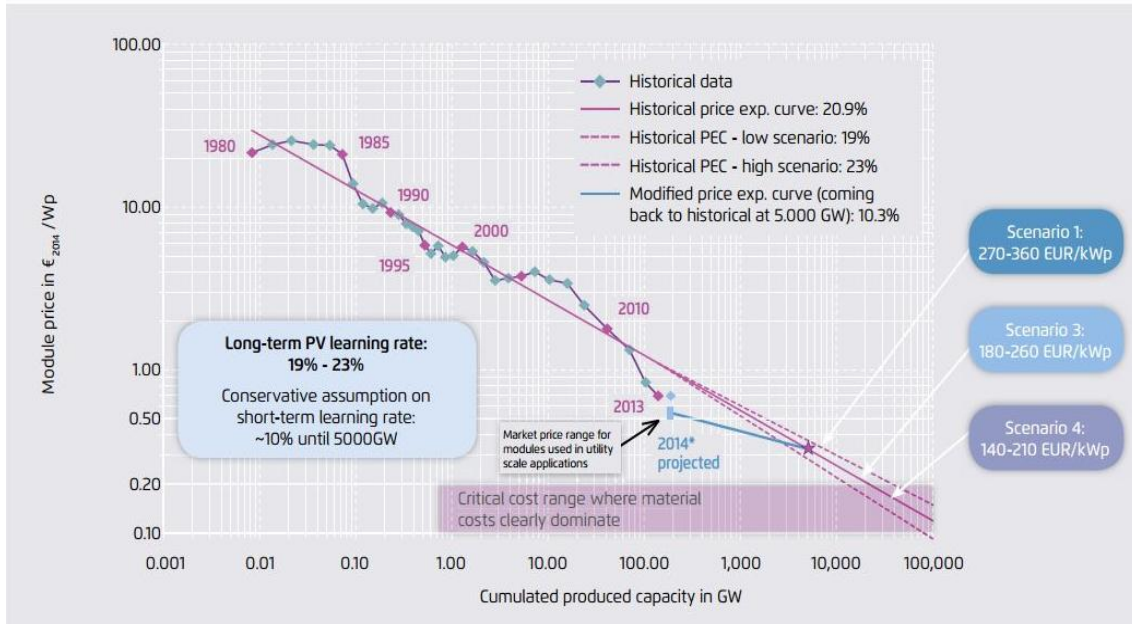


FIG. 5.3 Price of solar modules and experience curve. Source: Fraunhofer ISE, 2015. *Current and Future Cost of Photovoltaics. Long-term Scenarios for Market Development, System Prices and LCOE of Utility-Scale PV Systems.* Study on behalf of Agora Energiewende.

In fact, as we can see in Fig. 5.3, power law functions have the property that, when plotting the logarithm of proficiency (cumulated production) against the logarithm of experience (the unitary cost C_n), the result is a straight line. The slope of such straight line is a , which expresses the percentage decrease in the logarithm of the unitary cost at the increasing of the log-cumulated production. In order to know the relationship which directly links the variation of the unit cost at each doubling of cumulated capacity, let's now introduce the learning rate (LR). According to the 2015 Fraunhofer ISE study estimates, the learning rate ranges between 0.19 and 0.23. We take the average 0.21 as a proxy. This means that, each time the cumulated capacity doubles, the unitary cost C_n will decrease by 21%. In such a way:

$$PR = \frac{C_n}{C_0} = \frac{C_0(1 - 0.21)}{C_0} = 1 - LR = 0.79$$

This leads to $a = \frac{\ln 0.79}{\ln 2} = -0.34$.

As for the growth rate of the PV industry, there are different forecasts, based on the degree of optimism of future scenarios. According to the aforementioned 2015 Fraunhofer ISE study on the PV market, in a pessimistic scenario the 2015-2050 CAGR will be 5%, in the intermediate scenario it will be 7.5%, while, in the optimistic one, the growth rate will be 10%. Such low growth rates, compared to the historical 44% growth of 2000-2013, are justified by the fact that the market, in the future period considered, will not be as relatively young as it has been until now, and will not be able to sustain such high growth rates anymore. However, since this is a global estimate, let's have a look at more local forecasts, relative to the market in which we're operating (the Italian one). According to an European Commission publication⁴⁵, the solar market in Italy will grow by 7.3% in the period 2015-2030. Even this estimate is in line with the more moderate growth trend projected for the future, so we take as a proxy for *growth* 7.5%.

We thus obtain that

$$\alpha_c = a \cdot growth = -0.025$$

Finally, the LCOE(t) function, expressed in €/kWh, is given by the following equation:

$$LCOE_t = 0.087 e^{-0.025 t}$$

where t is the time expressed in years starting from 2014.

This is the equation according to which our cost of electricity production will evolve during time.

Updating last equation for $t_0 = 2015$ as a starting time, we obtain:

$$LCOE_t = 0.085 e^{-0.025 t}$$

⁴⁵ European Commission, 2010. *EU Energy Trends to 2030*. Luxembourg: Publications Office of the European Union.

Then we can compute the total cost of building the plant now, just multiplying the $LCOE_{2015}$ by the total electricity output we're expecting to produce over the lifetime of the PV plant:

$$\text{Cost of building the plant now} = Q \cdot LCOE_{2015} = 1.48 \cdot 10^8 \text{ EUR}$$

5.2. The variables involved

5.2.1. The carbon price

As we saw in the past chapters, the carbon price has a peculiar distribution, which we modeled first through a VG process and then using a BS model. Both models demonstrated to have their advantages and limitations, when compared.

In this chapter, our aim is to price the real option in an analytical way. Because of this, we now choose to perform the valuation using the BS model rather than the VG one. In fact, it is not possible (to the best of our knowledge) to find a closed-form expression of the option value if one of the underlying components follows a dynamics such as the VG one. Instead, with a relatively simpler model such as the BS, we will be able to analytically solve the real option valuation problem.

5.2.2. The LCOE

As we saw in section 5.1.3, the LCOE is time-dependent, thus it is one of the variables involved in our real option problem. Since LCOE represents the unit cost for each kWh, the total investment cost of our plant over the years is found multiplying the LCOE by the total electricity our plant will produce during its economic life, taking as base year $t = 2015$:

$$\text{Total cost of PV project} = Q \cdot LCOE_t = 1.48 \cdot 10^8 \cdot e^{-0.025 t}$$

There is another variable playing a relevant role in the decision to invest, namely the oil price.

5.2.3. The oil price

Oil is a commodity traded on financial markets, whose price varies stochastically over time. For the purposes of this chapter, since we're more interested in investigating the effects of a stochastically varying carbon price rather than the ones given by the oil price variations, we'll assume a far simpler dynamics for our fuel. Specifically, we model the oil price by a deterministic process, as follows:

$$dD_t = \alpha_D D_t dt$$

Or, equivalently,

$$D_t = D_0 e^{\alpha_D t}$$

where D_t represents the price (in EUR) for each ton of oil at time t , D_0 is the current oil price ($t_0 = 2015$) and α_D is a parameter to be fitted on historical data.

Analyzing the West Texas Intermediate (WTI) crude oil historical spot prices and using the maximum likelihood (ML) estimation method, we can find a value for α_D . Our curve fitting procedure returns the following value for the estimator:

$$\alpha_D = 0.0777$$

The red line in Fig. 5.4 represents the curve fitted to oil prices. As we can see, the exponential curve seems to be a good fit to our data and to capture, to some extent, the overall trend of oil prices. Nevertheless, the high volatility of oil prices during the last ten years leads to uncertainty over future scenarios. For instance, estimating α_D using different time samples, we obtain different results. Even though the most likely estimate is the previous one, in the final part of this thesis we will also take into consideration the other estimates reported in Table 5.2.

Time range	$\hat{\alpha}_D$
1986-2015	0.0777
2008-2015	0.0271
2009 (Oct.)-2015	0.0005

TABLE 5.2 Oil parameter estimator for different time ranges

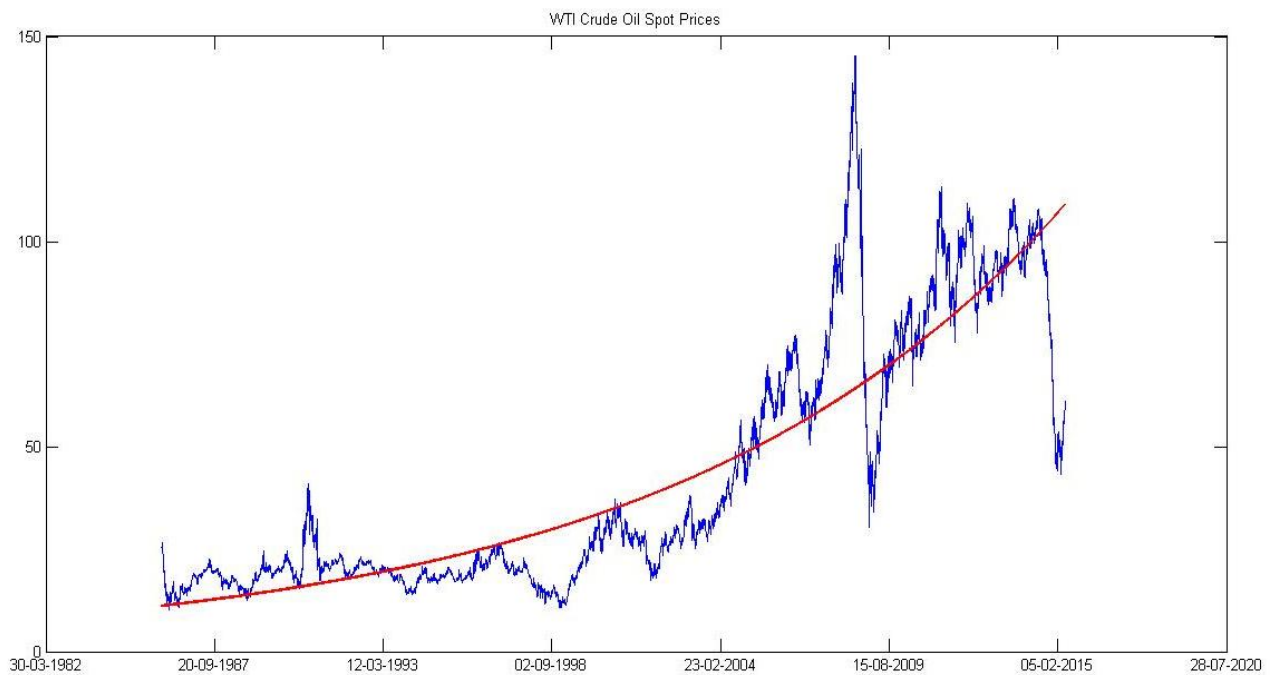


FIG. 5.4 Oil spot prices 1986-2015 in USD/barrel, real and fitted curve.

5.2.4. Benefits and costs deriving from switching

When we decide to switch to the clean energy plant, we face some annual benefits and costs and some sunk costs, that are costs which, once incurred, are not recoverable, thus making the investment irreversible.

For the sake of clarity, we report the three dynamics of the variables influencing our costs and benefits:

$$dC_t = \alpha_C C_t dt \quad (5.1)$$

$$dD_t = \alpha_D D_t dt \quad (5.2)$$

$$dP_t = k(\theta - P_t)dt + \sigma P_t dz \quad (5.3)$$

where in (5.1) we wrote C in lieu of $LCOE$, while (5.2) and (5.3) represent the process for the oil and carbon price, respectively.

The sunk or irreversible costs we incur when we decide to switch type of plant are: the decommissioning costs c_1 (= 1 million €) and the total cost of the PV project, $Q \cdot C_t$, which depends on time. We call such sunk costs K :

$$\begin{aligned} K(t) &= c_1 + Q \cdot C_t = \\ &= c_1 + Q \cdot C_0 \cdot e^{\alpha_C t} \\ &= 10^6 + 1.48 \cdot 10^8 \cdot e^{-0.025 t} \end{aligned}$$

The annual benefits we get by switching include:

- savings deriving from not having to buy oil anymore = $\int_t^{T_{pv}+t} B D_t e^{-\mu_D(s-t)} ds$
- savings deriving from not having to buy the allowances = $\int_t^{T_{pv}+t} X P_t e^{-\mu_P(s-t)} ds$
- savings from not having to manage the oil plant = $\int_t^{T_{pv}+t} Op \cdot e^{-r(s-t)} ds$

In fact, as we recall, the oil-fired plant has annual operating costs $Op = 0.5 \cdot 10^6$ €, the number of tons of oil per year used in order to power the plant is $B = 1.48 \cdot 10^4$ tons/year, the number of tons of CO₂ emitted every year by the oil plant is $X = 46,200$ tons, while the lifetime of the PV plant is $T_{pv} = 25$ years. The risk-free rate, r , is assumed to be equal to 5%. The two other discount rates, μ_D and μ_P , are the risk-adjusted discount rates required by an investor in the oil and in the EUA markets, respectively. For the sake of simplicity, in what follows we will assume them both equal to the risk free rate, r .

The annual electricity output remains the same before and after the switch, therefore it has no effects on benefits nor costs. Thus, the benefits are equal to:

$$\begin{aligned}
\Phi(D_t, P_t, t) &= \int_t^{T_{pv}+t} BD_t e^{-r(s-t)} ds + \int_t^{T_{pv}+t} XP_t e^{-r(s-t)} ds + \int_t^{T_{pv}+t} Op \cdot e^{-r(s-t)} ds = \\
&= [1 - e^{-r(T_{pv})}] \left(\frac{B}{r} D_t + \frac{X}{r} P_t + \frac{Op}{r} \right) = \\
&= [1 - e^{-0.05(25)}] \left(\frac{1.48 \cdot 10^4}{0.05} D_t + \frac{46,200}{0.05} P_t + \frac{0.5 \cdot 10^6}{0.05} \right)
\end{aligned}$$

In the expression above, recall that $D_t = D_0 e^{\alpha_D t}$, so that $\Phi(D_t, P_t, t) = \Phi(P_t, t)$, where α_D assumes the value we fitted in paragraph 4.2.2., 0.0777. As of the time of writing, the crude oil price is 58.88 \$/barrel, so, in the calibration of the model, we will use this value as D_0 (expressed in €/ton). Instead, we will keep the estimated exponential factor α_D in order to define the speed at which the oil price will increase in the future.

As we said, as of the time of writing, the crude oil price is 58.88 \$/barrel, while the EUA price is 7.25 €/ton (as of 05/22/2015). Converting the oil price into €/ton as well, and filling the formulas above with these values, we find the corresponding values for Φ and K :

$$\Phi = 0.93 \cdot 10^8 \text{ EUR}$$

$$K = 1.49 \cdot 10^8 \text{ EUR}$$

At this point one could think that it would be convenient switching to PV technology as soon as $\Phi(D_t, P_t, t) > K_t$. This conclusion would in fact miss an important point, as we will see in what follows.

5.3. The option value

As we saw, there are : 1) uncertainty over the future profits; 2) irreversibility (presence of some sunk costs) and 3) the possibility to postpone our investment decision. These

three conditions together suggest that a simple DCF analysis would not be adequate enough to assess the value of our investment, as it would miss considering the value of flexibility. In fact, the opportunity we have to switch the production process and to invest in a clean energy plant is a real option and it can be given a value, as shown in the seminal text by Dixit and Pindyck (1994)⁴⁶ on real option theory. Like financial options, real options give their owner the right, but not the obligation, to do something, specifically to undertake certain business activities. In the same way as a financial call option gives the owner the right to buy the underlying asset, the real call option gives the owner the right to invest in the underlying project. This right has a price, and must be considered when deciding when it is optimal to make the investment.

The option value is given by:

$$F(P_t, D_t, t) = \max_{\tau} E [e^{-\mu(\tau-t)} (\Phi(D_t, P_t, t) - K_t)]$$

where μ is the risk-adjusted discount rate of this type of investment and the maximum is taken over all stopping times τ with $t < \tau < T$, where T is the residual lifetime of the oil plant, 25 years. As we can see from this formulation, this is an American-style real call option, in that it can be exercised at any time τ prior to maturity.

In the remaining part of this chapter, we will show how to find such a value in an analytical way.

5.3.1. Analytical solution of the real option problem

As Dixit and Pindyck (1994) explain, to find the value of a real option, we could either use dynamic programming or the contingent claims analysis. Here, the first step we take in order to find the option value is using the contingent claims analysis. Contingent claims are assets whose value depends upon the price of at least another asset, like our real option value does. Merton (1977) showed that any contingent claim could be described by a peculiar PDE, subject to specific boundary conditions. He computed the PDE using arbitrage arguments, nevertheless, he also showed that such PDE remained valid even if arbitrage was not allowed. This enables us to find a value even for assets

⁴⁶ Dixit, Pindyck, 1994. *Investment Under Uncertainty*. Princeton, N.J.: Princeton University Press.

which are not traded, like assets and options incorporated in real investment projects. Contingent claims analysis consists in constructing a riskless replicating portfolio of existing traded assets able to indeed replicate the return of the claim we're trying to give a value. Being riskless, such a portfolio must earn a risk-free rate of return.

Since the hedging portfolio must consist of the underlying assets, the contingent claim and riskless bonds, in the case of real options it is usually difficult to make such portfolio riskless, since the assets of which it is made of are not usually traded. The solution to this problem consists in looking for actively traded assets which are perfectly correlated to the ones included in the portfolio. However, even this task could be challenging. Yet, since we're interested only in the assets' market equilibrium rates of return, a way to overcome the problem is to use an asset pricing model such as the CAPM in order to find such returns.

Let's put into practice what we said above. Since in this chapter we're considering oil price as deterministic and not stochastic, $F(P_t, D_t, t) = F(P_t, t)$. By Itô's lemma, we have⁴⁷:

$$\begin{aligned} dF(P_t, t) &= F_P dP_t + \frac{1}{2} F_{PP} (dP_t)^2 + F_t dt = \\ &= \left[\frac{1}{2} \sigma^2 P_t^2 F_{PP} + k(\theta - P_t) F_P + F_t \right] dt + \sigma P_t F_P dz \end{aligned}$$

From this equation, and knowing that the expected capital gain is $E[dF(P_t, t)]/dt$, we can find the expected rate of return, equal to:

$$E[R] = \frac{\frac{1}{2} \sigma^2 P_t^2 F_{PP} + k(\theta - P_t) F_P + F_t}{F}$$

and its standard deviation:

$$\sigma(R) = \frac{\sigma P_t F_P}{F}$$

According to the CAPM,

⁴⁷ In the expression and in what follows, $F_P = \frac{\delta F}{\delta P}$, $F_{PP} = \frac{\delta^2 F}{\delta^2 P}$, $F_t = \frac{\delta F}{\delta t}$ and $\Phi_P = \frac{\delta \Phi}{\delta P}$.

$$E[R] = r + \lambda\rho\sigma(R) \quad (5.4)$$

where λ is the market price of risk and is equal to $\frac{E[R_m]-r}{\sigma_m}$, r is the risk-free rate, ρ is the correlation between the market and the asset we're considering, $E[R_m]$ is the expected return given by the market and σ_m is its standard deviation.

Substituting the expected return of our asset and its standard deviation into (5.4), we get:

$$\frac{1}{2}\sigma^2 P_t^2 F_{PP} + k(\theta - P_t)F_P + F_t = rF + \lambda\rho\sigma P_t F_P$$

Rearranging,

$$\frac{1}{2}\sigma^2 P_t^2 F_{PP} + [k(\theta - P_t) - \lambda\rho\sigma P_t]F_P + F_t = rF \quad (5.5)$$

subject to:

$$\lim_{P \rightarrow +\infty} F(P_t, t) = +\infty \quad (5.6)$$

$$\lim_{t \rightarrow +\infty} F(P_t, t) = +\infty \quad (5.7)$$

$$\lim_{P \rightarrow 0^+} F(P_t, t) = 0 \quad (5.8)$$

The first two boundary conditions are given by the fact that, when the price of the allowances goes to infinity, the option value becomes infinite too and the same happens when time goes to infinity. In fact, recall that $C_t = C_0 e^{\alpha_C t}$ and $D_t = D_0 e^{\alpha_D t}$ and that $\alpha_C < 0$, while $\alpha_D > 0$. Thus, as time approaches infinity, according to the dynamics we defined, the price of oil goes to infinity too, while the LCOE tends to zero. The boundary condition (5.8) is instead given by the fact that, being the price of the EUAs the only source of uncertainty, the option value tends to zero as the price of the allowances approaches zero as well.

The base case: $D_t = D_{2015}$ and $LCOE_t = LCOE_{2015}$

Before analytically solving the problem as we presented it, let's reduce it at its simplest form, namely allowing for one variable only, the price of the allowances, and

considering everything else as a constant. This means that we consider the oil price to always remain at the current value, $D_t = D_{2015}$, as well as the LCOE, $C_t = C_{2015}$. In this base case, in order to find the analytical solution, we will follow the procedure described by Tsekrekos (2009)⁴⁸.

With D_t and C_t constant, the PDE in (5.5) reduces to:

$$\frac{1}{2}\sigma^2 P_t^2 F_{PP} + [k(\theta - P_t) - \lambda\rho\sigma P_t]F_P = rF \quad (5.9)$$

subject to (5.6) and (5.8).

We can rewrite the PDE as follows:

$$P_t F_{PP} + \frac{2}{\sigma^2 P_t} [k(\theta - P_t) - \lambda\rho\sigma P_t] F_P - \frac{2r}{\sigma^2 P_t} F = 0$$

$$P_t F_{PP} + \left[\frac{2k\theta}{\sigma^2 P_t} - \frac{2(k+\lambda\rho\sigma)}{\sigma^2} \right] F_P - \frac{2r}{\sigma^2 P_t} F = 0 \quad (5.10)$$

In order to solve it, let's now introduce a particular function, called confluent hypergeometric function. In mathematics, this function is known to be solution to the general confluent hypergeometric differential equation, as we can see in Abramowitz and Stegun (1972)⁴⁹. Such equation is given by:

$$w''(z) + \left[\frac{2A}{z} + 2f'(z) + \frac{bh'(z)}{h(z)} - h'(z) - \frac{h''(z)}{h'(z)} \right] w'(z) + \left[\left(\frac{bh'(z)}{h(z)} - h'(z) - \frac{h''(z)}{h'(z)} \right) \right. \\ \left. \left(\frac{A}{z} + f'(z) \right) + \frac{A(A-1)}{z^2} + \frac{2Af'(z)}{z} + f''(z) + [f'(z)]^2 - \frac{a[h'(z)]^2}{h(z)} \right] w(z) = 0$$

and its general solution is:

$$w(z) = Cz^{-A} e^{-f(z)} M(a, b, h(z)) + Dz^{-A} e^{-f(z)} U(a, b, h(z))$$

⁴⁸ Tsekrekos, 2009. *The Effect of Mean Reversion on Entry and Exit Decisions Under Uncertainty*. Journal of Economic Dynamics and Control, doi:10.1016/j.jedc.2009.10.015

⁴⁹ Abramowitz, Stegun (1972). *Handbook of Mathematical Functions with Formulas, Graphs and Mathematical Tables*. National Bureau of Standards Applied Mathematics Series. Dover Publications, New York.

where $M(a, b, h(z))$ is the Kummer's confluent hypergeometric function and $U(a, b, h(z))$ is the Tricomi's confluent hypergeometric function, respectively equal to:

$$M(a, b, z) = 1 + \frac{az}{b} + \frac{a(a+1)z^2}{b(b+1)2!} + \frac{a(a+1)(a+2)z^3}{b(b+1)(b+2)3!} + \dots$$

$$+ \frac{a(a+1)(a+2) \dots (a+n-1)z^n}{b(b+1)(b+2) \dots (b+n-1)n!} + \dots$$

$$U(a, b, h(z)) = \frac{\pi}{\sin b\pi} \left[\frac{M(a, b, h(z))}{\Gamma(1+a-b)\Gamma(b)} - [h(z)]^{1-b} \frac{M(1+a-b, 2-b, h(z))}{\Gamma(a)\Gamma(2-b)} \right]$$

In order to solve (5.10), we can note that our PDE can be viewed as a particular case of the general confluent differential equation. In fact, as Tsekrekos (2009) shows, if we set $A = -\gamma$, $f(z) = 0$ and $h(z) = \frac{2k\theta}{\sigma^2 z}$, we get:

$$w''(z) + \left[-\frac{2\gamma}{z} - \frac{b}{z} + \frac{2k\theta}{\sigma^2 z^2} + \frac{2}{z} \right] w'(z) + \left[\left(-\frac{b}{z} + \frac{2k\theta}{\sigma^2 z^2} + \frac{2}{z} \right) \left(-\frac{\gamma}{z} \right) + \frac{\gamma(\gamma+1)}{z^2} - \frac{a}{z} \frac{2k\theta}{\sigma^2 z^2} \right] w(z) = 0$$

$$zw''(z) + \left[-2\gamma - b + \frac{2k\theta}{\sigma^2 z} + 2 \right] w'(z) + \left[\frac{b\gamma - 2\gamma + \gamma(\gamma+1)}{z} - \frac{2k\theta(\gamma+a)}{\sigma^2 z^2} \right] w(z) = 0$$

whose solution is:

$$w(z) = Cz^\gamma M\left(a, b, \frac{2k\theta}{\sigma^2 z}\right) + Dz^\gamma U\left(a, b, \frac{2k\theta}{\sigma^2 z}\right)$$

If we compare the differential equation we just found with (4.10), letting $z = P_t$ and $w(z) = F(P_t)$, we can see the two equations coincide if and only if

$$\begin{cases} 2 - 2\gamma - b = -\frac{2(k + \lambda\rho\sigma)}{\sigma^2} \\ b\gamma - 2\gamma + \gamma(\gamma+1) = -\frac{2r}{\sigma^2} \\ 2k\theta(\gamma+a) = 0 \end{cases}$$

Solving the system, we get:

$$\gamma_{1,2} = \frac{2(k + \lambda\rho\sigma) + \sigma^2 \pm \sqrt{8r\sigma^2 + (-2k - 2\lambda\rho\sigma - \sigma^2)^2}}{2\sigma^2}$$

$$b_{1,2} = 2 - 2\gamma_{1,2} + \frac{2(k + \lambda\rho\sigma)}{\sigma^2}$$

$$a = -\gamma_{1,2}$$

According to (5.6) and (5.8), we rule out the set that depends on the negative root γ_2 , which leads us to the following solution:

$$F(P_t) = \left[CM\left(-\gamma_1, b_1, \frac{2k\theta}{\sigma^2 P_t}\right) + DU\left(-\gamma_1, b_1, \frac{2k\theta}{\sigma^2 P_t}\right) \right] P_t^{\gamma_1} \quad (5.11)$$

Now, substituting the formulation for Tricomi's confluent hypergeometric function into (5.11), we obtain:

$$\begin{aligned} F(P_t) &= \left[CM\left(-\gamma_1, b_1, \frac{2k\theta}{\sigma^2 P_t}\right) + D \frac{\pi}{\sin b_1 \pi} \left[\frac{M\left(-\gamma_1, b_1, \frac{2k\theta}{\sigma^2 P_t}\right)}{\Gamma(1 - \gamma_1 - b_1)\Gamma(b_1)} - \right. \right. \\ &\quad \left. \left. - \left[\frac{2k\theta}{\sigma^2 P_t} \right]^{1-b_1} \frac{M\left(1 - \gamma_1 - b_1, 2 - b_1, \frac{2k\theta}{\sigma^2 P_t}\right)}{\Gamma(-\gamma_1)\Gamma(2 - b_1)} \right] \right] P_t^{\gamma_1} = \\ &= \left[M\left(-\gamma_1, b_1, \frac{2k\theta}{\sigma^2 P_t}\right) \left[C + \frac{D\pi}{\sin b_1 \pi \cdot \Gamma(1 - \gamma_1 - b_1)\Gamma(b_1)} \right] + \right. \\ &\quad \left. + \left[\frac{2k\theta}{\sigma^2 P_t} \right]^{1-b_1} M\left(1 - \gamma_1 - b_1, 2 - b_1, \frac{2k\theta}{\sigma^2 P_t}\right) \left[\frac{-D\pi}{\sin b_1 \pi} \right] \right] P_t^{\gamma_1} \end{aligned}$$

Since the two factors in square brackets are constants, we can write:

$$F(P_t) = \left[M\left(-\gamma_1, b_1, \frac{2k\theta}{\sigma^2 P_t}\right) q_1 + \left[\frac{2k\theta}{\sigma^2 P_t} \right]^{1-b_1} M\left(1 - \gamma_1 - b_1, 2 - b_1, \frac{2k\theta}{\sigma^2 P_t}\right) q_2 \right] P_t^{\gamma_1}$$

Now, from (5.8), and knowing that the Kummer function has an asymptotic behavior of this kind: $\lim_{x \rightarrow +\infty} M(a, b, x) = \frac{\Gamma(b)}{\Gamma(a)} e^x x^{a-b}$, we have:

$$\lim_{P \rightarrow 0^+} q_1 \frac{\Gamma(b_1)}{\Gamma(-\gamma_1)} e^x x^{-\gamma_1 - b_1} + q_2 x^{1-b_1} \frac{\Gamma(2 - b_1)}{\Gamma(1 - \gamma_1 - b_1)} e^x x^{-1 - \gamma_1} = const$$

In fact, the presence of the factor $P_t^{\gamma_1}$ guarantees that $F(P_t)$ goes to zero, provided that the term in brackets does not go to infinity, namely that it is equal to a constant.

This leads to:

$$q_2 = -q_1 \frac{\Gamma(b_1)\Gamma(1 - \gamma_1 - b_1)}{\Gamma(-\gamma_1)\Gamma(2 - b_1)} = \omega q_1$$

In fact, the factor which multiplies *const* is $\frac{\Gamma(1-\gamma_1-b_1)}{\Gamma(2-b_1)} x^{\gamma_1+b_1} e^{-x}$, which goes to zero when $x \rightarrow +\infty$.

If we substitute this equation in the solution we found above, we get:

$$F(P_t) = q_1 \left[M\left(-\gamma_1, b_1, \frac{2k\theta}{\sigma^2 P_t}\right) + \omega \left[\frac{2k\theta}{\sigma^2 P_t}\right]^{1-b_1} M\left(1 - \gamma_1 - b_1, 2 - b_1, \frac{2k\theta}{\sigma^2 P_t}\right) \right] P_t^{\gamma_1} \quad (5.12)$$

where q_1 is a constant to be determined along with the optimal trigger value P_t^* , using the so-called value-matching and smooth-pasting conditions, respectively equal to:

$$F(P_t^*) = \Phi(P_t^*) - K$$

$$F_P(P_t^*) = \Phi_P(P_t^*)$$

which ensure not only that in the trigger point the option value function has the same value as the costs-benefits function, but also that their slopes are equal.

The deterministic LCOE and oil price case

Returning to the initial formulation of the problem, let's now consider what happens when both the oil price and LCOE are deterministic. At the beginning of this chapter, we were left with the task of solving the PDE in (5.5) subject to (5.6), (5.7) and (5.8). For convenience, we report them here:

$$\frac{1}{2} \sigma^2 P_t^2 F_{PP} + [k(\theta - P_t) - \lambda \rho \sigma P_t] F_P + F_t = rF \quad (5.5)$$

subject to:

$$\begin{cases} \lim_{P \rightarrow +\infty} F(P_t, t) = +\infty & (4.6) \\ \lim_{t \rightarrow +\infty} F(P_t, t) = +\infty & (4.7) \\ \lim_{P \rightarrow 0^+} F(P_t, t) = 0 & (4.8) \end{cases}$$

As we can see, the only difference arising from the comparison between (5.9) and (5.5) is the presence of the time derivative F_t . Our guess for the solution is thus:

$$F(P_t, t) = \tilde{F}(P_t)e^{gt} \quad (5.13)$$

where $\tilde{F}(P_t)$ represents the solution (5.12) of the base case we found above, while g is a constant to be found, as we will see in what follows.

In fact, substituting the guessed solution in (5.5) we obtain:

$$\frac{1}{2}\sigma^2 P_t^2 \tilde{F}_{PP} e^{gt} + [k(\theta - P_t) - \lambda\rho\sigma P_t] \tilde{F}_P e^{gt} + g\tilde{F} e^{gt} = r\tilde{F} e^{gt}$$

which leads to:

$$\frac{1}{2}\sigma^2 P_t^2 \tilde{F}_{PP} + [k(\theta - P_t) - \lambda\rho\sigma P_t] \tilde{F}_P = (r - g)\tilde{F} \quad (5.14)$$

As we can see, (5.14) is equivalent to (5.9), with the only difference of having $(r - g)$ instead of just r multiplying \tilde{F} . This means that $\tilde{F}(P_t)$ is equal to (5.12) (even in this case we rule out the negative root γ_2 because of (5.6) and (5.8) and even in this case we can use (5.8) and the asymptotic property of the Kummer function to reduce the two constants C and D in (5.11) to just one). The only difference concerns the definition of the parameters γ and b , in which we must take into account the presence of the different factor multiplying \tilde{F} in the PDE, leading to:

$$\gamma_1 = \frac{2(k + \lambda\rho\sigma) + \sigma^2 + \sqrt{8(r - g)\sigma^2 + (-2k - 2\lambda\rho\sigma - \sigma^2)^2}}{2\sigma^2}$$

$$b_1 = 2 - 2\gamma_1 + \frac{2(k + \lambda\rho\sigma)}{\sigma^2}$$

Thus, the solution to (5.5) is

$$F(P_t, t) = q_1 P_t^{\gamma_1} e^{gt} \left[M\left(-\gamma_1, b_1, \frac{2k\theta}{\sigma^2 P_t}\right) + \omega \left[\frac{2k\theta}{\sigma^2 P_t}\right]^{1-b_1} M\left(1 - \gamma_1 - b_1, 2 - b_1, \frac{2k\theta}{\sigma^2 P_t}\right) \right]$$

$$\text{with } \omega = -\frac{\Gamma(b_1)\Gamma(1-\gamma_1-b_1)}{\Gamma(-\gamma_1)\Gamma(2-b_1)}.$$

As before, the trigger value P_t^* and the unknown constant q_1 can be found by solving the following system of equations:

$$F(P_t^*, t) = \Phi(P_t^*, t) - K(t) \quad (4.15)$$

$$F_P(P_t^*, t) = \Phi_P(P_t^*, t) \quad (4.16)$$

In addition to these usual value-matching (5.15) and smooth-pasting (5.16) conditions, now we need a third equation in order to determine the value of the third unknown, g , and we can use (5.14) to this purpose (see Appendix C for the expressions of \tilde{F}_{PP} and \tilde{F}_P and for the explicit expression of $\Phi_P(P_t, t)$ as well):

$$g = r - \frac{\frac{1}{2}\sigma^2 P_t^2 \tilde{F}_{PP} - [k(\theta - P_t) - \lambda\rho\sigma P_t] \tilde{F}_P}{\tilde{F}}$$

Thus, the system of equations to be solved is:

$$\left\{ \begin{array}{l} F(P_t^*, t) = \Phi(P_t^*, t) - c_1 + Q \cdot C_0 \cdot e^{\alpha_c t} \\ F_P(P_t^*, t) = \Phi_P(P_t^*, t) \\ g = r - \frac{\frac{1}{2}\sigma^2 P_t^{*2} \tilde{F}_{PP} - [k(\theta - P_t^*) - \lambda\rho\sigma P_t^*] \tilde{F}_P}{\tilde{F}} \end{array} \right.$$

5.3.2. Results

The results of the resolution of (5.14) along with (5.15) and (5.16) are reported in Table 5.4.

t	P_t^*	g	q_1	error
0	155.10	0.3091	4.490	5.69e-14
0.2	150.15	0.3072	4.535	3.61e-15
0.4	146.10	0.3104	4.690	1.42e-14
0.5	144.97	0.3167	5.040	8.00e-15
0.6	142.04	0.3137	4.847	3.60e-15
0.8	137.51	0.3148	4.881	5.20e-17
1.0	132.09	0.3113	4.680	3.00e-12
1.2	128.03	0.3153	4.888	8.01e-15
1.4	121.38	0.3052	4.409	2.22e-14
1.6	115.23	0.2970	4.102	9.22e-16
1.8	110.21	0.2963	4.139	9.56e-17
2.0	100.04	0.2490	2.785	2.87e-13
2.2	95.28	0.2511	2.957	3.12e-17
2.4	90.39	0.2526	3.136	9.15e-16
2.6	82.57	0.2152	2.534	9.06e-16
2.8	75.70	0.1846	2.253	8.91e-16
3.0	68.58	0.1452	2.010	6.16e-10
3.2	63.56	0.1499	2.339	5.43e-18
3.4	58.31	0.1523	2.723	8.91e-16
3.6	55.55	0.2053	3.908	4.98e-15
3.8	51.52	0.2342	5.001	8.97e-16
4.0	45.46	0.2339	5.766	8.94e-16
4.2	41.11	0.2661	7.321	3.52e-19
4.4	35.89	0.2933	8.972	8.91e-16
4.6	27.97	0.3086	10.954	6.32e-18
4.8	19.37	0.3799	8.839	4.16e-15
5.8	0.16	0.4195	1.264	8.93e-16

TABLE 5.3 Trigger value P_t^* , g , and q_1 for each fixed time t . The error is computed as the square of the norm of the residuals.

Each one of the triads in Table 5.3 represents the point in which all three curves in the 4-D space go to zero: the PDE, the value-matching condition and the smooth-pasting one. If we take one of the arrays in Table 5.3, say the one for $t = 4$, we can graphically see that $P^* = 45.46$ is the trigger value in which all three curves equal zero (see Fig. 5.5). As it is natural to expect, unlike the value-matching and smooth-pasting conditions, whose values are equal to zero only when they're evaluated at the trigger point P^* , the PDE, when evaluated at the values of g and q_1 corresponding to $t=4$, always equals zero for any value of P .

As we can see from Table 5.3 and from Fig. 5.6, the threshold P^* is a decreasing function of time. This is an intuitive result: as time goes by, it becomes more and more convenient to consider switching to a PV plant, since the oil price keeps increasing with time, while the LCOE of PV technology keeps on getting lower, shifting the costs-benefits balance. This will require a progressively lower trigger price for the allowances. According to the graph, the grid parity⁵⁰ will likely be reached in less than six years from now, that is in 2021, even with very low emission allowances prices (in fact the trigger price tends to zero as t approaches 6 years). Instead, at the moment, we would have the grid parity only if the price of allowances were around 155 €. This is not the case, since, at the time we're writing this thesis, the EUA trades at 7.25 € (as of 05/22/2015).

⁵⁰ Usually the term “grid parity” is intended as the point in time in which the cost of producing electricity by means of an alternative energy source is equal to the price of purchasing power from the electricity grid, so it's a term usually meant for ratepayers. We use it in this context as the point in time in which the electricity producer is indifferent between using a PV energy source rather than fossil fuels.

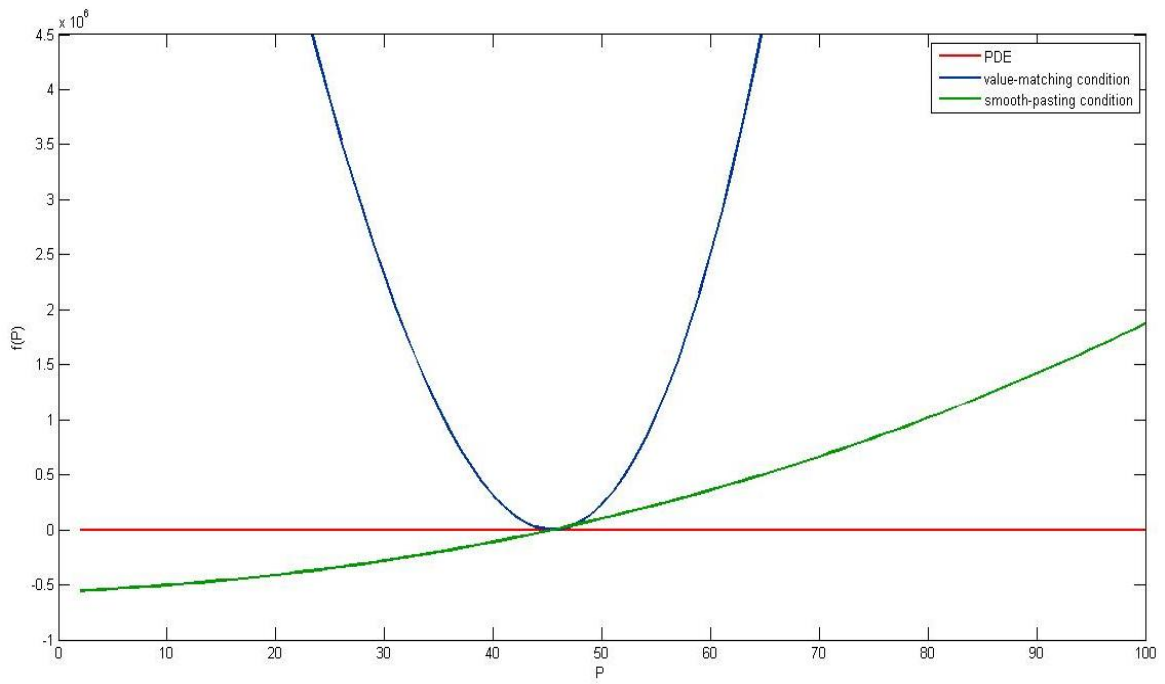


FIG. 5.5 Trigger point P^* for $t = 4$

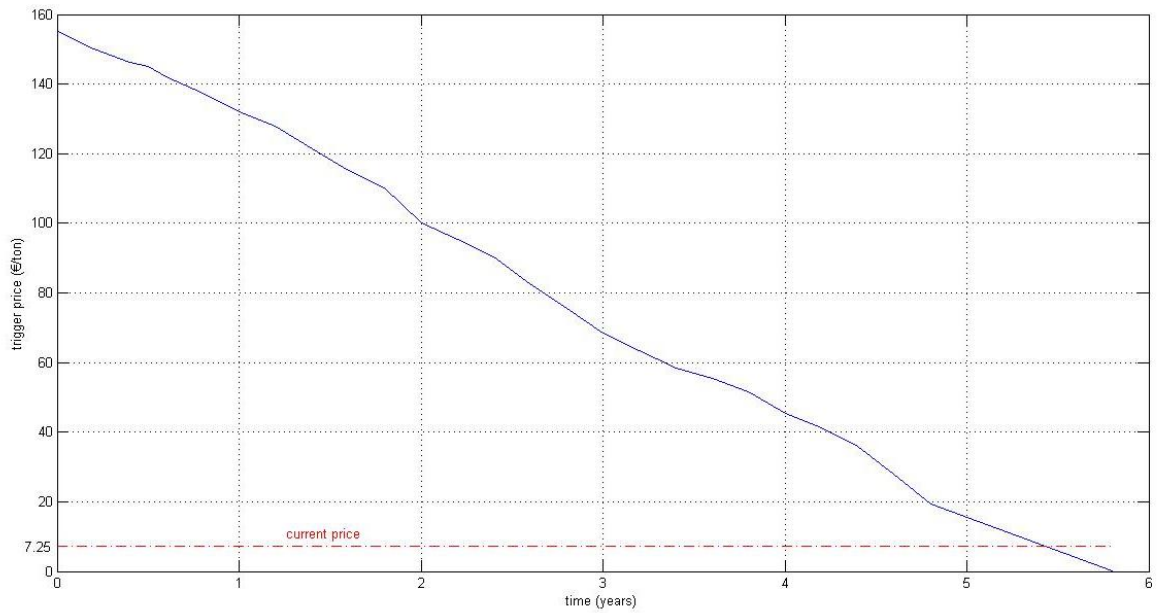


FIG. 5.6 Trigger prices P^* for each fixed time (first scenario)

However, we must underline that this result is highly dependent on the trend we estimated for the future LCOE, oil and carbon prices.

While the estimate for the exponential factor defining the trend of LCOE is quite robust, since technological improvement will almost certainly drive down the costs of producing electricity with PV technology, the same cannot be said for the oil dynamics parameter, α_D . In fact, the price is likely to increase in the long-term, due to oil scarcity which will eventually lead to the depletion of all oil fields, but we don't know for sure at which pace prices will be increasing in the future. Thus, in order to define the impact of oil prices on our real option problem, we defined three alternative scenarios, each one with a different growth rate for the oil price.

The first scenario is the one we outlined above, where the oil price is expected to increase according to an exponential curve fitted to the whole sample available for WTI prices: from 1986 to nowadays. As we saw in Fig. 5.4, there is a huge gap between what prices used to be back in the '80s and '90s and what they are now: it is natural for the exponential factor to reflect this discrepancy, with a fitted value of 0.0777.

Instead, if we choose to focus on recent years only and we base our estimate on a smaller sample, say from the last seven years, the trend is less defined and the value in the exponential parameter will reflect this. In fact, the estimator $\hat{\alpha}_D$ on the sample ranging between [Jul. 2008-Jul. 2015] is equal to 0.0271. This lower but still positive value suggests that prices will be rising in the future, even if at a slower pace than the one estimated before. In the second scenario simulation we use this lower value instead of the one found fitting the exponential on the whole historical data sample.

The third scenario is the one in which the oil price does not change at all: $\hat{\alpha}_D$ is supposed to be equal to 0, so that the oil price is fixed and equal to today's price. In this scenario we can analyze how the threshold changes and how much more time it will take in order to get to the grid parity.

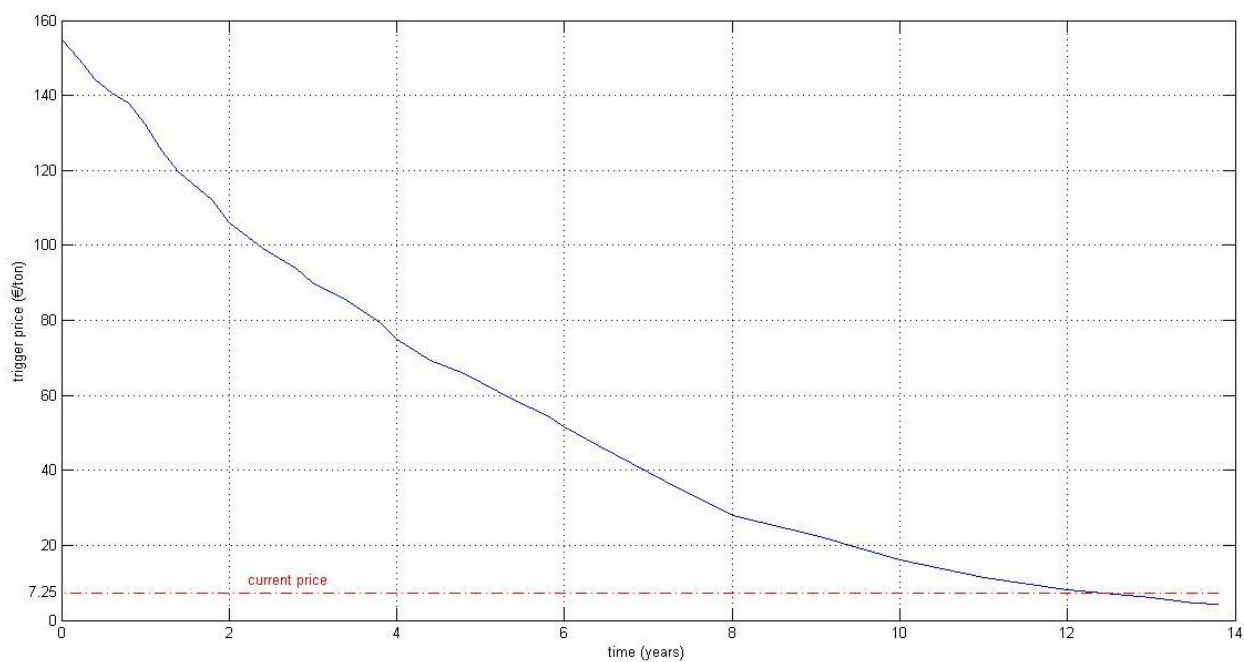


FIG. 5.7 Trigger prices P^* for each fixed time (second scenario)

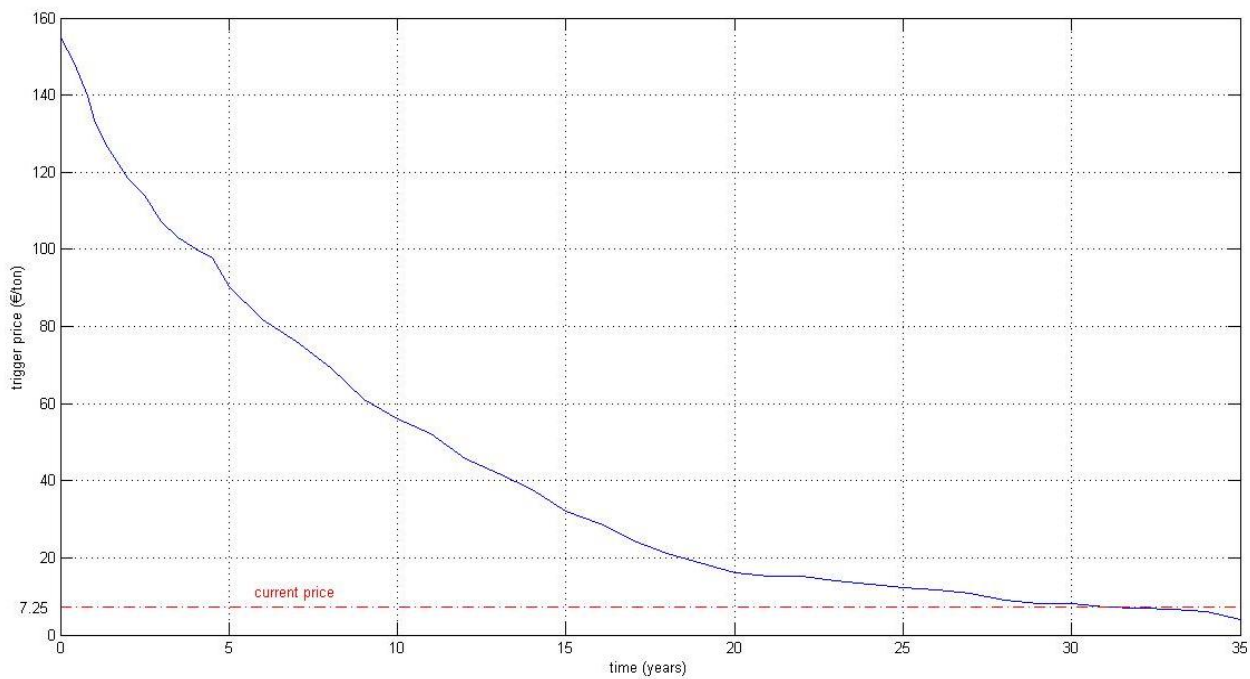


FIG. 5.8 Trigger prices P^* for each fixed time (third scenario)

As we can see from Fig. 5.6, 5.7 and 5.8, the oil price plays a relevant role in the definition of the trigger price P^* . At the current EUA price, as the exponential factor $\hat{\alpha}_D$ fitted for the oil price curve gets progressively lower, the time of grid parity goes farther and farther, shifting from less than 6 years in the first scenario, to slightly more than 12 years in the second one, reaching 31 years in the third one.

In this last scenario simulation, the oil price no longer influences the trigger price P^* , which is the result of the LCOE and carbon price dynamics only. Without the “help” of increasing oil prices, at the current EUA price, grid parity would be reached in a considerable amount of time. This result differs a lot from the one we found in the first scenario. With a fixed oil price, it takes about six times the time it took before in order to make it convenient to switch to alternative energy sources.

This underpins the role of oil prices in determining the optimal timing of the renewable energy investment, stressing their relevance. However, as we can see from the three scenario graphs, also the EUA price can substantially influence the result. In fact, if EUA prices were a little higher, let's say around 30 €/ton, in the case of the third scenario, grid parity would only take half the time in order to be reached, about 15 years, thus leading to a 50% reduction in optimal timing with respect to the current level of prices. This can be seen even in the first and second scenario, where a 30 €/ton EUA price would lead to a 20% and 35% reduction in grid parity, respectively.

It is worth noticing that, among the three scenarios proposed, the most likely to happen is the first one, as confirmed by the latest World Bank report on commodity markets outlook (World Bank, 2015). In fact, the exponential factor estimated in the mentioned report is equal to 0.0665, a value much more similar to the one we estimated in our first scenario (0.0777), than it is to the one of our second scenario (0.0271).

Conclusions

In our work, we presented a comprehensive analysis of carbon prices in the EU ETS framework, with the purpose of valuating a renewable energy investment project by means of a real option approach.

After a contextualizing introduction on the past and current state of political environmental intervention in the economy, the statistical features of carbon prices have been analyzed in detail. Unlike other financial products, which all fall into a precise asset category (equity, fixed income, FX, commodities, derivatives), carbon is a special asset which may resemble energy commodities in some aspects but differentiates itself in others, in the sense that its price somewhat depends on an exogenous political decision, which caps the total supply of the product. This aspect reflects in the price distribution, featuring extreme events such as the jump occurring between the first and second trading phase, as well as heavy tails and leptokurtic behavior.

Two different assumptions have been made to explain the particular distribution characterizing asset prices. First, log-returns have been fitted to a VG model, which performed very well in matching the empirical distribution, even when calibrated to the entire sample, demonstrating the capacity of adequately explaining even extreme events and jump in prices. Then, the calibration process has been implemented using a different stochastic process, the BS, which demonstrated its ability in better predicting future prices. For this reason, and most of all for its higher analytical tractability, this second model has been chosen to perform the real option valuation which motivates our work.

In order to accomplish this task, first we have defined the investment project setup, along with the analysis of the time dependent dynamics characterizing the levelized cost of electricity of photovoltaic technology and the oil price. After having identified the

variables determining the costs and benefits deriving from the project, we have proceeded to price the real option by analytically solving the partial differential equation (PDE) obtained by means of stochastic calculus tools. The closed-form solution to the PDE, representing the value of the investment opportunity, paired with real options theory's value-matching and smooth-pasting conditions, enabled us to come across the value of EUA prices triggering the convenience of the renewable energy investment, at each fixed point in time.

The results highlight not only EUA's role in determining the optimal timing for switching from fossil fuels to green sources of energy, but also its connection to the future oil price dynamics. In fact, the solution to the real options valuation problem depends in a significant way on the dynamics of the energy source about to be abandoned, namely on oil price, in addition to the price of allowances. In order to assess the dependency of the result on the definition of the process describing oil prices, we have performed three simulation scenarios, each with a different speed of growth of oil prices.

Initially, we calibrated the oil price process on a wide sample of available historical data coming from crude oil spot prices (ranging from 1986 to 2015). The trend is fairly defined and the estimation suggests oil prices will be increasing at a moderate pace in the future. In this first scenario, if EUA prices stay at current levels, grid parity, defined as the time in which the cost of production of electricity by means of renewable sources equals that of producing it through fossil fuels, will be reached in less than six years. If instead we calibrate the oil price process on a smaller sample, considering the past seven years only, the trend is less pronounced and oil is expected to grow at a lower rate. In this case, grid parity shifts at about twelve years. Finally, in the third scenario we have supposed the oil price will not change at all in the future, remaining fixed at the current price. In this case, grid parity is expected to be reached in about thirty years from now.

According to these findings, the price of fossil fuels plays a relevant role in the definition of the time of grid parity. Nevertheless, we must underline that, among the three scenarios proposed, the most likely to happen is the first one, as confirmed by the latest World Bank report on commodity markets outlook (World Bank, 2015). Thus,

according to our results, this bodes a likely rise in renewables in the years to come, influencing in a positive way the time of grid parity.

However, with regard to the effectiveness of the ETS, it should be noted the still not enough exploited potential of emission allowances, as they would allow grid parity to come earlier in time, whichever scenario will actually take place. This is particularly true for low growth rates of the oil price: were the third scenario to take place, an EUA price around 30 €/ton would bring grid parity forward of about sixteen years, from 2046 to 2030, with respect to what it would be with the current EUA price. Even in the first and second scenario, such a higher price of allowances would allow for grid parity to be achieved earlier in time.

In conclusion, it is likely that renewable energy, in the near future, will become an interesting and economically convenient alternative to fossil fuels for electric utilities. Nevertheless, the price of allowances should be higher in order for the ETS to actually have the desired impact on the economy, and to readily boost low carbon investments. Thus, a political intervention would be advisable, in order to keep the allowance prices above a floor value. Such a price management mechanism has already been implemented in three other emission trading programs, the northeastern US Regional Greenhouse Gas Initiative (RGGI), the California emission trading program and the Quebec one. The floor is implemented as a minimum bid in auctions and in all three programs it has been successful in enhancing environmental outcomes. Hence, it would be interesting to assess the impact of such a price floor on the EU ETS carbon market as well.

On a final note, a possible extension of this work could be analyzing how the result changes by changing the underlying process of EUA prices. This can be done for example by assuming a VG process and finding the trigger price through a numerical procedure, by means of a Monte Carlo simulation. The comparison of such results with the ones obtained in this study can help shed further light and improve accuracy on the optimal timing of grid parity.

Appendix

A. Codes (created for the Matlab[®] environment)

A.1. Statistical analysis of the data sample

```

% DAILY RETURNS

% Unit root test (Dickey-Fuller), normality test (Jarque-Bera)
% autocorrelation check

[num,txt]=xlsread('maria_selezionati');
logdata=log(num);
[h,pvalue_dickey]=adftest(logdata)
rend=logdata(2:length(logdata))-logdata(1:(length(logdata)-1));

[d,pvalue_jarque]=jbttest(rend)
Kurtosis=kurtosis(rend)
Skewness=skewness(rend)

media=mean(rend)
varianza=var(rend)
c=length(rend);
figure
hist(rend,200)
hold on
maxmin=(max(rend)-min(rend))/200;
x=min(rend):maxmin:max(rend);
sigma=sqrt(varianza);
y=normpdf(x,media,sigma)*(c*maxmin);
plot(x,y,'r')
title('Normality Check')
legend('Actual data','Normal PDF')

vector=mle(rend,'distribution','normal');
mu=vector(1);
sigma=vector(2);

vettoredate1=txt;
v2=datenum(vettoredate1,'dd/mm/yyyy');

figure
plot(v2,logdata);
datetick('x','dd-mm-yyyy','keepticks')
title('Log(relative stock value)')

figure
plot(v2(2:length(v2)),rend);

```

```

ax=gca;
ax.XTick=rend;
datetick('x','dd-mm-yyyy','keepticks')
title('Log-returns')

% test whether the logdata series matches a random walk
[h_walk,pValue_walk] = vratiotest(logdata)

% test whether an i.i.d. random walk is a reasonable model for the
stock series
[h2,pValue2] = vratiotest(logdata,'IID',true)

figure
autocorr(rend)
title('Return autocorrelation')
figure
rsquare=(rend.^2)*10000;
autocorr(rsquare)
title('Square return autocorrelation')

figure
autocorr(abs(rend))
title('Absolute log-returns autocorrelation')

theta=[0.1:0.1:2]';
ACF=zeros(21,20);
for i=1:20
    auto=autocorr((abs(rend)).^theta(i));
    ACF(:,i)=auto;
end
ACF1=ACF(2:end,:);
[~,lags]=autocorr(abs(rend));
lags1=lags(2:end);
figure
surface(theta,lags1,ACF1)
title('ACF of Powers of Log>Returns')
xlabel('theta')
ylabel('lag number')
zlabel('autocorrelation')

figure
autocorr((abs(rend)).^0.5)
title('ACF of Square Root of Absolute Log>Returns')

%%%%%%%%%%%%%%%%%%%%%%%%%%%%%%%%%%%%%%%%%%%%%%%%%%%%%%%%%%%%%%%%%%%%%%%%

% MONTHLY RETURNS

vettoredate=datevec(txt,'dd/mm/yyyy');
matrice=[vettoredate((2:size(vettoredate,1)),:),rend];
datain='08-Sep-2005';
datafin='07-Oct-2014';
if vettoredate(1,3)>vettoredate((length(vettoredate)),3)
    mesi=months(datain,datafin)+2;
else
    mesi=months(datain,datafin)+1;
end
rmensili=zeros(mesi,1);

```


A.2. VG model calibration

```

%%
% Compute the VG parameters (main body)

% The estimates for alpha, mu, sigma and theta respectively are
% reported in the x vector

[num,~]=xlsread('maria_selezionati'); % load carbon prices

VGpdf_function = @(p) MLE_ESTIMATE(p, num);
start = [2.5,1,1,1]';
lbounds = [1e-7; -1e7; 1e-7; -1e7];
ubounds = [1e7; 1e7; 1e7; 1e7];

% first solve with the interior-point algorithm
options = optimset('Algorithm', 'interior-point', 'TolFun', 1e-8);
[x0,~,~,output0]=fmincon(VGpdf_function, start, [],[],[],[], lbounds,
ubounds, [],options)
% improve the estimate with the sqp algorithm
options = optimset('Algorithm', 'sqp', 'TolFun', 1e-8);
[x,fval,exitflag,output]=fmincon(VGpdf_function, x0, [],[],[],[],
lbounds, ubounds, [],options);

%%
% Compute CIs using a normal approximation for params
params = x;
data = num;
N = length(data)-1;
pdf = @(d,al,mu,si,th) (-MLE_ESTIMATE3(d,al,mu,si,th));

acov = mlecov(params, data, 'pdf', pdf);
std_params = sqrt(diag(acov));
%std_params(1) = alpha standard deviation
%std_params(2) = mu standard deviation
%std_params(3) = sigma standard deviation
%std_params(4) = theta standard deviation

sign = 0.05;
l = norminv(1-sign/2,0,1);
lb = x - l*std_params/sqrt(N);
ub = x + l*std_params/sqrt(N);

disp(['Confidence Interval Lower Bound at ' num2str(sign) '%']);
disp(num2str(lb))
disp(['Confidence Interval Upper Bound at ' num2str(sign) '%']);
disp(num2str(ub))

% Compute the VG parameters (function)

% Maximum Likelihood Estimation of parameters with VG density function

function val=MLE_ESTIMATE(parametri, num)

alpha = parametri(1);

```

```

mu = parametri(2);
sigma = parametri(3);
theta = parametri(4);
logdata=log(num);
rend=logdata(2:length(logdata))-logdata(1:(length(logdata)-1));

sigma2 = sigma^2;
n=alpha-0.5;
temp = sqrt(theta^2+2*alpha*sigma2);
w=(abs(rend-mu)*temp)/(sigma2);

VGpdf = sqrt(2/pi)*(((alpha^alpha)*exp((rend-
mu)*theta/sigma2))/(sigma*gamma(alpha)).* ...
    ((abs(rend-mu)/temp).^n).*besselk(n,w);

val=-sum(log(VGpdf));

end

%%%%%%%%%%%%%%%%%%%%%%%%%%%%%%%%%%%%%%%%%%%%%%%%%%%%%%%%%%%%%%%%%%%%%%%%

```

A.3. Goodness of fit of the estimated VG model - graphical test

```

% Graph (to be run after MLE_main)
% actual data compared to the VG pdf obtained with the estimated
parameters

logdata=log(num);
rend=logdata(2:length(logdata))-logdata(1:(length(logdata)-1));
c=length(rend);
maxmin=(max(rend)-min(rend))/900;
figure
hist(rend,900)
hold on
observed=hist(rend,900);
observedCut=observed(1:end-1);
bin=min(rend):maxmin:max(rend);

alpha = x(1);
mu = x(2);
sigma = x(3);
theta = x(4);

sigma2 = sigma^2;
n=alpha-0.5;
temp = sqrt(theta^2+2*alpha*sigma2);
w=(abs(bin-mu)*temp)/(sigma2);

y = sqrt(2/pi)*(((alpha^alpha)*exp((bin-
mu)*theta/sigma2))/(sigma*gamma(alpha)).* ...
    ((abs(bin-mu)/temp).^n).*besselk(n,w).*(c*maxmin);
plot(bin,y,'r')
title('Goodness of Fit Check')
legend ('Actual data','VG PDF')

```

A.4. Goodness of fit of the estimated VG model – Pearson’s chi squared test

```
% Chi squared goodness of fit test
% (to be run after MLE_GRAPH)

theoretical=y(1:end-2);
h=(observedCut-theoretical).^2./theoretical;
chi2_test_statistic=sum(h)
degrees=length(theoretical)-4;
critical_value=chi2inv(0.95,degrees)
```

A.5. Oil parameters estimation

```
% Curve fitting of crude oil spot prices via mle

% Load WTI spot historical data
[num,dates]=xlsread('WTI_all');
v=datetime(dates,'dd/mm/yyyy');
% Delete entries in which WTI was not traded
i=1;
for j=1:length(num)
    if isnan(num(j))==0
        Oilmatrix(i,1)=v(j);
        Oilmatrix(i,2)=num(j);
        i=i+1;
    end
end

% Exponential curve fitting
modelFun = @(p,x) p(1) .* exp(p(2) .* x);
startingVals = [30 0.08]; % guesses for D_0 and alpha_D
years=Oilmatrix(:,1)./365.24-2014;
coefEsts = nlinfit(years, Oilmatrix(:,2), modelFun, startingVals)

% Plot prices
figure
plot(Oilmatrix(:,1),Oilmatrix(:,2))
datetick('x','dd-mm-yyyy','keepticks')
hold on
line(Oilmatrix(:,1), modelFun(coefEsts, years), 'Color','r');
title('WTI Crude Oil Spot Prices')
```

A.6. BS model calibration

```
% Parameters estimation of carbon spot prices following a Brennan-
Schwartz
% process - main body
```

```

[num,~]=xlsread('maria_selezionati'); % load carbon prices

BS_fun = @(p) PARAMETERS_BS_fun(p, num);
start = [0.5,0.1,0.2]';
lbounds = [1e-7; -1e7; 1e-7];
ubounds = [1e7; 1e7; 1e7];

% x=[k,theta,sigma]

% first solve with the interior-point algorithm
options = optimset('Algorithm', 'interior-point', 'TolFun', 1e-8);
[x0,~,~,output0]=fmincon(BS_fun, start, [],[],[],[], lbounds, ubounds,
[],options)
% improve the estimate with the sqp algorithm
options = optimset('Algorithm', 'sqp', 'TolFun', 1e-8);
[x,fval,exitflag,output]=fmincon(BS_fun, x0, [],[],[],[], lbounds,
ubounds, [],options);

% display results
k = x(1)
theta =x(2)
sigma =x(3)

% Parameters estimation of carbon spot prices following a Brennan-
% Schwartz process - function

function sumlog=PARAMETERS_BS_fun(parameters, num)

% define the parameter vector
k = parameters(1);
theta = parameters(2);
sigma = parameters(3);

xi=num(2:end); % x(t)
xminus1=num(1:end-1); % x(t-1)
dt=1/250;
% define the BS log-likelihood function
mui=xminus1+k.*(theta-xminus1).*dt;
sigmai=sigma.*xminus1.*sqrt(dt);
hlp1=log(sqrt(2*pi*sigmai.^2));
hlp2=(xi-mui).^2./(2.*sigmai.^2)+hlp1;
sumlog=sum(hlp2);

end

```

A.7. Goodness of fit of the estimated BS model – graphical test

```

% Compute theoretical probabilities given the estimated parameters

k=0.364;
theta=8.3789;
sigma=0.5195;

```

```

xi=num2(2:end);
ximinus1=num2(1:end-1);
dt=1/250;
% define the approximated BS pdf
mui=ximinus1+k.*(theta-ximinus1).*dt;
sigmai=sigma.*ximinus1.*sqrt(dt);

y = 1./(sqrt(2*pi.*sigmai.^2)).*exp((- (xi-mui).^2)./(2.*sigmai.^2));

% Divide prices in bins and compute the theoretical probability
% relatively to each bin
yth=zeros(300,1);
bin=(max(xi)-min(xi))./300;
xth=min(xi):bin:max(xi);
xthCut=xth(2:end);
for i=1:length(xi)
    for j=1:299
        if xthCut(j)<xi(i) && xi(i)<xthCut(j+1)
            yth(j)=yth(j)+y(i);
        end
    end
end
end

% CDF graphs

% Empirical CDF:
figure
cdfplot(xi)
hold on
% Theoretical CDF:
yplot=cumsum(yth);
yplotnorm=yplot./max(yplot);

plot(xthCut,yplotnorm,'r')
title('CDF')
legend('Empirical CDF','Theoretical CDF')

% PDF graphs

% Empirical PDF:
figure
hist(xi,300)
hold on
% Theoretical PDF:
yplot=yth;

plot(xthCut,yplot,'r')
title('PDF')
legend('Empirical PDF','Theoretical PDF')

```

A.8. Resolution of the system of equations in order to find the trigger price

```

%% Parameter values
B= 1.48*10^4;    % number of tons of oil used per year
X= 46200;       % number of tons of CO2 emitted per year
Op= 0.5*10^6;   % operative costs
r= 0.05;        % risk free rate
alfac= -0.025;  % LCOE parameter
alfad= 0.0777;  % oil parameter
D00=60.18;      % oil spot price in $/barrel as of 05/21/15
D0=D00*7.46/1.14; % oil price in €/ton (exchange rate as of 05/21/15)
k=0.364;        % carbon parameter
theta= 8.3789;  % carbon parameter
sigma=0.5199;   % carbon parameter

lambda=0.5;
ro=0;
%lambda=(Rm-r)/sigmam; % market price of risk

% Set time (in years):
t =1;

%%
% call function
FThreshold = @(x) (FIND_threshold_fun2(x, ...
B,X,Op,r,alfac,alfad,D0,k,theta,sigma,lambda,ro,t));
FThresholdNorm = @(x) (norm(FIND_threshold_fun2(x, ...
B,X,Op,r,alfac,alfad,D0,k,theta,sigma,lambda,ro,t))^2);

lbounds = [1e-7; 0; 0]; %lower bounds
ubounds = [1e7; 0.4201; +Inf]; %upper bounds
start = [33,0.06,11]'; % starting guess at the solution

%% First solver : fsolve. Solve the system of equations
algorithm = 'Levenberg-Marquardt';
options=optimset('Display','iter', 'Algorithm', algorithm,...
'MaxFunEvals',1600000,'MaxIter',10000,'Diagnostics','on','TolX', ...
1e-8,'TolFun',1e-8); % Option to display output
% Call solver
[x0,fval0,exitflag0,output0] = fsolve(FThreshold,start,options)
% error in the estimate
error=norm(fval0).^2

%% Second solver: fmincon. Minimizes the square norm of the vector of
% equations
algorithm = 'sqp';
options = optimset('Algorithm',algorithm,'FinDiffType','central', ...
'MaxFunEvals',10000,'TolX',1e-16,'TolFun', ...
1e-10,'MaxIter',10000,'Display','iter','UseParallel', 'always');
[x,fval,exitflag,output] = ...
fmincon(FThresholdNorm,start,[],[],[],[],lbounds,ubounds,[], options);
disp(FThresholdNorm(x))

```

```

% Third solver: lsqnonlin. Minimizes the sum of the squares of the
% vector of equations
algorithm = 'trust-region-reflective';
options = optimset('Algorithm',algorithm,'FinDiffType','central', ...
'MaxFunEvals',5000,'TolX',1e-16,'TolFun', ...
1e-16,'MaxIter',40000,'Display','iter','UseParallel', 'always');
[x1,resnorm,residual,exitflag1,output1] = ...
lsqnonlin(FThreshold,start,lbounds,ubounds, options)
disp(FThresholdNorm(x1))
disp(FThreshold(x1))

% Function FIND_threshold_fun2

% It computes the values of the equations useful to run
% "FIND_THRESHOLD.mat"

function val=FIND_threshold_fun2(parameters, ...
B,X,Op,r,alfac,alfad,D0,k,theta,sigma,lambda,ro,t)

% define vector of unknowns
P = parameters(1);
g = parameters(2);
q1 = parameters(3);

gam=(2*(k+lambda*ro*sigma)+sigma^2+sqrt(8*(r-g)*sigma^2+(-2*k-
2*lambda*ro*sigma-sigma^2)^2))/(2*sigma^2);
b=2-2*gam+(2*(k+lambda*ro*sigma))/sigma^2;
omega= -(gamma(b)*gamma(1-gam-b)/(gamma(-gam)*gamma(2-b)));

% Sunk costs
K= 10^6+1.48*10^8*exp(alfac*t);

% Annual benefits
phi= (1-exp(-r*(25)))*(B/r*D0*exp(alfad*t)+X/r*P+Op/r);
% phi derivative wrt P
phiP=(1-exp(-r*(25)))*X/r;

z=(2*k*theta)/(sigma^2*P);

% Option value
F = q1*P^gam*exp(g*t)*(kummer(-gam,b,z)+omega*z^(1-b)* ...
kummer(1-gam-b,2-b,z));

% F derivative wrt P
FP = P^(gam-1)*exp(g*t)*q1*(omega*z^(1-b)*(gam+b-1)* ...
(kummer(1-gam-b,2-b,z)+1/(2-b)*z*kummer(2-gam-b,3-b,z)) ...
+gam*kummer(-gam,b,z)+gam/b*z*kummer(1-gam,1+b,z));

% FP derivative wrt P
FPP = P^(gam-2)*exp(g*t)*q1*(omega*z^(1-b)*(gam+b-1)*(gam+b-2)* ...
kummer(1-gam-b,2-b,z)+omega*z^(1-b)*(gam+b-1)/(2-b)*z ...
*2*(gam+b-2)*kummer(2-gam-b,3-b,z)+gam*(gam-1)* ...
kummer(-gam,b,z)+ gam/b*z*2*(gam-1)*kummer(-gam+1,b+1,z) ...
-omega*z^(3-b)*(gam+b-1)*(2-gam-b)/((2-b)*(3-b))* ...
kummer(3-gam-b,4-b,z)-gam/b*z^(2)*(1-gam)/(1+b)*kummer ...
(2-gam,b+2,z));

```

```

% F derivative wrt t
Ft = P^gam*q1*g*exp(g*t)*(kummer(-gam,b,z)+omega*z^(1-b) ...
    *kummer(1-gam-b,2-b,z));

% system of three equations
% 3 unknowns: P,q1,g

% pde
e1=0.5*sigma^2*P^2*FPP+(k*(theta-P)-lambda*ro*sigma*P)*FP+Ft-r*F;
% value-matching condition
e2= F-phi+K;
%smooth-pasting condition
e3= FP-phiP;

val=[e1;e2;e3];

end

%%%%%%%%%%%%%

```

A.9. Forecast of carbon prices using the VG, BS and GBM models

```

%% load data
loadData; % X is the vector containing EUA prices
nsim = 1e4; % number of simulations

%=====
%%%%%%%%%% VG model %%%%%%%%%%%
%=====
% as before, calibrate the VG model, this time on second phase prices
% only
VGpdf_function = @(p) MLE_ESTIMATE(X, p);
start = ones(4,1);
lbounds = [1e-7; -1e7; 1e-7; -1e7];
ubounds = [1e7; 1e7; 1e7; 1e7];

options = optimset('Algorithm', 'interior-point', 'TolFun', 1e-8);
[x0,~,~,output0]=fmincon(VGpdf_function, start, [],[],[],[], lbounds,
ubounds, [], options);
options = optimset('Algorithm', 'sqp', 'TolFun', 1e-8);
[x,fval,exitflag,output]=fmincon(VGpdf_function, x0, [],[],[],[],
lbounds, ubounds, [], options);
% x = [alpha, mu, sigma, theta]
BICVG = 2*fval+length(x)*log(length(X)); % Bayesian Information
%Criterion

% second period estimates
alpha = x(1);
mu = x(2);
sigma = x(3);
theta = x(4);

```

```

% ===== find a simulated path of prices coming from a VG
% distribution (run VG_AMERICAN first)
Xsim=S1;

% graph plotting empirical vs. forecasted prices
figure
subplot(2,2,1)
plot(date,X)
hold on
%plot(mean(Xsim,2),'r')
plot(date,mean(Xsim,1),'r')
title('VG')
xlabel('time')
set(gca,'XTick',[733310:650:735879 735965])
ylabel('P')
legend('Empirical prices','Forecasted prices')
datetick('x','dd-mm-yyyy','keepticks')
%xlim(date([1 end]))
xlim([733310 735965])
hold on

RMSE = sqrt(mean(X-mean(Xsim,1))^2); % root mean square error
disp(RMSE)

%=====
%##### BS model #####
%=====
% parameters found calibrating the BS model on second period prices
Estlambda=0.364;
Estmu=8.3789;
Estsigma=0.5195;

% ===== find a simulated path of prices coming from a BS
% distribution
Xsim = BS_sim(parametri, X(1), 1e4, length(X));

% graph plotting empirical vs. forecasted prices
subplot(2,2,2)
plot(date,X)
hold on
plot(date,mean(Xsim,2),'r')
title('BS')
xlabel('time')
set(gca,'XTick',[733310:650:735879 735965])
ylabel('P')
legend('Empirical prices','Forecasted prices')
datetick('x','dd-mm-yyyy','keepticks')
%xlim(date([1 end]))
xlim([733310 735965])
hold on

RMSE = sqrt(mean(X-mean(Xsim,2))^2);
disp(RMSE)

%=====

```

```

%%%%%%%%%% GBM model %%%%%%%%%%%
%=====

rend = diff(log(X));

% GBM parameters estimation

GBM_function = @(p) GBM(p, rend);
start = [0.2,0.2]';
lbounds = [-1e7; 1e-7];
ubounds = [1e7; 1e7];

% x=[mu,sigma]

options = optimset('Algorithm', 'interior-point', 'TolFun', 1e-8);
[x0,~,~,output0]=fmincon(GBM_function, start, [],[],[],[], lbounds,
ubounds, [],options)
options = optimset('Algorithm', 'sqp', 'TolFun', 1e-8);
[x,fval,exitflag,output]=fmincon(GBM_function, x0, [],[],[],[],
lbounds, ubounds, [],options);

mu=-0.05;
sigma=0.5267;

% ===== find a simulated path of prices coming from a GBM
% distribution
parametri = [mu,sigma];
Xsim = GBM_simula(parametri, X(1), 1e4, Itempo);

% graph plotting empirical vs. forecasted prices
subplot(2,2,4)
plot(date,X)
hold on
%plot(mean(Xsim,1)', 'r')
plot(date,mean(Xsim,2), 'r')
title('GBM')
xlabel('time')
set(gca, 'XTick', [733310:650:735879 735965])
ylabel('P')
legend('Empirical prices', 'Forecasted prices')
datetick('x', 'dd-mm-yyyy', 'keepticks')
%xlim(date([1 end]))
xlim([733310 735965])
hold on

BICGBM = 2*GBM(mu, rend)+length(parametri)*log(length(X));

RMSE = sqrt(mean(X-mean(Xsim,2))^2);
disp(RMSE)

%%%%%%%%%%

```


BS_sim.m

```
function [Xsim] = BS_sim(parametri, x0, Nsim, N)

lambda = parametri(1);
mu = parametri(2);
sigma = parametri(3);

% Eulero scheme simulation
noise = randn(N,Nsim);

Xsim = NaN(N,Nsim);
Xsim(1,:) = x0;
dt=1/250;

for k = 2:N
    Xsim(k,:) = Xsim(k-1,:)+lambda*(mu-Xsim(k-
1,:))*dt+sigma*sqrt(dt)*(Xsim(k-1,:).*noise(k-1,:));
end

%%%%%%%%%%%%%%%%%%%%%%%%%%%%%%%%%%%%%%%%%%%%%%%%%%%%%%%%%%%%%%%%%%%%%%%%%
```

GBM_simula.m

```
function [S, tempi] = GBM_simula(parametri, s0, nsim, tempi)

mu = parametri(1);
sigma = parametri(2);

delta_t = diff(tempi);
m = (mu-0.5*sigma^2)*delta_t;

S = NaN(length(tempi), nsim);
S(1,:) = s0;
E = repmat(sigma*sqrt(delta_t), 1,nsim);
stoc =normrnd(0,1,length(delta_t), nsim).* E;
for k = 2:length(tempi)
    S(k,:) = S(k-1,:).*exp(m(k-1)+stoc(k-1,:));
end
```

B. Emissions by year and country

The following Tables illustrate our own elaboration of the dataset available on the European Environment agency website (<http://www.eea.europa.eu/data-and-maps/data/european-union-emissions-trading-scheme-eu-ets-data-from-citl-6>). The dataset mainly comes from the EU Transaction Log (EUTL), which provides data on emissions and allowances, by country, sector and year. The values are expressed in million tons of CO₂ equivalent.

B.1. Allocated allowances vs. verified emissions by all industry sectors

	2005	2006	2007	2008	2009	2010	2011	2012	2013	Total 2005- 2007	Total 2008- 2012
Austria											
1. Total allocated allowances	32.41	32.65	32.73	30.72	30.72	30.96	30.96	30.96	36.65	97.79	154.33
2. Verified emissions	33.37	32.38	31.75	32.08	27.36	30.92	30.60	28.39	29.85	97.51	149.34
Belgium											
1. Total allocated allowances	58.31	59.95	60.43	55.38	56.80	56.03	56.56	68.12	66.08	178.69	292.88
2. Verified emissions	55.36	54.78	52.80	55.46	46.21	50.10	46.20	43.01	45.23	162.93	240.98
Bulgaria											
1. Total allocated allowances	0.00	0.00	0.00	38.30	40.60	35.27	41.54	42.94	25.71	0.00	198.65
2. Verified emissions			39.18	38.30	32.01	33.53	40.00	35.05	32.70	39.18	178.89
Croatia											
1. Total allocated allowances	0.00	0.00	0.00	0.00	0.00	0.00	0.00	0.00	5.29	0.00	0.00
2. Verified emissions									8.51		
Cyprus											
1. Total allocated allowances	5.47	5.61	5.90	4.82	5.09	5.37	5.84	6.24	1.20	16.98	27.35
2. Verified emissions	5.08	5.26	5.40	5.58	5.36	5.06	4.60	4.38	4.02	15.73	24.98
Czech Republic											
1. Total allocated allowances	96.92	96.92	96.92	85.56	85.91	86.08	86.43	88.98	49.42	290.76	432.96
2. Verified emissions	82.45	83.62	87.83	80.40	73.78	75.58	74.19	69.32	67.71	253.91	373.27
Denmark											
1. Total allocated allowances	37.30	32.28	27.90	23.91	23.84	23.83	23.83	26.85	26.39	97.49	122.25
2. Verified emissions	26.48	34.20	29.41	26.55	25.46	25.27	21.47	18.19	21.60	90.08	116.93

Estonia											
1. Total allocated allowances	16.75	18.20	21.34	11.68	11.86	11.86	15.95	14.24	8.26	56.29	65.58
2. Verified emissions	12.62	12.10	15.33	13.54	10.38	14.51	14.81	13.54	15.92	40.06	66.79
Finland											
1. Total allocated allowances	44.67	44.62	44.62	36.53	37.07	37.92	37.99	38.17	39.77	133.90	187.68
2. Verified emissions	33.10	44.62	42.54	36.16	34.35	41.30	35.08	29.50	31.50	120.26	176.40
France											
1. Total allocated allowances	150.41	149.97	149.78	129.57	128.57	133.23	134.07	134.53	139.90	450.15	659.97
2. Verified emissions	131.26	126.98	126.63	124.13	111.09	115.57	105.58	103.66	115.09	384.88	560.04
Germany											
1. Total allocated allowances	493.48	495.49	497.30	436.93	431.88	440.68	440.49	471.65	374.68	1486.27	2221.62
2. Verified emissions	475.05	478.07	487.15	472.85	428.29	454.86	450.35	452.59	480.94	1440.27	2258.95
Greece											
1. Total allocated allowances	71.16	71.16	71.16	63.69	63.25	64.65	76.02	73.95	51.42	213.49	341.55
2. Verified emissions	71.27	69.97	72.72	69.85	63.66	59.94	58.84	61.44	58.63	213.95	313.73
Hungary											
1. Total allocated allowances	30.24	31.43	31.41	25.12	23.60	25.70	24.96	32.76	21.23	93.08	132.14
2. Verified emissions	26.16	25.85	26.84	27.24	22.40	22.99	22.47	21.27	19.13	78.84	116.37
Iceland											
1. Total allocated allowances	0.00	0.00	0.00	0.00	0.00	0.00	0.00	0.00	0.00	0.00	0.00
2. Verified emissions									1.78		
Ireland											
1. Total allocated allowances	19.24	20.45	19.24	19.97	20.14	21.23	21.76	21.75	15.96	58.93	104.85
2. Verified emissions	22.44	21.71	21.25	20.38	17.22	17.37	15.77	16.90	15.69	65.39	87.64
Italy											
1. Total allocated allowances	216.15	205.05	203.26	212.20	209.01	199.97	195.33	192.72	185.90	624.46	1009.22
2. Verified emissions	225.99	227.44	226.41	220.68	184.88	191.49	189.96	179.08	164.40	679.83	966.08
Latvia											
1. Total allocated allowances	4.07	4.06	4.04	3.73	4.86	4.76	4.62	4.99	5.34	12.16	22.96
2. Verified emissions	2.85	2.94	2.85	2.74	2.49	3.24	2.92	2.74	2.65	8.64	14.14
Liechtenstein											
1. Total allocated allowances	0.00	0.00	0.00	0.02	0.02	0.02	0.02	0.02	0.00	0.00	0.09
2. Verified emissions				0.02	0.01	0.00	0.00	0.00	0.00		0.04
Lithuania											
1. Total allocated allowances	13.50	10.58	10.87	7.51	7.57	8.16	8.89	10.85	11.69	34.95	42.97
2. Verified emissions	6.60	6.52	6.00	6.10	5.79	6.39	5.61	5.72	7.46	19.12	29.61
Luxembourg											
1. Total allocated allowances	3.23	3.23	3.23	2.49	2.49	2.49	2.49	2.49	2.62	9.69	12.44
2. Verified emissions	2.60	2.71	2.57	2.10	2.18	2.25	2.05	1.99	1.85	7.88	10.57
Malta											
1. Total allocated allowances	2.09	2.17	2.29	2.11	2.12	2.16	2.17	2.16	1.13	6.54	10.72
2. Verified emissions	1.97	1.99	2.03	2.02	1.90	1.88	1.93	2.05	1.70	5.98	9.78

Netherlands											
1. Total allocated allowances	86.45	86.39	86.48	76.76	83.83	92.84	92.83	91.00	83.82	259.32	437.26
2. Verified emissions	80.35	76.70	79.87	83.51	81.03	84.74	79.97	76.43	86.80	236.93	405.67
Norway											
1. Total allocated allowances	0.00	0.00	0.00	7.54	20.57	14.34	14.75	18.18	25.01	0.00	75.37
2. Verified emissions				19.34	19.22	19.34	19.23	18.59	24.70		95.71
Poland											
1. Total allocated allowances	237.56	237.56	237.54	201.00	202.02	205.64	207.21	213.04	129.35	712.66	1028.90
2. Verified emissions	203.15	209.62	209.62	204.11	191.17	199.73	203.03	196.64	205.73	622.38	994.67
Portugal											
1. Total allocated allowances	36.91	36.91	36.91	30.41	30.77	32.36	32.99	32.94	30.42	110.73	159.47
2. Verified emissions	36.43	33.06	31.20	29.91	28.26	24.17	25.01	25.25	24.64	100.69	132.60
Romania											
1. Total allocated allowances	0.00	0.00	74.34	71.79	73.93	74.99	74.81	75.86	57.56	74.34	371.39
2. Verified emissions			69.61	63.82	49.06	47.34	51.24	47.86	42.41	69.61	259.32
Slovakia											
1. Total allocated allowances	30.47	30.49	30.49	32.17	32.14	32.36	32.62	33.43	32.24	91.44	162.71
2. Verified emissions	25.23	25.54	24.52	25.34	21.60	21.70	22.22	20.94	21.83	75.29	111.79
Slovenia											
1. Total allocated allowances	9.14	8.69	8.25	8.21	8.22	8.23	8.22	8.23	6.84	26.08	41.11
2. Verified emissions	8.72	8.84	9.05	8.86	8.07	8.13	7.99	7.61	7.39	26.61	40.66
Spain											
1. Total allocated allowances	172.16	166.21	159.74	154.15	151.46	150.01	151.45	154.15	154.50	498.11	761.21
2. Verified emissions	183.63	179.72	186.57	163.46	136.94	121.48	132.69	135.64	122.79	549.93	690.21
Sweden											
1. Total allocated allowances	22.29	22.48	22.85	20.77	21.09	23.55	22.72	22.75	37.84	67.62	110.88
2. Verified emissions	19.38	20.00	19.04	20.08	17.49	22.66	19.85	18.17	20.11	58.42	98.26
United Kingdom											
1. Total allocated allowances	206.07	206.01	215.88	217.84	240.06	256.14	253.84	255.87	173.52	627.95	1223.75
2. Verified emissions	242.51	251.16	256.58	265.06	231.94	237.34	220.87	231.26	225.52	750.26	1186.47

B.2. Verified emissions by all industry sectors and by the electricity generation sector

	2005	2006	2007	2008	2009	2010	2011	2012
Austria								
Public Electricity and Heat Production	12.79	11.71	10.51	10.41	9.38	10.88	10.56	9.10
All Industry Sectors	33.37	32.38	31.75	32.08	27.36	30.92	30.60	28.39
Belgium								
Public Electricity and Heat Production	24.54	23.27	22.50	20.52	20.87	21.45	18.51	17.97
All Industry Sectors	55.36	54.78	52.80	55.46	46.21	50.10	46.20	43.01
Bulgaria								
Public Electricity and Heat Production			29.72	31.24	28.53	30.52	35.36	30.55
All Industry Sectors			39.18	38.30	32.01	33.53	40.00	35.05
Cyprus								
Public Electricity and Heat Production	3.48	3.66	3.81	3.98	4.01	3.88	3.72	3.56
All Industry Sectors	5.08	5.26	5.40	5.58	5.36	5.06	4.60	4.38
Czech Republic								
Public Electricity and Heat Production	56.36	55.77	59.44	54.00	51.40	53.85	53.54	52.58
All Industry Sectors	82.45	83.62	87.83	80.40	73.78	75.58	74.19	69.32
Denmark								
Public Electricity and Heat Production	20.53	28.35	23.66	21.66	21.64	21.62	17.68	14.33
All Industry Sectors	26.48	34.20	29.41	26.55	25.46	25.27	21.47	18.19
Estonia								
Public Electricity and Heat Production	12.21	11.51	13.76	12.39	10.38	13.82	14.15	12.69
All Industry Sectors	12.62	12.10	15.33	13.54	10.38	14.51	14.81	13.54
Finland								
Public Electricity and Heat Production	18.90	29.76	27.68	21.08	22.23	27.70	21.70	17.86
All Industry Sectors	33.10	44.62	42.54	36.16	34.35	41.30	35.08	29.50
France								
Public Electricity and Heat Production	49.71	46.30	46.32	44.82	43.70	45.88	37.90	41.16
All Industry Sectors	131.26	126.98	126.63	124.13	111.09	115.57	105.58	103.66
Germany								
Public Electricity and Heat Production	337.15	339.77	348.20	330.28	309.05	320.74	318.49	333.99
All Industry Sectors	475.05	478.07	487.15	472.85	428.29	454.86	450.35	452.59
Greece								
Public Electricity and Heat Production	54.43	51.57	55.00	54.08	50.87	48.49	50.64	51.08
All Industry Sectors	71.27	69.97	72.72	69.85	63.66	59.94	58.84	61.44
Hungary								
Public Electricity and Heat Production	18.38	18.70	19.74	18.73	15.69	16.18	15.42	14.92
All Industry Sectors	26.16	25.85	26.84	27.24	22.40	22.99	22.47	21.27
Ireland								
Public Electricity and Heat Production	15.25	14.53	14.06	14.16	12.62	12.90	11.56	12.38
All Industry Sectors	22.44	21.71	21.25	20.38	17.22	17.37	15.77	16.90

Italy								
Public Electricity and Heat Production	119.66	120.78	120.30	113.49	97.27	93.14	91.80	91.08
All Industry Sectors	225.99	227.44	226.41	220.68	184.88	191.49	189.96	179.08
Latvia								
Public Electricity and Heat Production	1.99	2.02	1.91	1.87	1.84	2.20	2.01	1.80
All Industry Sectors	2.85	2.94	2.85	2.74	2.49	3.24	2.92	2.74
Lithuania								
Public Electricity and Heat Production	3.85	3.67	3.28	2.98	3.09	3.74	2.90	2.97
All Industry Sectors	6.60	6.52	6.00	6.10	5.79	6.39	5.61	5.72
Luxembourg								
Public Electricity and Heat Production	1.24	1.31	1.18	1.00	1.20	1.21	1.00	1.04
All Industry Sectors	2.60	2.71	2.57	2.10	2.18	2.25	2.05	1.99
Malta								
Public Electricity and Heat Production	2.00	2.01	2.05	2.01	1.92	1.89	1.94	2.06
All Industry Sectors	1.97	1.99	2.03	2.02	1.90	1.88	1.93	2.05
Netherlands								
Public Electricity and Heat Production	54.24	50.12	52.97	52.68	52.89	54.90	50.84	48.44
All Industry Sectors	80.35	76.70	79.87	83.51	81.03	84.74	79.97	76.43
Norway								
Public Electricity and Heat Production				0.79	1.79	2.35	2.11	1.54
All Industry Sectors				19.34	19.22	19.34	19.23	18.59
Poland								
Public Electricity and Heat Production	169.76	174.97	169.99	164.15	158.03	163.74	165.97	161.08
All Industry Sectors	203.15	209.62	209.62	204.11	191.17	199.73	203.03	196.64
Portugal								
Public Electricity and Heat Production	23.01	20.02	17.45	16.79	17.24	12.20	14.34	15.27
All Industry Sectors	36.43	33.06	31.20	29.91	28.26	24.17	25.01	25.25
Romania								
Public Electricity and Heat Production			38.54	36.52	31.39	27.97	31.94	29.14
All Industry Sectors			69.61	63.82	49.06	47.34	51.24	47.86
Slovakia								
Public Electricity and Heat Production	8.69	8.05	7.37	7.46	6.53	6.25	6.41	6.12
All Industry Sectors	25.23	25.54	24.52	25.34	21.60	21.70	22.22	20.94
Slovenia								
Public Electricity and Heat Production	6.32	6.37	6.59	6.38	6.08	6.20	6.25	5.98
All Industry Sectors	8.72	8.84	9.05	8.86	8.07	8.13	7.99	7.61
Spain								
Public Electricity and Heat Production	110.94	102.30	108.03	91.65	75.89	59.47	72.91	77.47
All Industry Sectors	183.63	179.72	186.57	163.46	136.94	121.48	132.69	135.64
Sweden								
Public Electricity and Heat Production	8.23	8.33	8.00	7.62	8.17	10.62	8.26	7.68
All Industry Sectors	19.38	20.00	19.04	20.08	17.49	22.66	19.85	18.17
United Kingdom								
Public Electricity and Heat Production	173.91	183.14	178.85	173.76	151.93	157.45	145.05	159.24
All Industry Sectors	242.51	251.16	256.58	265.06	231.94	237.34	220.87	231.26

C. Option value and benefit function derivatives

In order to compute the first and second derivative with respect to P of

$$\tilde{F}(P_t) = q_1 P_t^{\gamma_1} \left[M\left(-\gamma_1, b_1, \frac{2k\theta}{\sigma^2 P_t}\right) + \omega \left(\frac{2k\theta}{\sigma^2 P_t}\right)^{1-b_1} M\left(1 - \gamma_1 - b_1, 2 - b_1, \frac{2k\theta}{\sigma^2 P_t}\right) \right]$$

we must first recall the expression of the derivative of the Kummer function with respect to z:

$$M_z(a, b, z) = \frac{a}{b} M(a + 1, b + 1, z)$$

Thus we obtain:

$$\begin{aligned} \tilde{F}_P(P_t) = q_1 P_t^{\gamma_1-1} & \left\{ \omega \left(\frac{2k\theta}{\sigma^2 P_t}\right)^{1-b_1} (\gamma_1 + b_1 - 1) \left[M\left(1 - \gamma_1 - b_1, 2 - b_1, \frac{2k\theta}{\sigma^2 P_t}\right) + \right. \right. \\ & \left. \left. + \frac{1}{2 - b_1} \frac{2k\theta}{\sigma^2 P_t} M\left(2 - \gamma_1 - b_1, 3 - b_1, \frac{2k\theta}{\sigma^2 P_t}\right) \right] + \gamma_1 M\left(-\gamma_1, b_1, \frac{2k\theta}{\sigma^2 P_t}\right) + \right. \\ & \left. \frac{\gamma_1}{b_1} \frac{2k\theta}{\sigma^2 P_t} M\left(1 - \gamma_1, 1 + b_1, \frac{2k\theta}{\sigma^2 P_t}\right) \right\} \end{aligned}$$

and

$$\begin{aligned} \tilde{F}_{PP}(P_t) = q_1 P_t^{\gamma_1-2} & \left\{ \omega \left(\frac{2k\theta}{\sigma^2 P_t}\right)^{1-b_1} (\gamma_1 + b_1 - 1)(\gamma_1 + b_1 - 2) M\left(1 - \gamma_1 - b_1, 2 - b_1, \frac{2k\theta}{\sigma^2 P_t}\right) + \right. \\ & \left. + \omega \left(\frac{2k\theta}{\sigma^2 P_t}\right)^{2-b_1} \frac{2(\gamma_1 + b_1 - 1)(\gamma_1 + b_1 - 2)}{2 - b_1} M\left(2 - \gamma_1 - b_1, 3 - b_1, \frac{2k\theta}{\sigma^2 P_t}\right) + \right. \\ & \left. \gamma_1(\gamma_1 - 1) M\left(-\gamma_1, b_1, \frac{2k\theta}{\sigma^2 P_t}\right) + \frac{2\gamma_1(\gamma_1 - 1)}{b_1} \frac{2k\theta}{\sigma^2 P_t} M\left(1 - \gamma_1, 1 + b_1, \frac{2k\theta}{\sigma^2 P_t}\right) + \right. \\ & \left. + \omega \left(\frac{2k\theta}{\sigma^2 P_t}\right)^{3-b_1} \frac{(\gamma_1 + b_1 - 1)(\gamma_1 + b_1 - 2)}{(2 - b_1)(3 - b_1)} M\left(3 - \gamma_1 - b_1, 4 - b_1, \frac{2k\theta}{\sigma^2 P_t}\right) + \right. \\ & \left. + \frac{\gamma_1(\gamma_1 - 1)}{b_1(b_1 + 1)} \left(\frac{2k\theta}{\sigma^2 P_t}\right)^2 M\left(2 - \gamma_1, 2 + b_1, \frac{2k\theta}{\sigma^2 P_t}\right) \right\} \end{aligned}$$

As for the benefit function,

$$\Phi(D(t), P(t), t) = [1 - e^{-r(T_{pv})}] \left(\frac{B}{r} D(t) + \frac{X}{r} P(t) + \frac{Op}{r} \right),$$

its derivative with respect to P is equal to

$$\Phi_P(D(t), P(t), t) = [1 - e^{-r(T_{pv})}] \frac{X}{r}.$$

Bibliography

Abramowitz, M. - Stegun, I.A. (1972). *Handbook of Mathematical Functions with Formulas, Graphs and Mathematical Tables*. National Bureau of Standards Applied Mathematics Series. Dover Publications, New York.

Agora Energiewende (2015): Calculator of Levelized Cost of Electricity for Photovoltaics; www.agora-energiewende.org/pv-cost

Agritre, 2011. *Documentazione Tecnica a Fini Autorizzativi. Documenti Strutturali. Relazione Tecnica Metodologica di Dismissione Impianto e Ripristino dei Luoghi*. Available at: http://www.ambiente.provincia.foggia.it/attachments/article/201/10-625-SAG-S-002_01_%20Relazione%20Dismissione.pdf [accessed on 06/18/15].

Andersen, M.S. - Ekins, P. (2009). *Carbon-Energy Taxation. Lessons from Europe*. New York: Oxford University Press.

Anger, N. (2008). *Emission Trading Beyond Europe: Linking Schemes in a Post-Kyoto World*. *Energy Economics*, **30**, 4, 2028-2049. DOI: 10.1016/j.eneco.2007.08.002.

Bai, K. - Russel, J. - Tiao, G. (2001). *Kurtosis of GARCH and Stochastic Volatility Models with Non-normal Innovation*. University of Chicago.

Bansal, P. - Hoffman, A. (2012). *The Oxford Handbook of Business and the Natural Environment*. Oxford University Press.

Bee, M. - Santi, F. (2013). *Finanza quantitativa con R*. Apogeo - Idee editoriali Feltrinelli.

Biondi, T. - Moretto, M. (2014). *Solar Grid Parity Dynamics in Italy: a Real Option Approach*. Energy, <http://dx.doi.org/10.1016/j.energy.2014.11.072>

Björk, T. (2009). *Arbitrage Theory in Continuous Time (3rd ed.)*. Oxford University Press.

Bloomberg New Energy Finance, 2015. *Sustainable Energy in America: 2015 Factbook*. London, UK: Bloomberg New Energy Finance; Washington, DC: The Business Council for Sustainable Energy.

Brennan, M.J. – Schwartz, E.S. (1980). *Analyzing Convertible Bonds*. The Journal of Financial and Quantitative Analysis, 15, 4, Proceedings of 15th Annual Conference of the Western Finance Association, June 19-21, 1980, San Diego, California, 907-929.

Campbell, J. - Lo, A.W. - MacKinlay, C. (1997). *The Econometrics of Financial Markets*. Princeton, NJ: Princeton University Press.

Carrol, A. - Lipartito, K. - Post, J. - Werhane, P. (2012). *Corporate Responsibility – The American Experience*. Cambridge University Press.

Carr, P. - Geman, H. - Madan, D. B. - Yor, M. (2002). *The fine structure of asset returns: An empirical investigation*. The Journal of Business 75, 2, 305–332.

Carr, P. - Geman, H. - Madan, D. B. - Yor, M. (2003). *Stochastic Volatility for Lévy Processes*. Mathematical Finance, 13, 3, 345-382.

Carr, P. - Madan, D.B. - Chang, E. (1998). *The Variance Gamma Process and Option Pricing*. European Finance Review, 2, 79-105.

Carr, P. - Wu, L. (2003). *The Finite Moment Log Stable Process and Option Pricing*. The Journal of Finance, **58**, 2.

Carr, P. - Wu, L. (2004). *Time-changed Lévy Processes and Option Pricing*. Journal of Financial Economics, **71**, 113-141.

Coase, R.H. (1960). *The Problem of Social Cost*. Journal of Law and Economics, **3**, 1-44.

Cont, R. (2001). *Empirical Properties of Asset Returns: Stylized Facts and Statistical Issues*. Quantitative Finance, **1**, 223-236.

Cont, R. - Potters, M. - Bouchaud, J.P., (1997). *Scaling in stock market data: stable laws and beyond - Scale Invariance and Beyond*. (Proc. CNRS Workshop on Scale Invariance, Les Houches, 1997) ed. Dubrulle, Graner and Sornette (Berlin: Springer).

Cont, R. - Tankov, P., (2004). *Financial Modelling with Jump Processes*. Chapman and Hall/CRC Press, London.

Cramton, P. - Kerr, S. (2002). *Tradable Carbon Permit Auctions: How and Why to Auction not Grandfather*. Energy Policy, **30**, 333-345.

Dales, J. (1968). *Pollution Property and Prices*. University of Toronto Press, Toronto.

Dixit, A.K. - Pindyck, R.S. (1994). *Investment Under Uncertainty*. Princeton, N.J.: Princeton University Press.

European Commission, *Structural Reform of the European Carbon Market*, accessed January 8, 2015, <http://ec.europa.eu/clima/policies/ets/reform/> .

European Commission (2010). *EU Energy Trends to 2030*. Luxembourg: Publications Office of the European Union.

European Commission (2013). *The EU Emissions Trading System (EU ETS)*. European Union Publications Office.

European Environmental Agency, 2011. *1970s*. Available at <http://www.eea.europa.eu/environmental-time-line/1970s> [accessed on 01/22/15].

EIA (US Energy Information Administration), 2015. *Electric Power Monthly -Table 6.7.A. Capacity Factor for Utility Scale Generators Primarily Using Fossil Fuels, January 2013- April 2015*. Available at: http://www.eia.gov/electricity/monthly/epm_table_grapher.cfm?t=epmt_6_07_a [accessed on 05/23/15].

EIA (US Energy Information Administration), 2015. *Table 8.4 . Average Power Plant Operating Expenses for Major US Investor-Owned Electric Utilities, 2003 through 2013*. Available at: http://www.eia.gov/electricity/annual/html/epa_08_04.html [accessed on 06/18/15].

Enipedia. *Livorno Powerplant*. Available at: http://enipedia.tudelft.nl/wiki/Livorno_Powerplant. [Accessed on 06/18/15].

Figueroa-Lopez, J. E. - Lancette, S.R. - Lee, K. - Mi, Y. (2011). *Estimation of NIG and VG Models for High Frequency Financial Data*. Handbook For Modeling High-Frequency Data In Finance, J. Wiley.

Finlay, R. (2009). *The Variance Gamma (VG) Model with Long Range Dependence*. Doctoral Thesis, School of Mathematics and Statistics, University of Sidney.

Fraunhofer ISE, 2015. *Current and Future Cost of Photovoltaics. Long-term Scenarios for Market Development, System Prices and LCOE of Utility-Scale PV Systems*. Study on behalf of Agora Energiewende.

Gouriéroux, C. - Monfort, A. - Renault, E. (1993). *Indirect Inference*. Journal of Applied Econometrics, **8**, S85-S118

Granger, C.W.J. - Ding, Z. (1995). *Some Properties of Absolute Returns: an Alternative Measure of Risk*. Annales d'Économie et de Statistique, **40**, 67-91.

Granger, C.W.J. - Ding, Z. - Spear, S. (1997). *Stylized Facts on the Temporal and Distributional Properties of Daily Data from Speculative Markets*. Department of Economics, UC San Diego.

Harrison, D. - Radov, D.B. (2002). *Evaluation of Alternative Initial Allocation Mechanisms in a European Union Greenhouse Gas Emissions Allowance Trading Scheme*. Report by National Economic Research Associates prepared for DG Environment, European Commission.

Heyde, C. - Liu, S. (2001). *Empirical Realities for a Minimal Description Risky Asset Model. The Need for Fractal Features*. Journal of the Korean Mathematical Society (5), **38**, 1047-1059.

Huld, T. - Müller, R. - Gambardella, A. (2012). *A New Solar Radiation Database for Estimating PV Performance in Europe and Africa*. Solar Energy, **86**, 1803-1815.

Hull, J. (2012). *Options, Futures, and Other Derivatives (8th ed.)*. Pearson education.

IEA (2008). *Energy Efficiency Indicators for Public Electricity Production from Fossil Fuels*. IEA information paper, OECD/IEA, Paris.

IEA (2014). *Technology Roadmap: Solar Photovoltaic Energy*. OECD/IEA, Paris.

IPCC 2006, *2006 IPCC Guidelines for National Greenhouse Gas Inventories*, prepared by the National Greenhouse Gas Inventories Programme, Eggleston H.S., Buendia L., Miwa K., Ngara T., and Tanabe K. (eds). Published: IGES, Japan.

Jaffe, J. - Stavins, R.N. (2008). *Linkage of Tradable Permit Systems in International Climate Policy Architecture*. NBER Working Paper N° 14432. National Bureau of Economic Research, Cambridge, MA.

Kou, S.G. (2008). *Jump-Diffusion Models for Asset Pricing in Financial Engineering*. Handbooks in OR & MS, Vol 15, 73-116.

Madan, D.B. - Carr, P.P. - Chang, E.C. (1998). *The Variance Gamma Process and Option Pricing*. European Finance Review, **2**, 79-105.

Madan, D.B. - Seneta, E. (1990). *The Variance Gamma (VG) Model for Share Market Returns*. Journal of Business, **63**, 511-524.

McLeish, D.L. (1982). *A Robust Alternative to the Normal Distribution*. The Canadian Journal of Statistics, **10**, 89-102.

Merton, R.C. (1976). *Option Pricing When Underlying Stock Returns Are Discontinuous*. Journal of Financial Economics, **3**, 125-144.

Merton, R. C. , (1977). *On the Pricing of Contingent Claims and the Modigliani-Miller Theorem*. Journal of Financial Economics , **5**, 241-249.

Müller, U. A. - Dacorogna, M. M. - Pictet, O. V. (1998). *Heavy tails in high-frequency financial data. A Practical Guide to Heavy Tails: Statistical Techniques and Applications*. Boston: Birkhäuser, 55-77.

Pearson, K. - Jeffery, G.B. - Elderton, E.M. (1929). *On the Distribution of the First Product-Moment Coefficient in Samples Drawn from an Indefinitely Large Normal Population*. *Biometrika*, **21**, 164-201.

Phillips, P.C.B. - Yu, J. (2006). *Maximum Likelihood and Gaussian Estimation of Continuous Time Models in Finance*. Research Collection School of Economics.

Reuters, *EU Parliament Rejects Carbon Market Rescue Fix*, April 16, 2013, <http://www.reuters.com/article/2013/04/16/us-eu-ets-vote-idUSBRE93F0NT20130416> .

Rogers, L.C.G. - Zhang, L. (2011). *An Asset Return Model Capturing Stylized Facts*. *Mathematics and Financial Economics* (2), **5**, 101-119.

Sarkar, S. (2003). *The Effect of Mean Reversion on Investment Under Uncertainty*. *Journal of Economic Dynamics and Control*, **28** (2), 377-396.

Schoutens, W. (2003). *Lévy Processes in Finance. Pricing Financial Derivatives*. John Wiley & Sons, England.

Šúri, M. - Huld, T.A. - Dunlop, E.D. - Ossenbrink, H.A. (2007). *Potential of Solar Electricity Generation in the European Union Member States and Candidate Countries*. *Solar Energy*, **81**, 1295–1305, <http://re.jrc.ec.europa.eu/pvgis/>.

Stavins, R.N. (1998). *What Can We Learn from the Grand Policy Experiment? Lessons from SO2 Allowance Trading*. *Journal of Economic Perspectives*, **12**, 3, 69-88.

Taylor, S. (2008). *Modelling Financial Time Series (2nd ed.)*. World scientific Publishing.

Teichroew, D. (1957). *The Mixture of Normal Distributions with Different Variances*. *The Annals of Mathematical Statistics*, **28**, 510-512.

Tietenberg, T.H. (1990). *Economic Instruments for Environmental Regulation*. Oxford Review of Economic Policy, **6**, 1, 17-33.

Tsekrekos, A.E. (2009). *The Effect of Mean Reversion on Entry and Exit Decisions Under Uncertainty*. Journal of Economic Dynamics and Control, doi:10.1016/j.jedc.2009.10.015

World Bank, (2014). *States and Trends of Carbon Pricing 2014*. Washington, DC: World Bank. Doi: 10.1596/978-1-4648-0268-3. License: Creative Commons Attribution CC BY 3.0 IGO.

World Bank, (2015). *Commodity Markets Outlook. April 2015 Quarterly Report*. World Bank Group.